

University of Southampton Research Repository ePrints Soton

Copyright © and Moral Rights for this thesis are retained by the author and/or other copyright owners. A copy can be downloaded for personal non-commercial research or study, without prior permission or charge. This thesis cannot be reproduced or quoted extensively from without first obtaining permission in writing from the copyright holder/s. The content must not be changed in any way or sold commercially in any format or medium without the formal permission of the copyright holders.

When referring to this work, full bibliographic details including the author, title, awarding institution and date of the thesis must be given e.g.

AUTHOR (year of submission) "Full thesis title", University of Southampton, name of the University School or Department, PhD Thesis, pagination

UNIVERSITY OF SOUTHAMPTON
SCHOOL OF OCEANOGRAPHIC SCIENCE

Lab-on-a-chip Systems for the Analysis of Phytoplankton RNA

By Mahadji Bahi

Thesis for degree of doctor of Engineering / Bioelectronics

January 2013

Abstract

Monitoring microorganisms in natural water is central to understanding and managing risks to human health and ecosystems. Some phytoplankton can produce toxic blooms which are harmful to aquatic ecosystems and human health. *Kariena brevis* is responsible for Harmful Algal Blooms and produces brevetoxin which can lead to gastrointestinal and neurological problems in mammals. Traditional methods for Harmful Algal Bloom monitoring require sample collection and preservation for later study in laboratories where they are generally processed using microscopy which can take many hours or days. Laboratory equipment for this application has been adapted for ship-board use. Portable instrument systems that incorporate sample preparation and detection have been also developed for environmental applications. However, very few are suitable for deployment in the environment (either as a hand-held or *in situ* system) and often require laboratory infrastructure or personnel to facilitate sample collection and processing. Current *in situ* systems are large, expensive, and require expert users to operate them. Thus these existing systems do not provide marine science with the high spatial resolution data required to enable a better understanding of the diversity, function and community structure of marine microorganisms. Ideal *in situ* sensors should provide sample analysis over wide areas and at many depths for long periods of time. This remains a significant challenge. One possible solution is to develop numerous cheap sensors which could be incorporated into autonomous underwater vehicles or an argofloats network. Micro systems are excellent candidates as when mature, they could be mass produced to enable them to meet this particular spatial mapping requirement. The use of fully automatic and accurate micro total analysis systems, also known as lab-on-a-chip, can overcome the challenges of highly integrated *in situ* systems for incorporation into environmental monitoring vehicles and stations. Lab-on-a-chip technology appears well suited for environmental monitoring with its main advantages being the possibility of miniaturization, portability, reduced reagent consumption and automation. Molecular biology tools combined with microfluidic technology have been seen as a potential technical solution for *in situ* environmental applications. The purpose of this work has been to develop key functions in independent microchips that perform elements of a complete biological assay for ribonucleic acid phytoplankton metrology from the sample preparation to the detection step. Specifically the system is being developed to analyse the large subunit of the ribulose-bisphosphate carboxylase (*rbcL*) gene of phytoplankton *Kariena brevis*, a species responsible for Harmful Algal Blooms. This thesis reports the development of three lab-on-a-chip devices which perform microalga cell lysis, nucleic acid purification and real-time ribonucleic acid detection. The aim was to demonstrate proof-of concept for each device separately in order to obviate the need to tackle the complications of system integration (which remains a challenge), while understanding performance needed and comparing that achieved to the most likely scenarios for real-world applications. Future research should integrate these separate chips into an integrated single chip design to achieve fully automated chips with “sample-in” to “answer-out” capability.

Acknowledgements

I would like to express my great thanks to my supervisors Doctor Matthew Mowlem and Professor Peter Statham for their guidance, encouragement and support during the course of my study.

Declaration of Authorship

I, Mahadji Majid Bahi, declare that the thesis entitled

‘Lab-on-a-chip Systems for the Analysis of Phytoplankton RNA’

and the work presented in the thesis is both my own and have been generated by me as the result of my own original research. I confirm that:

- this work was done wholly or mainly while in candidature for a research degree at the University of Southampton ;
- where any part of this thesis has previously been submitted for a degree or any other qualification at this University or any other institution, this has been clearly stated;
- where I have consulted the published work of others, this is always clearly attributed;
- Where I have quoted from the work of others, the source is always given. With the exception of such quotations, this thesis is entirely my own work;
- I have acknowledged all main sources of help;
- Where the thesis is based on work done by myself jointly with others, I have made clear exactly what was done by others and what I have contributed myself;
- part of this work have been published as:
 - “*Electroporation and lysis of marine microalga *Karenia brevis* for RNA extraction and amplification*” by M. M. Bahi, M.-N. Tsaloglou, M. Mowlem and H. Morgan. (published) (Bahi, Tsaloglou et al. 2010)
 - “*On-chip real-time nucleic acid sequence-based amplification for RNA detection and amplification*” by M.-N. Tsaloglou, M. M. Bahi, E.M Waugh, H. Morgan and M. Mowlem. (published)(Tsaloglou, Bahi et al. 2011)

Contents

Abstract	2
Acknowledgements	3
Declaration of Authorship	4
Contents	5
List of Figures	9
List of Tables	14
Nomenclature	15
Chapter 1 Introduction	17
1.1. Research motivations and objectives	19
1.1.1. Main criteria and solutions for nucleic acid <i>in situ</i> sensors	23
1.1.1.a Low cell number detection	23
1.1.1.b Viable cells detection	24
1.1.1.c Transportable system and assay cost	24
1.1.1.d Ease of use	25
1.1.2. Scope and outline of this thesis	26
1.1.3. Statement of novelty	27
1.1.4. Contribution of the author and co-workers	28
1.1.5. Additional activities during my PhD	29
1.2. Nucleic acid analysis overview	31
1.2.1. Introduction to PCR and NASBA	32
1.3. Current nucleic acid amplification-based lab-on-a-chip devices with “sample-in” to “answer-out” capability	39
1.3.1. Sample preparation techniques in lab-on-a-chip with potential “sample-in” to “answer-out” capability	41
1.3.1.a Silica-based extraction techniques	41
1.3.1.b Antibodies-conjugated magnetic microbeads for cancer cells capture an nucleic acids extraction	45
1.3.1.c Mechanical filtering and membrane-based nucleic acid capture and extraction	45
1.3.2. Biological assay and integration level in lab-on-a-chip devices with potential “sample-in” to “answer-out” capability	46
1.3.2.a PCR-based lab-on-a-chip devices with “sample-in” to “answer-out” capability	46
1.3.2.b NASBA-based lab-on-a-chip devices with “sample-in” to “answer-out” capability	50
1.4. Lab-on-a-chip systems challenges	54

1.4.1. Small volume and sample preparation challenges	54
1.4.2. Biocompatibility and surface adsorption challenges	55
1.4.3. Reagent storage challenges.....	58
1.4.4. Detection techniques challenges.....	58
1.4.5. Nucleic acid analyse time versus high temporal resolution	59
1.4.6. Microfluidic interconnections standard challenges	60
1.4.7. Fluidic automation and integration.....	60
1.4.8. Fabrication challenges	60
Chapter 2 Cell lysis microchip.....	61
2.1. Cell lysis microchip summary	63
2.2. An introduction to dielectrophoresis and electroporation	65
2.2.1. Electrostatic concept and polarisation effect	65
2.2.2. Dielectrophoresis background	66
2.2.2.a Cells parameters for dielectrophoresis:	70
2.2.3. Electroporation Theory.....	72
2.3. State of art of electroporation for cell lysis on-chip.....	75
2.4. Electroporation and lysis of the phytoplankton <i>Karenia brevis</i> for RNA extraction and amplification	76
2.4.1. Materials and methods.....	76
2.4.1.a Cell culture	77
2.4.1.b Sample preparation	77
2.4.1.c Electroporation experimental	78
2.4.2. Results	78
2.5. Discussion and conclusion.....	83
Chapter 3 RNA sample preparation microdevice.....	85
3.1. RNA sample preparation microdevice summary	87
3.2. Nucleic acid preparation method and quantification	89
3.2.1. Sample extraction methods.....	89
3.2.2. Measurement of nucleic acid quantity and quality	92
3.2.2.a UV absorption methods.....	92
3.2.2.b Gel-electrophoresis methods	92
3.2.2.c Staining methods	93
3.2.2.d Amplification methods.....	93
3.3. State-of-art of microdevices for nucleic acid extraction	94

3.3.1.a Membrane technology	95
3.3.1.b Antibody coated beads technology	96
3.3.1.c Functionalized (oligo-dT) magnetic beads technology	97
3.4. A simple sample preparation platform for environmental applications	100
3.4.1. Materials and methods.....	101
3.4.1.a Algal cultures	101
3.4.1.b Bench-top sample preparation and RNA purification	101
3.4.1.c Sample preparation microfluidic device	101
3.4.1.d Sample preparation experimental procedure	104
3.4.1.e Cell number filtration capacity	106
3.4.1.f RNA capture efficiency	106
3.4.1.g Sample preparation microdevice operation range	107
3.4.1.h Sample preparation microfluidic performance assessment	107
3.4.1.i RNA quality assessment	108
3.4.1.j RNA quantity assessment	108
3.4.1.k Suitability for subsequent amplification	108
3.4.2. Results	109
3.4.2.a Cell number filtration capacity	109
3.4.2.b RNA capture efficiency.....	109
3.4.2.c Sample preparation microdevice operation range	110
3.4.2.d Sample preparation microfluidic performance assessment with mixed population	112
3.4.3. Discussion and conclusion	115
3.4.3.a Current challenges.....	115
3.4.3.b Possible improvements.....	116
Chapter 4 RNA amplification on-chip	119
4.1. RNA amplification on-chip summary.....	121
4.2. NASBA-based microdevices	123
4.3. On-chip real-time nucleic acid sequence-based amplification for RNA detection and amplification	124
4.3.1. Materials and methods.....	125
4.3.1.a Algae culture	125
4.3.1.b Sample preparation	125
4.3.1.c Bench top NASBA	125
4.3.1.d Microchip fabrication.....	125
4.3.1.e Material compatibility assessment	126
4.3.1.f On-chip NASBA and fluorescence setup.....	126
4.4. Results	128

4.4.1.a Material compatibility assessment	128
4.4.1.b On-chip NASBA and fluorescence setup	129
4.5. Discussion and conclusion	131
Chapter 5 Discussion and further work	135
5.1. Conclusion	137
5.1.1. Sample preparation	139
5.1.2. Integration	140
5.2. Further work	142
5.2.1. Sample preparation	142
5.2.2. Integration and automation	143
References	144
Appendix A – NASBA design	157

List of Figures

Figure 1 Principle of on-site and point-of-care diagnostics, diagram adapted from Puren et al. (Puren, Gerlach et al. 2010).	20
Figure 2 A photo of a standalone fluidic handling system and on the right a photo of the ESP. Taken from (Preston, Harris et al. 2011).	23
Figure 3 “The blue shaded areas denote the thin layer occupied by <i>Dinophysis</i> cells.” Taken from (Anderson, Cembella et al. 2011).	25
Figure 4 Overview of nucleic acid analysis, techniques and microfluidic technology, adapted from Lui et al. Surface-enhanced Raman scattering (SERS) and surface plasma resonance (SPR) are optical detection methods (Lui, Cady et al. 2009).	31
Figure 5 Schematic diagrams of the (a) PCR and (b) NASBA reactions. In PCR, DNA is first denatured at 95 C and then primers anneal to the single DNA strands at 50–60 C, depending on the target. Finally, taq DNA polymerase catalyses the synthesis of 2n–2n double stranded DNA molecules, where n is the number of amplification cycles. Typically, 20 cycles, at 5 min per cycle, are required for one million fold amplification. NASBA is a complex process which amplifies mRNA using T7 RNA polymerase, reverse transcriptase and RNase H. NASBA needs approximately five cycles at an isothermal temperature of 41 C, to yield one million antisense single RNA copies, since 10–100 copies are produced in each transcription step.(Tsaloglou, Bahi et al. 2011)	35
Figure 6 “Phase transitions in solutions containing molecular beacons. Schematic representation of the phases. As the temperature is raised, the fluorescent probe–target duplex (phase 1) dissociates into a nonfluorescent molecular beacon in a closed conformation and a randomly coiled target oligonucleotide (phase 2). As the temperature is raised even higher, the hairpin stem of the molecular beacon unravels into a fluorescent randomly coiled oligonucleotide (phase 3).” Taken from (Bonnet, Tyagi et al. 1999; Vet and Marras 2005).	37
Figure 7 “An optical micrograph of the DNA purification/real-time PCR microchip is shown. The nucleic acid purification region is shown in (A) while the real-time PCR region is shown in (B). The fluid connections are (1) sample input, (2) waste outlet, (3) PCR reagent input, and (4) reaction outlet. The large white arrow denotes the lateral path for fluorescent excitation for real-time PCR.” Taken from (Cady, Stelick et al. 2005).	41
Figure 8 Photograph of the bench top instrument using a microfluidic chip, Peltier element, electrical connections and touch screen control panel. Taken from (Shaw, Joyce et al. 2011).	42
Figure 9 “Method for silica bead immobilisation on PDMS surface. (A) Before loading the beads, all ports are sealed except for the Input and Waste Output. (B) 3 mL of plain silica bead solution flows into the input, left to dry, and exposed to UV-ozone for bonding. (C) Unbound beads are washed away with dH2O, leaving a (D) layer of silica beads bonded to the walls of the RPC (E–F) Bright-field micrographs of the immobilised 10 mm silica beads on the PDMS walls of the RNA purification chamber.” Taken from (Dimov, Garcia-Cordero et al. 2008).	43
Figure 10 Photograph of Left: Final chip design with fluid inputs and outputs and functional regions labelled. Right: Picture of a chip prototype demonstrating its credit card-like size.(Sauer-Budge, Mirer et al. 2009)	44
Figure 11 “The fluorescence excitation/detection system is shown. A 480 nm wavelength LED (A) is used to illuminate the PCR chamber of the microfluidic detection chip (C) through a chrome-plated glass waveguide (B). Upon fluorescence of the real-time PCR reaction.” Taken from (Cady, Stelick et al. 2005).	46

Figure 12 Photograph of “Left: Schematic of instrument functionality and photo of chip/instrument interface. The interface block is raised to show the position of the chip (red arrow). Right: Picture of instrument. The black arrow points to the door of the chip/in.” Taken from (Sauer-Budge, Mirer et al. 2009).	47
Figure 13 “Schematic (top) and photograph (bottom) of the microfluidic device, showing the thermally activated silica monolith (A) within the microfluidic device, the position of the carbon electrodes (B–H) and the locations of the gel encapsulated reagents. The additional channel between electrodes G and H provides the potential for future integration with capillary electrophoresis for detection of PCR products.” Taken from (Shaw, Joyce et al. 2011).	48
Figure 14 “(a) Experimental setup of the proposed 3D microfluidic system. (b) Schematic diagram and the designed parameters of the 3D microfluidic incubator in both top-sectional view (b-1), and cross-sectional view (b-2), during the membrane-deformation process (b-3) and during the membrane recovery process (b-4). (c) The working principle of the suction-based microfluidic control module.” Taken from (Lien, Chuang et al. 2010).	49
Figure 15 Illustration of the relation between miniaturisation and analyte amount.	55
Figure 16 “Synthesis of PEG-NH ₂ (A) and the two-step surface modification procedure (B).” Taken from (Zhang, Feng et al. 2009).	57
Figure 17 Illustration of biocompatibility, PMMA substrate coated with PEG, taken from (Bi, Meng et al. 2006).	57
Figure 18 Particles under uniform field, the net force on the dipole is zero because an equal and opposite force acts on each half of the dipole.	66
Figure 19 In non uniform field, the electrostatic force on each half of the sphere will be different, resulting in a net force on it.	67
Figure 20 (a) Plot of the Clausius-Mossotti factor for a <i>K. brevis</i> cell (simple model) in low conductive medium, calculated using Equation 5 and the parameters in Table 5. In red $\text{Re}(f_{\text{CM}})$, in bleu $\text{Im}(f_{\text{CM}})$ (imaginary part of the Clausius-Mossotti factor), positive DEP occurs until 100 Mhz. (b) Plot of the Clausius-Mossotti factor for a <i>K. brevis</i> cell (simple model) in seawater, in red $\text{Re}(f_{\text{CM}})$, in bleu $\text{Im}(f_{\text{CM}})$. Weak positive DEP occurs from 3 GHz for <i>K. brevis</i> cells in seawater.	69
Figure 21 A single concentric shell model, typically used for modelling biological cells.	70
Figure 22 Plot of the Clausius-Mossotti factor for <i>K. brevis</i> cells, calculated using Equation 11 and the parameters in Table 6. In bleu $\text{Re}(f_{\text{CM}})$, in red $\text{Im}(f_{\text{CM}})$	71
Figure 23 “Formation of an aqueous pore according to the model of electroporation. From top to bottom: the intact bilayer; the formation of a hydrophobic pore; the transition to a hydrophilic pore and a limited expansion of the pore radius corresponding to a reversible breakdown; unlimited expansion of the pore radius corresponding to an irreversible breakdown.” Taken from (Pavlin, Kotnik et al. 2008).	72
Figure 24 Plot of the approximate transmembrane potential induced on a <i>K. brevis</i> cell. The calculation is based on the Equation 13 using parameters in Table 7 . In bleu the absolute value of the transmembrane potential, in red its real part and green its imaginary part.	74
Figure 25 (a) Image of microchip using a UK pound coin for size reference. (b) Light microscopy image (20 magnification) of <i>K. brevis</i> cells captured on the micro-electrodes upon the application of 1 V at 200 kHz for 10 s.	77
Figure 26 Estimation of the capture efficiency.	79
Figure 27 Membrane deformation and pore formation of <i>K. brevis</i> cells: (a) pre-electroporation under cell trapping of 1 V field at 200 kHz for 20 s. Two distinct cells, encircled white, can be observed trapped on the micro-electrodes. (b) Post-electroporation of 60 V field at 600 kHz for 5 s. Membranes of the encircled cells are becoming disrupted owing to the	

formation of pores by the continued application of an electric field. (c) Post-electroporation of 60 V at 600 kHz for 10 s. Poration of the encircled cells is so extensive that intracellular material is escaping into the iso-osmotic low-conductivity buffer. (d) Post-electroporation of 60 V at 600 kHz for 15 s, the encircled cells have become completely disrupted and no distinct cell membranes can be observed..... 79

Figure 28 Micrographs showing the process of single-cell electroporation of *K. brevis* temporary cysts. (a) Bright-field images on the application of 45 V at 600 kHz captured at (i) 0 s (ii) 30 s (iii) 1 min (iv) 1.5 min and (v) 2 min. (b) Epi-fluorescence images collected simultaneously at an excitation of 536 nm and emission of 593 nm. 80

Figure 29 Identification of optimal electroporation conditions: (a) On-chip lysis using a 1 V field for five different time intervals: (i) yield and purity results (black bars, relative yield; grey bars, relative fluorescence) and (ii) NABSA amplification data. Triangles, positive control; white circles, 1 s; crosses, 30 s; black circles, 60 s; plus symbols, 90 s; squares, 120 s. Increasing duration of electroporation led to increased yield of RNA extracted from the cell lysate. (b) On-chip lysis using a 30 V field for five different time intervals: (i) Yield and purity results (black bars, relative yield; grey bars, relative fluorescence) and (ii) NABSA amplification data. White triangles, positive control; diamonds, 1 s; squares, 30 s; crosses, 60 s; circles, 90 s; black triangles, 120 s. Electroporation that lasted longer than 60 s caused the yield of RNA extracted from the cell lysate to decrease. (c) On-chip lysis using a 60 V field for different time intervals: (i) Yield and purity results (black-filled bars, relative yield; grey-filled bars, relative fluorescence) and (ii) NABSA amplification data. Black circles, positive control; triangles, 1 s; white circles, 30 s; crosses, 60 s. Data show that electroporation of 60 V was more effective than the bench-top alternative but appeared to degrade the quality of extracted RNA from the lysate. 82

Figure 30 Principle of nucleic acid adsorption on silica substrate. 91

Figure 31 Institut für Mikrotechnik's instrument for the sample preparation chip. Taken from (Baier, Hansen-Hagge et al. 2009). 95

Figure 32 Photograph of“(A) Sample and buffer solutions pass through the microchannel of the RNA microextractor at sample and buffer flow rates of 15 mL/h, respectively, without an external magnetic field. In this case, the magnetic beads and other lysate components flow into outlet #2. (B) Sample and buffer solutions pass through the microchannel with an external magnetic flux of 0.14 T. The magnetic beads are laterally drawn and flow into outlet #1, while the other substances flow into outlet #2.” Taken from (Lee, Jung et al. 2010). 97

Figure 33 Sample preparation microdevice. (a) exploded view (95 mm long, 37 mm wide and 6 mm thick) with integrated aluminium oxide filter. 102

Figure 34 Sample preparation microdevice. Detailed exploded view of the microchip top part. 102

Figure 35 Sample preparation microdevice. Detailed exploded view of the microchip bottom part. 103

Figure 36 Sample preparation microdevice. Schematic of the microfluidic system setup, the sample is dispensed by a syringe pump, a manual 3 way valves allow switching between the two outputs. A personal computer running LabVIEW™ was used to control a National Instruments data acquisition card (NI-6281 USB), which control the holder temperature..... 103

Figure 37 Sample preparation microdevice. Schematics of the microchip and illustration of the flow control and the operation process of the microdevice capable of performing RNA extraction,: (1) cells pre-concentration; (2) cells lysis and incubation process for total RNA binding with aluminium oxide filter; (3) washing and digestion of DNA by DNase washing buffer; and (4) RNA elution..... 104

Figure 38 Schematics of the microfluidic setup for the pressure measurement. The pressure is monitored with a differential pressure sensor, its output signal is conditioned and acquired with a National Instruments data acquisition card (PCI-6289). The inlet was connected to 4 syringe pumps driving each 1 mL syringe (2 x fresh cells and 2 x artificial water) and 500 µL of each syringe (Artificial seawater then Fresh cells)was alternatively dispensed..... 106

Figure 39 Pressure measured across the filter for on-chip concentration of <i>Tetraselmis suecica</i> cells. 2 mL of artificial seawater media (Erd Schreiber media) and fresh cells were dispensed alternately in 500 μ L aliquots at 200 μ L/min and pressure recorded every second.	109
Figure 40 Comparison of extraction methods using bench-top and on-chip RNA extraction and purification techniques. These data were obtained from pure total RNA from 1,000 <i>K. brevis</i> cells previously extracted on-bench (n=2). The bar plot shows the percentage of total RNA recovery of the initial concentration, the error bars represent the standard deviation of the experiments.	110
Figure 41 Graphs showing the range of operation for the sample preparation device with the species <i>Karenia mikimotoi</i> and <i>K. brevis</i> . (a) Bioanalyzer 2100 total RNA fluorescence data from 1,000, 250, 100, 50, 30, and 10 <i>Karenia mikimotoi</i> cells extracted on-chip. With table summarizing total RNA yields obtained using the on-chip method. (b) Bioanalyzer 2100 total RNA fluorescence data from 120,000, 30,000, 25,000, 12,000, 1,000, 500 and 250 <i>K. brevis</i> cells extracted on-chip. With table summarizing total RNA yields obtained using the on-chip method.	111
Figure 42 NASBA amplification data. (a) Data for 5,000, 2,500, 500, 250,125 <i>K. brevis</i> cells with 10,000 <i>Tetraselmis suecica</i> cells extracted using the bench-top miniMAG® lysis-extraction system (each of the five lines show average measurements based on three replicates of the experiment, the error bars represent the standard deviation of the experiments). White triangles represent the negative control. (b) Data for 5,000, 2,500, 500, 250,125 <i>K. brevis</i> cells with 10,000 <i>Tetraselmis suecica</i> cells extracted using the sample preparation microdevice (each of the five lines show average measurements based on three replicates of the experiment, the error bars represent the standard deviation of the experiments). White triangles represent the negative control.	113
Figure 43 Bioanalyzer total RNA fluorescence data. (a) Open circles are data for 5,000, 2,500, 500, 250,125 <i>K. brevis</i> cells with 10,000 <i>Tetraselmis suecica</i> cells (n=3, n represents the number of replicated experiments) extracted using the bench-top miniMAG® lysis-extraction system. (b) Open squares are data for 5,000, 2,500, 500, 250,125 <i>K. brevis</i> cells with 10,000 <i>Tetraselmis suecica</i> cells (n=3, n represents the number of replicated experiments) extracted using the sample preparation microdevice. The error bars represent the standard deviation of the experiments.	114
Figure 44 Automated lab-on-a-chip system for sample preconcentration, nucleic acid extraction, amplification, and real-time fluorescent detection. (a) Sample preparation chip, (b) Sample preparation instrument (c) NASBA chip, (d) NASBA instrument. Taken from (Gulliksen and Hansen-Hagge 2012).	123
Figure 45 Illustration of the microchip with dimensions of all features shown.	126
Figure 46 (a) Schematic of optical geometry, where D1 and D2 are dichroic mirrors, N is notch filter, and BP670 is band pass filter at 670 nm. (b) Microchip as housed in thermoregulated chip holder shown with a 20x objective.	128
Figure 47 Adsorption of BSA labelled onto PMMA microchips. Microscope fluorescence pictures - Alexa 488 λ_{ex} = 495 nm, λ_{em} = 519 nm. (a) BSA treated PMMA chip after water rinse, b) native PMMA microchip after water rinse.	129
Figure 48 Adsorption of BSA labelled onto COC microchips. Microscope fluorescence pictures - Alexa 488 λ_{ex} = 495 nm, λ_{em} = 519 nm. (a) BSA treated COC chip after water rinse, b) native COC microchip after water rinse.	129
Figure 49 (a) <i>K. brevis</i> cells amplified on-chip results for 100 cells (crosses), 50 cells (triangles) and 10 cells (squares) and negative control (circles), the background (DC) fluorescence from the polymer has been subtracted. (b) The standard curve analysis of NASBA.	130
Figure 50 <i>K. brevis</i> cells amplified bench-top (a) and on-chip (b). Results for 400 cells (empty circles), 100 cells (full circles) and 10 cells (full triangles). For the on-chip data, the background (DC) fluorescence from the polymer has been subtracted. Taken from (Tsaloglou, Bahi et al. 2011).	130

Figure 51 (a) Data for 400 *K. brevis* cells equivalent amplified bench-top (open circles). Dashed line is the fitted fluorescence curve, solid black line is TOD based on negative controls and solid grey line is TOD based on the average of the first five points of measured fluorescence. (b) Relationship between nominal cell number and the observed logarithm of the $k_1\alpha_1\alpha_2^2$ as obtained by on-chip (full circles) and bench-top (red open circles) experiments. Taken from (Tsaloglou, Bahi et al. 2011). 131

Figure 52 Schematics of the real-time PCR system with integrated sample preparation and fluorescence detection. Taken from (Xu, Hsieh et al. 2010)..... 132

Figure 53 Illustration of a micromixer. “The three rectangles on the left represent a peristaltic micropump and A and B represent two spots which will eventually mix in the rotary micromixer”. Taken from (Tabeling 2009). 140

List of Tables

Table 1 Design criteria versus technical solutions.....	26
Table 2 Summary of nucleic acid amplification-based laboratory on-chip devices with “sample-in” to “answer-out” capability.....	53
Table 3 Typical diffusivities for various species in water at room temperature, adapted from (Squires and Quake 2005).	55
Table 5 Parameters used for the simulation of Clausius-Mossotti factor for <i>K. brevis</i> cells in low conductivity medium and seawater.....	69
Table 6 Parameters used for the simulation of Clausius-Mossotti factor using the multi-shell model for <i>K. brevis</i> cells in low conductivity medium.....	71
Table 7 Parameters used for the calculation of transmembrane potential on <i>K. brevis</i> cells.....	74
Table 8 Analysis of the cells lysis microchip.....	84
Table 10 Summary of microdevices for nucleic acid extraction.....	99
Table 11 Bioanalyzer total RNA fluorescence and NASBA amplification curve kinetic parameters from sample extracted on-chip and bench-top with standard deviation of triplicate samples.....	115
Table 12 Analysis of the sample preparation microdevice.....	117
Table 14 Summary of the NASBA microdevice-based system.....	133
Table 15 Summary of the general discussion.....	143

Nomenclature

This nomenclature is in alphabetical order and includes the page number where the abbreviations are first referenced.

VE	external electric field	67	EMW	Edward M. Waugh	28
AC	alternating current.....	68	ESP	Environmental Sample Processor.....	22
AH	Andy Harris	28	EtBr	ethidium bromide	89
AMG	Autonomous Microbial Genosensor	23	ϵ_0	vacuum permittivity	65
AMV-RT	avian myeloblastosis virus reverse transcriptase	33	FAM	Carboxyfluorescein	50
AOM	aluminium oxide membrane	95	f_{CM}	Clausius-Mossotti factor	67
AUV	autonomous underwater vehicle	21	$f_{CM\ cell}$	Clausius-Mossotti factor for the particle/medium system together	70
BC	Barbara Cortese	28	$f_{CM\ cytoplasm-membrane}$	Clausius-Mossotti factor for the particle itself	70
BHQ	Black Hole Quencher	125	FRET	Fluorescence resonance energy transfer	36
BSA	bovine serum albumin	51	GuSCN	guanidinium thiocyanate	89
CCD	charge-coupled device.....	29	HAB	harmful algal bloom	19
cDNA	complementary deoxyribonucleic acid	32	HPLC	high-performance liquid chromatography	22
COC	cyclic-olefin copolymer	45	HPV	human papillomavirus.....	27
COP	cyclic olefin polymer.....	45	IC	internal control	60
CsCl	caesium chloride.....	89	$Im(f_{CM})$	imaginary part of the Clausius-Mossotti factor	69
Cy5	cyanine 5	124	<i>K. Brevis</i>	Kariena brevis	20
DC	direct current	68	LED	light emitting diode	22
DEP	dielectrophoresis.....	27	MBARI	Monterey Bay Aquarium Research Institute	22
DNA	deoxyribonucleic acid.....	22	MIQE	Minimum Information for Publication of Quantitative Real-Time PCR Experiments	101
Dnase	Deoxyribonuclease	90	MMB	Mahadji Majid Bahi	28
DRIE	deep reactive ion etching	29	MNT	Maria-Nefeli Tsaloglou	28
dsDNA	double stranded DNA	33	mRNA	messenger RNA	27
ECL	electrochemiluminescent	37			

NASBA			
nucleic acid sequence-based amplification	20	RT-PCR	
OD ₂₆₀		reverse transcriptase polymerase chain reaction	20
absorbance unit	92	SERS	
-OH		Surface-enhanced Raman scattering	31
silica hydroxyl	90	SPE	
Oligo (dT)		solid phase extraction	41
oligodeoxythymidylic acid	45	SPR	
PCR		surface plasma resonance	31
polymerase chain reaction	22	ssDNA	
PDA		single-stranded DNA	93
personal digital assistant	124	TOD	
PDMS		threshold of detection	37
polydimethylsiloxane	28	TTP	
PEG		time to positivity	113
polyethylene glycol	50	α_1, α_2^2	
PI		the transcription rate	38
propidium iodide	76	α_3	
PID		the time point at which the amplification begins of the	
proportional-integrative-derivative	105	linear phase	38
PMMA		$\Delta\psi$	
poly-methyl methacrylate	28	transmembrane potential	73
PMT		ϵ	
photomultiplier tube	46	electrical permittivity	65
POC		$\epsilon_{(\lambda,ex)}$	
point-of-care	21	fluorophores molar extinction coefficient	36
poly-A		$\epsilon_{\text{cytoplasm-membrane}}$	
polyadenylation-A	92	equivalent complex permittivity for the particle	70
qPCR		ϵ_{medium}	
quantitative polymerase chain reaction	22	permittivity of the suspending medium	67
Q_y		$\epsilon_{\text{particle}}$	
fluorescent molecule quantum yield	36	complex permittivity of the particle	68
rbcL		θ	
ribulose-bisphosphate carboxylase	20	angle	73
$\text{Re}(f_{\text{CM}})$		λY_0	
real part of the Clausius-Mossotti factor	67	maximal fluorescence	38
RIN		μTAS	
RNA integrity number	93	micro total analysis systems	21
RNA		ρ_{ext}	
ribonucleic acid	20	external resistivity	73
RNase		ρ_{int}	
Ribonuclease	90	internal resistivity	73
RNase H		σ	
ribonuclease H	33	conductivity	68
ROX		$\Phi_{\text{F}(\lambda,em)}$	
Carboxy-X-rhodamine	50	fluorescence intensity	36
rRNA		$\phi_{o(\lambda,ex)}$	
ribosomal RNA	22	the excitation light source optical power	36
		ω	
		frequency	68

Chapter 1 Introduction

1.1. Research motivations and objectives

The ocean has an important role in climate variability and change (Sarmiento and Gruber 2006). Ocean observatory systems are central components in understanding how the ocean and life in it works. Life in the sea is dependent on the biogeochemical status of the ocean and is influenced by changes in its physical state and circulation. Nutrient concentrations are primary factors that drive natural biogeochemical cycles. Some nutrients play a controlling role in primary productivity and carbon sequestration in sea water. Over the past few years a range of sensors have been developed to detect nutrients such as ammonium (Sasaki, Ando et al. 1998; Masserini and Fanning 2000), nitrate (Sasaki, Ando et al. 1998), nitrite (Masserini and Fanning 2000), phosphate (Cleary, Slater et al. 2009), manganese (Okamura, Kimoto et al. 2001). Quantification of the different biological components present in an ecosystem is one of the first tasks of any ecological investigation. Recognizing, and enumerating different microorganisms such as protozoa, toxic and/or non toxic microalgae, bacteria, and viruses that thrive in natural waters is very important for local ecosystems (Marie, Brussaard et al. 1999).

Monitoring microorganisms in natural water is central to understanding and managing risks to human health and ecosystems (Burkholder, Noga et al. 1992; Giovannoni and Rappé 2000; Zehr, Hewson et al. 2008; DeLong 2009). Some phytoplankton can produce toxic blooms which are harmful to aquatic ecosystems and human health and can lead to major financial losses for fishery, tourism and healthcare industries, estimated at €584 million in the European Union for 2005 (Granéli and Turner 2006). Harmful algal blooms (HABs) are common in some areas (Giacobbe, Penna et al. 2007) and are increasing in frequency (Hallegraeff 1993) with climate change (Peperzak 2005). Enumeration of organisms such as viruses infecting algae and bacteria can also be beneficial in understanding the marine environment (Marie, Brussaard et al. 1999). For example, *Prochlorococcus* is the smallest and most abundant photosynthetic primary producer microbe in the ocean and occupies a key position at the base of the marine food web. Moreover, *Synechococcus* are a type of cyanobacteria which can cause destructive blooms and produce neurotoxins (Suzuki, Taylor et al. 2000). Another important type of phytoplankton, *Coccolithophores* are single-celled marine plants that live in large numbers throughout the upper layers of the ocean and could be an important indicator on climate change (Iglesias-Rodriguez, Halloran et al. 2008). Consequently, *in situ* or on-site monitoring and enumeration of phytoplankton could offer important insight into ecosystem and biogeochemical processes and function. The increasing number of potentially harmful species in natural seawater calls for fast, sensitive, and cost-effective portable detection systems. Monitoring HABs is a necessity for threat detection as well as for the characterisation of ecosystem and biogeochemical processes. Real-time measurements of population fluctuations of HAB-forming species would assist in the understanding of species development and could be used as a tool to identify temporal and spatial variability in organism growth (Anderson, Cembella et al. 2011; Erickson, Hashemi et al. 2011).

Kariena brevis (*K. brevis*) is responsible for HABs and produces brevetoxin which can lead to gastrointestinal and neurological problems in mammals (Doucette, Logan et al. 1997; Watkins, Reich et al. 2008; Grimes 2009; Plakas and Dickey 2010). Early detection of HABs can help to reduce toxicity of contaminated areas (Khan, Benabderrazik et al. 2010). We decided to detect the large subunit of the ribulose-bisphosphate carboxylase (*rbcL*) gene of *K. brevis* as an exemplary target application for HABs monitoring.

Nucleic acid analysis techniques have been widely used for clinical diagnostics (Ferrari, Cremonesi et al. 1996; Buckingham 2012) and environmental monitoring (Burton 1996), and have demonstrated a significant number of applications for the measurement of toxic phytoplankton species to potentially observe bloom formation (Casper, Paul et al. 2004). Ribonucleic acid (RNA) is one of the key regulatory molecules in eukaryotic cells, bacteria and viruses (Romano, Shurtliff et al. 1995), and can be an indicator for environmental pollution and toxicity (Cook 2003; Palchetti and Mascini 2008). It is often the case that only a few RNA copies are present in environmental samples, which also contain a mixture of other bio-molecules, debris and particles. This makes RNA detection extremely difficult by direct analysis. Nucleic acid amplification is often necessary to increase the number of RNA copies to a detectable level. Two commonly used RNA amplification techniques are reverse transcriptase polymerase chain reaction (RT-PCR) (Bustin 2000; Burchill, Perebolte et al. 2002) and nucleic acid sequence-based amplification (NASBA) (Compton 1991). These types of assays are used in a variety of fields including healthcare (Ferrari, Cremonesi et al. 1996), homeland security (Lim, Simpson et al. 2005), food (Cook 2003) and environmental monitoring (Burton 1996; Gilbride, Lee et al. 2006). However, currently biological samples have to be processed at a central laboratory due to the requirements of specialised equipment and reagents, as well as trained personnel for operation (Puren, Gerlach et al. 2010). This can be expensive and time-consuming, as summarised in Figure 1.

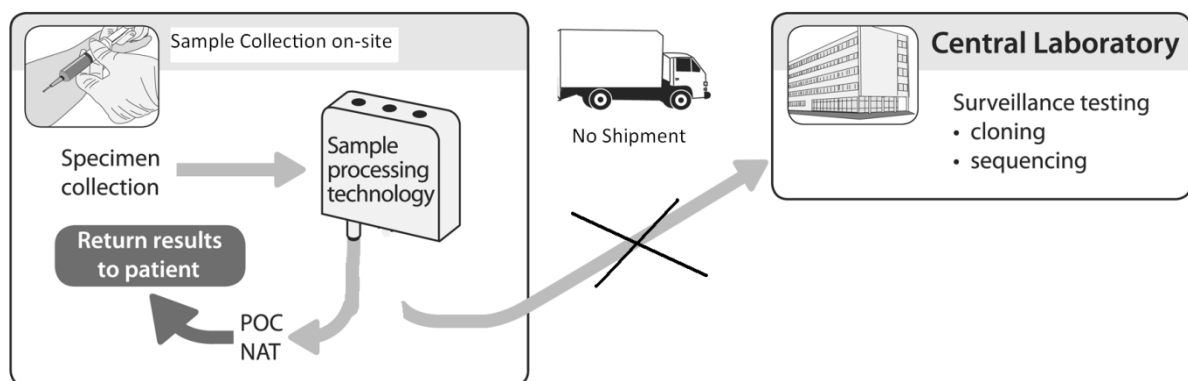


Figure 1 Principle of on-site and point-of-care diagnostics, diagram adapted from Puren et al. (Puren, Gerlach et al. 2010).

Traditional methods for HAB monitoring require sample collection and preservation for later study in the laboratory (Galluzzi, Penna et al. 2004; Anderson 2009). Alternative laboratory equipment has

been adapted for ship-board use. For example, instruments which utilise optical characters specific to the target organism have been developed and mounted on-board research vessels (Kirkpatrick, Orrico et al. 2003). Red Tide is a common name for a phenomenon where blooms of certain algal species (i.e. *K. brevis*), which contain red-brown pigments (i.e. the pigment *fucoxanthin*), cause the water to appear to be colored red ¹. This approach thus has great potential for monitoring those HABs species which have this specific pigment (in contrast to Chlorophyll-a that is the most common pigment found in phytoplankton), but for the vast majority of other species alternative approaches to cell detection are needed. Moreover in some cases this method is slow and does not provide the temporal and spatial resolution (i.e. particular location and depth (Gentien, Lunven et al. 1995)) essential for a true understanding of HAB evolution (Rantajaervi, Olsonen et al. 1998; Vila, Camp et al. 2001; Anderson, Cembella et al. 2011; Erickson, Hashemi et al. 2011). This can only be addressed using submersible sensors small enough to be integrated into autonomous underwater vehicles (AUV) and Argo float station networks (Anderson, Cembella et al. 2011; Erickson, Hashemi et al. 2011).

The use of fully automatic and accurate micro total analysis systems (μ TAS), also known as lab-on-a-chip (Manz, Graber et al. 1990) can overcome the challenges of point-of-care (POC) diagnostics, and enable *in situ* and on-site environmental monitoring (Prien 2007; Yager, Domingo et al. 2008; Erickson, Hashemi et al. 2011). This technology has the potential to replace bulky and expensive traditional laboratory equipment with cheap, smaller and faster micro-systems. Their size is typically millimetres to a few centimetres (Adams, Enzelberger et al. 2003). Lab-on-a-chip devices offer possible advantages such as portability, low consumption of valuable reagents and samples, rapid analysis times, cost effectiveness (for sample usage), and the possibility of developing disposable consumables and thus reducing contamination. The lab-on-a-chip concept is based on the integration of multiple laboratory functions onto a chip format. The overall objective is to achieve fully automated chips with “sample-in” to “answer-out” capability and to produce inexpensive disposable microdevices with low production costs. In an environmental context the aim may also be to produce numerous devices with small resource consumption that can be used for long periods of time. In the past few years, the field of lab-on-a-chip devices with “sample-in” to “answer-out” capability has shown a promising impact for environmental (Palchetti and Mascini 2008; Sieben, Floquet et al. 2010; Am, Zhiwei et al. 2011; Beaton, Sieben et al. 2011) and clinical (Baier, Hansen-Hagge et al. 2009; Lien, Chuang et al. 2010; Gulliksen and Hansen-Hagge 2012) applications. Lab-on-a-chip technology appears well suited to environmental monitoring with its main advantages being the possibility of miniaturisation, portability, reduced reagent consumption and automation. The availability of a rapid microfluidic test for phytoplankton monitoring would greatly accelerate the detection of toxic species and improve sensitivity and general monitoring performance. The lab-on-a-chip field has seen important progress with applications in enzymatic analysis (Wang 2002), polymerase chain reaction

¹ http://www.sccoos.org/data/habs/about_habs.php

(PCR)-based nucleic acids analysis, proteomic analysis (Lee 2001) and immunoassays analysis (Lee, Lee et al. 2009; Wu, Hsu et al. 2010).

Section 1.3 (page 39) gives a general introduction to lab-on-a-chip devices for microorganism detection, discusses different nucleic acid amplification based lab-on-a-chip devices with “sample-in” to “answer-out” capability, and evaluates their potential suitability for seawater monitoring.

Outside of the lab-on-a-chip chip field, two instruments have been developed based on molecular biology analysis for environmental *in situ* applications, including sample preparation functions. The Environmental Sample Processor (ESP) developed by the Monterey Bay Aquarium Research Institute (MBARI) is an electromechanical / fluidic system designed to collect water samples, concentrate microorganisms, and automate molecular biology analysis (Greenfield, Marin et al. 2006). The original ESP utilizes deoxyribonucleic acid (DNA) probes and protein arrays to detect target molecules, and can also archive sample for future laboratory analyses. MBARI recently demonstrated the first *in situ* macro system for quantitative polymerase chain reaction (qPCR) analysis, deployed on a coastal mooring (Preston, Harris et al. 2011; Robidart, Preston et al. 2011). The system combined the originally designed ESP with a fluidic handling system based on sequential injection analysis (see Figure 2). This system was deployed in the ocean for one month. The ESP could collect 1 litre of sample onto a filter for subsequent thermal-chemical lysis (i.e. 85 °C for 8 minutes in a 3 M guanidine thiocyanate lysis buffer). Following the lysis step the lysate was loaded onto a high-performance liquid chromatography (HPLC) column for solid phase extraction (see an introduction to solid phase extraction techniques in section 3.2.1, page 89). Nucleic acids were eluted with 60 µL of water. Then the pure nucleic acids were transferred to the PCR module with light emitting diode (LED) fluorescence induced multiplex detection channels. Full nucleic acid analysis was completed in 2 hours. During deployment (1 month) the system collected and processed 22 samples. However the system was only performing semi quantitative analysis, and the HPLC column efficiency decreased with repeated use. PCR reagents were stored in coiled tubing at the ambient temperature and showed stability for up to 5 months. The system is commercially available through Spyglass Biosecurity in partnership with McLane Research Laboratories. Although it is a great demonstration of autonomous *in situ* ribosomal RNA (rRNA) detection, the macro system is only suitable for mooring or buoy deployment and did not demonstrate realistic long term deployment (ideally 1 year) potential. Ideal *in situ* sensors should provide sample analysis at each particular location and depth and only a microsystem incorporated in AUVs could meet this spatial mapping requirement.

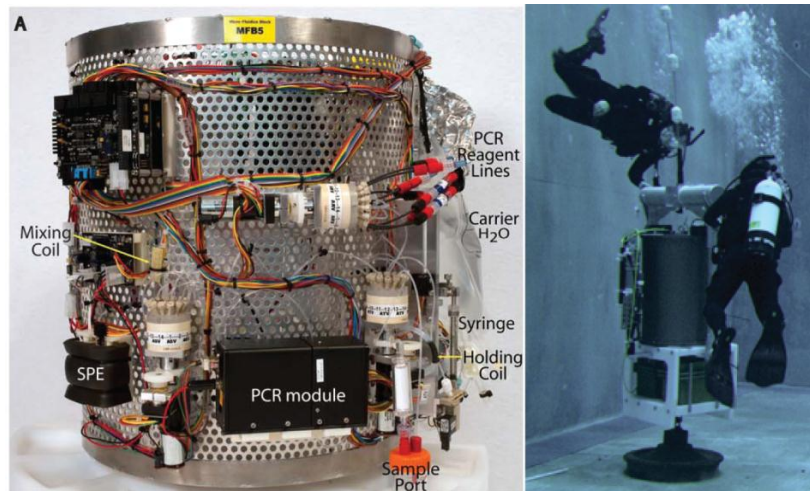


Figure 2 A photo of a standalone fluidic handling system and on the right a photo of the ESP. Taken from (Preston, Harris et al. 2011).

Another instrument is under development at the University of South Florida: the Autonomous Microbial Genosensor (AMG) (Casper, Patterson et al. 2007; Fries, Paul et al. 2007). This system is designed for *in situ* detection of *K. brevis* using NASBA and has achieved a 3-day-long subsurface deployment. The AMG collects samples, filters cells and extracts nucleic acid using cartridges contained in a rotating carousel. However no detailed description has been given in terms of performance. The ESP and AMG are the only fully autonomous instruments reported for “medium term” (< 3 months) *in situ* nucleic acid analysis, they are macro scale devices and to our knowledge do not use lab-on-a-chip technology. However the ESP and AMG systems are great demonstrations of the maturity of nucleic acid systems for *in situ* seawater applications. It must be noted that the ESP has been under development for 13 years (the first ESP generation was initiated by MBARI in 1999). The development of this system is a result of a team work of 16 people and collaborations with 6 different institutions and laboratories.

1.1.1. Main criteria and solutions for nucleic acid *in situ* sensors

A discussion of the main criteria for nucleic acid *in situ* sensors set by scientific objectives follows below.

1.1.1.a Low cell number detection

Nucleic-acid-based technology has the potential to detect target organisms at low concentrations (e.g. 1 cell (Delaney, Ulrich et al. 2011), 20 copies (Mas, Soriano et al. 1998)). However, very few nucleic acid based sensors have been developed for seawater environmental monitoring (Greenfield, Marin et al. 2006; Casper, Patterson et al. 2007; Fries, Paul et al. 2007; Preston, Harris et al. 2011) (see above). To prevent possible environmental damage and risks to human health caused by HABs, such as *K. brevis*, portable and integrated systems combining molecular biology and high performance detection could be used. This could enable prompt response (e.g. shutting of beaches or fisheries) or control and

limitation of the spread of the bloom (e.g. exposure to toxins produce by *K. brevis* could be reduced using titanium dioxide photocatalysis) (Khan, Benabderrazik et al. 2010). The lower the limit of detection of the target species the more likely that bloom-related problems could be mitigated or prevented. Concentrations of toxic phytoplankton species that can cause damage to marine life can be as low as 1,000 cells per litre (1 cell/mL) (Blasco, Levasseur et al. 2003; Chang 2011). For oceanographic research applications low phytoplankton concentration detection is required in order to understand the influence of slight environmental condition changes.

1.1.1.b Viable cells detection

For an estimation of the impact of target organisms, a degree of discrimination between live and dead (or inactive) cells would be beneficial. Since DNA can persist for long periods in dead cells, attention has turned to the analysis of shorter lived RNA as a marker for viability, as it is only present in active or recently moribund cells (Birch, Dawson et al. 2001). NASBA technology was chosen as the amplification method used in this thesis because it has already been shown that RNA amplification with NASBA is particularly suitable for early detection and quantification of harmful microalga *K. brevis* on a macro scale system (Casper, Patterson et al. 2007). NASBA is an isothermal process of nucleic acid amplification which occurs at 41 °C, making it ideal for lab-on-a-chip applications due to its simple temperature control requirement. The advantage of it being isothermal is that there is no need for thermocycling at high temperatures, which is necessary in the case of a RT-PCR approach.

1.1.1.c Transportable system and assay cost

Monitoring for biochemical molecules in seawater requires reliable *in situ* sensors that can withstand long-term deployment and accuracy and make measurements at high temporal and spatial resolutions (Prien 2007; Erickson, Hashemi et al. 2011). The ultimate goal for seawater monitoring systems is to make them submersible and remotely operable *in situ*. Integrated into an Argo float as a part of a network, *in situ* sensors should accomplish a measurement every metre to achieve an accurate measurement of phytoplankton population fluctuations. In some extreme cases phytoplankton are only present in a 10 cm layer (see Figure 3) which therefore calls for a minimum sampling rate of 1 sample/5 cm (Anderson, Cembella et al. 2011).

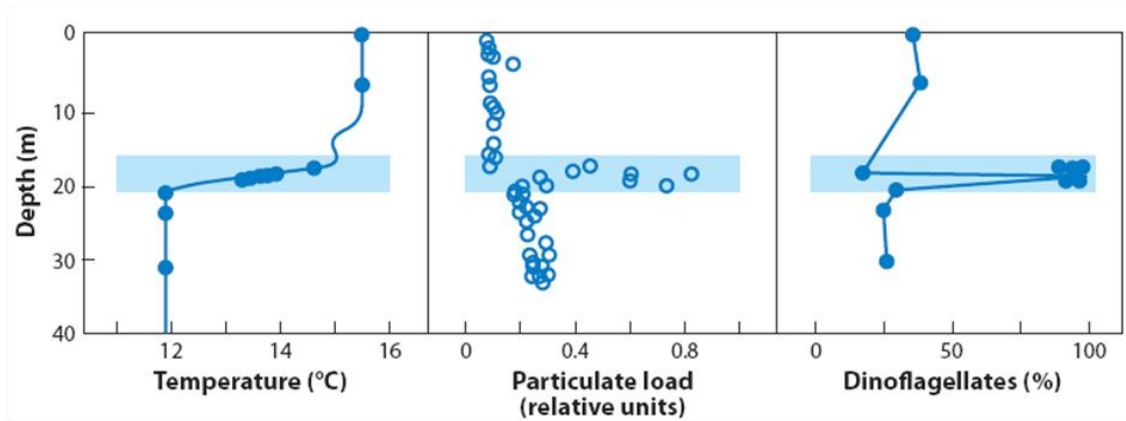


Figure 3 “The blue shaded areas denote the thin layer occupied by *Dinophysis* cells.” Taken from (Anderson, Cembella et al. 2011).

Typical deployment requirements are on the order of one year and critical factors are robustness, reagent consumption, power requirements and waste storage. The lab-on-a-chip technology, which allows handling of micro-litre volumes, can decrease reagent/sample consumption and allows compact integration resulting in small and portable sensors. A first realistic goal will be to develop a transportable microfluidic based system for hand-held operation in the field or for operation at coastal stations.

1.1.1.d Ease of use

For seawater applications, sensors might be deployed on buoys, coastal station or on remotely-operated vehicles. To be deployed using these structures sensors have to be fully automated and autonomous. For single on-site measurements such as coastal testing, full automation is not required, as an operator or user can support the system operation. This is particularly true for sample handling (i.e. sample collection) and fluid manipulation (i.e. manual pump for fluid actuation).

Summary of requirements

The system requirements and engineering solutions to address these are summarized in the Table 1 below:

Summary of the main criteria and solutions	
Detection of viable targets	Early detection and fast response
<ul style="list-style-type: none">Molecular biology analysis for nucleic acid detection (specifically RNA) is only produced by viable cells.	<ul style="list-style-type: none">NASBA amplifies RNA which is detected using molecular beacons technology resulting in low limits of detection and rapid analysis.
On-site detection system	Ease of use
<ul style="list-style-type: none">Functions integration using the lab-on-a-chip technology.	<ul style="list-style-type: none">Electronics automation and smart microfluidic design.

Table 1 Design criteria versus technical solutions.

Additional requirements for the *in situ* device also include stability and reproducibility of measurements, chip material chemical compatibility with samples and reagents, insensitivity to particulate contamination, and ability to be re-used for cost reduction (i.e. mechanics and electronics parts). In the section 1.4 (page 54) development challenges for a fully integrated device are discussed.

1.1.2. Scope and outline of this thesis

The development of integrated systems for nucleic acid analysis is driven by the requirement for fast and simple diagnostic systems. The purpose of this work has been to develop key functions in independent microchips that perform elements of a complete biological assay for measurement of phytoplankton RNA, from the sample preparation step to the detection step. The aim was to demonstrate proof-of concept for each device separately. This removes the complications of system integration (which remain a challenge) whilst enabling innovation and optimisation of devices for each process. The sample preparation system presented here (see Chapter 3) can receive and treat fresh samples to obtain a pure solution of nucleic acids, which in turn, can be transferred to the amplification chip (see Chapter 4). Specifically the system is being developed to analyse the *rbcL* gene of phytoplankton *K. brevis* a species responsible for HABs. The long term goal of this work is to integrate these separate chips into an integrated single chip design. We chose *K. brevis* as the model for harmful marine microalgae, because this species causes dense blooms which indiscriminately kill fish and invertebrates (Granéli and Turner 2006; Khan, Benabderrazik et al. 2010; Plakas and Dickey 2010). They also synthesise brevetoxin (Lin, Risk et al. 1981), which causes neurotoxic shellfish poisoning in humans (Watkins, Reich et al. 2008; Khan, Benabderrazik et al. 2010), and are rare and very difficult to culture even for experienced marine cytologists. Finally some phytoplankton can enter a robust dormant state which can make the cell lysis process very challenging in comparison to

mammalian cells. For example *K. brevis* can form robust cysts (Van Dolah, Lidie et al. 2009; Anderson, Cembella et al. 2011).

1.1.3. Statement of novelty

The long term objective is to develop the unique microfluidic based sensors with “sample-in” to “answer-out” capability for environmental phytoplankton analysis (see section 1.3, page 39). As discussed in the *Research motivations and objectives* section, two instruments have been previously developed based on molecular biology analysis for environmental *in situ* applications: the ESP (Greenfield, Marin et al. 2006) and the AMG (Casper, Patterson et al. 2007; Fries, Paul et al. 2007). Both are macro scale systems that do not use the lab-on-a-chip technology. The Institut für Mikrotechnik Mainz in collaboration with the University of Oslo developed a lab-on-a-chip based system for detection of human papillomavirus (HPV) E6/E7 messenger RNA (mRNA) using NASBA (Gulliksen and Hansen-Hagge 2012). This resulted in the final development of two stand alone bench top automated platforms using microchips, one for sample preparation and one for amplification and detection (see section 1.3.2.b, page 50).

Chapter 2 Cell lysis microchip

We have demonstrated, we believe for the first time, electrical field-based cell concentration and lysis on-chip for subsequent RNA analysis. The method we have developed and optimized could be incorporated within a complete microfluidic RNA extraction and amplification system.

Cell electroporation was first presented in the 1960s (Coster 1965). It has been thoroughly applied and developed using mammalian and bacterial cells. Sedgwick et al. described a device for the isolation and electroporation of single human cells (Sedgwick, Caron et al. 2008). Human cells are generally weaker than plant cells, moreover only a qualitative assessment of the lysis efficiency was demonstrated. Lysis or electroporation of algal cells (and in particular cysts) is much more difficult, and to our knowledge has not been reported in the literature. Furthermore, the effect of the electric field (and the entire process) on cellular RNA has not previously been studied. The novelty is also in the application to environmental and marine science.

An array of interdigitated electrodes was used to both concentrate cells by positive dielectrophoresis (DEP) and subsequently perform electric field-mediated cell lysis. The system efficiency was characterised using microscopy techniques and the on-bench NASBA amplification method.

Chapter 3 RNA sample preparation microdevice

We developed a new microchip for environmental sample preparation that enables rapid concentration of cells from large volumes (~ mL range) onto an on-chip filter where they are chemically lysed, the RNA extracted, purified and eluted. The novelty stems from the use of an on-chip filter which is also

used for solid phase extraction and purification of RNA. This is also the first demonstration of a filter used in a microdevice for both concentration and solid phase extraction for the environmental application and study of phytoplankton in particular (Scholin 2010).

The use of an on-chip filter has been subsequently published. Kim, Mauk et al (2010) used an aluminium oxide membrane for DNA and RNA extraction and amplification (Kim, Mauk et al. 2010). Their system did not include the lysis and concentration steps on-chip, therefore no assessment of the device's performance in realistic conditions (i.e. complex sample matrix - mixed population) was demonstrated. Our device has been demonstrated and tested with mixed cell populations. The sample is collected and concentrated on a nanoporous aluminium oxide filter where it is subsequently chemically lysed and left for incubation. The total RNA is captured onto the aluminium oxide filter in the presence of a chaotropic salt solution and extracted by solid phase extraction using commercial guanidine thiocyanate chaotropic lysis and washing buffers (Nuclisens miniMAG© kit, bioMérieux, Netherlands) based on the Boom method (Boom, Sol et al. 1990).

Chapter 4 RNA amplification on-chip

We have 1) developed the first poly-methyl methacrylate (PMMA) based chip for real-time NASBA and 2) applied on-chip NASBA to detection and amplification of phytoplankton RNA; both for the first time. Casper et al. developed a portable macro scale NASBA incubator system for phytoplankton RNA detection, not based on the lab-on-a-chip technology (Casper, Patterson et al. 2007). Dimov et al demonstrated an on-chip NASBA system (made from polydimethylsiloxane (PDMS)) incorporating both the RNA elution step and annealing step for *Escherichia coli*, but sample collection and lysis were performed off-chip (Dimov, Garcia-Cordero et al. 2008).

1.1.4. Contribution of the author and co-workers

Due to the multidisciplinary field of lab-on-a-chip, cooperation has been essential. All co-workers have been indispensable towards obtaining the outlined goal in this thesis

- Matt Mowlem and Hywel Morgan secured funding,
- Matt Mowlem, Hywel Morgan and Maria-Nefeli Tsaloglou supervised all work,
- Experimental contributors: Mahadji Majid Bahi (MMB), Maria-Nefeli Tsaloglou (MNT), Barbara Cortese (BC), Edward M. Waugh (EMW) and Andy Harris (AH).

MNT modified and optimised the NASBA assay for *K. brevis* and *Tetraselmis suecica* species, and assisted in maintaining *K. brevis* cultures. MMB adapted the *K. brevis* NASBA assay to enable detection of *Dunaliella primolecta*. All data presented in this thesis has been collected in experiments performed by MMB.

For the Cell lysis microdevice, MMB performed the experiments on-chip, and the MATLAB™ simulation. MMB designed fluorescence experiments, acquired fluorescence microscopy images and analysed the data.

For the RNA sample preparation microdevice, MMB developed the automation for the extraction microdevice, wrote the LabVIEW™ program, designed the chip layout, the assembly technique and mechanical packaging. BC fabricated the chips. AH developed and assembled the thermoregulation system. MMB designed and performed the on-chip and on-bench extraction experiments, the pressure testing experiment, Bioanalyzer 2100 measurements and on bench NASBA assays. MMB modified the initial MATLAB™ program developed by EMW for NASBA curve fitting. MMB analysed all data presented.

For the RNA amplification on-chip microdevice, MMB developed the optical setup for fluorescence measurement on-chip. MMB designed and assembled microchips and all optical, thermal, electronics and mechanical components MMB developed the automation for the NASBA on-chip system and wrote the LabVIEW™ program. BC fabricated the chips. AH developed and assembled the thermoregulation system. MMB performed and designed the on-chip adsorption experiment, and initial NASBA experiments. MMB and MNT carried out the final on-chip NASBA assays.

All journal papers produced as part of this thesis include a detailed contribution of authors section.

1.1.5. Additional activities during my PhD

The work presented in this thesis was mainly carried out at the National Oceanography Centre of Southampton and at the University of Southampton in the period from October 2008 to October 2011. During this time period, I have also contributed to and assisted with other projects within the Matt Mowlem group that are not presented in this thesis:

- the ammonium project with the study of the fluorescence properties of the chemical reaction ammonium – orthophthaldialdehyde,
- The study of feasibility of an integrated detection system using a charge-coupled device (CCD) sensors, but this idea has not been enforced due to financial and time constraint,
- Training and test of clean-room based fabrication process (i.e. deep reactive ion etching (DRIE)),
- Testing of custom lysis buffers for the phytoplankton *Dunalliella primolecta*
- Testing of commercial buffers' functions (Nuclisens, Biomérieux),
- The LABONFOIL European project with the contribution in characterising a CCD based detection system for NASBA application and in assisting European collaborators during their visits in our laboratories.

Matt Mowlem also kindly supported me to participate to the national entrepreneurial Environment YES competition (finished 3rd, participated with Victoire Rerolle, David Owsianka and Alex Beaton)², the 2011 KPMG International Case Competition and the Southampton Ernst & Young Business Simulation Competition (finished 1st). These experiences helped me to raise my commercial awareness and inspired me during my PhD in seeking attitudes and behaviour, such as creativity, risk taking and a can-do attitude.

² <http://www.soton.ac.uk/ris/news/studentenvironmentalenterprise.shtml>

1.2. Nucleic acid analysis overview

The identification of DNA sequences and RNA sequences may help in the monitoring of microorganisms such as protozoa, toxic and/or non toxic microalgae, bacteria, and viruses that thrive in natural waters (Gilbride, Lee et al. 2006). In medical diagnostic applications nucleic acid analysis helps in the detection of genetic diseases and other health conditions, such as precancerous states, bacterial and, viral infections (Myers and Lee 2008; Lui, Cady et al. 2009; Torres-Chavolla and Alocilja 2009). Nucleic acid analysis requires the following:

- Sample collection and concentration, especially from dilute environmental samples.
- Sample preparation: separation and purification of nucleic acid from other constituent molecules and contaminants.
- Analytic assay, hybridisation for large nucleic acid concentrations or nucleic acid amplification for low concentrations.
- Nucleic acid detection and quantification, ideally real-time, and interpretation of the result(s) (Lui, Cady et al. 2009).

Implementation of the above functionalities is the objective for a “sample-in” to “answer-out” device. One approach is to complete all the steps in a lab-on-a-chip platform. A schematic overview of nucleic acid analysis and its application to lab-on-a-chip platforms is shown in Figure 4.

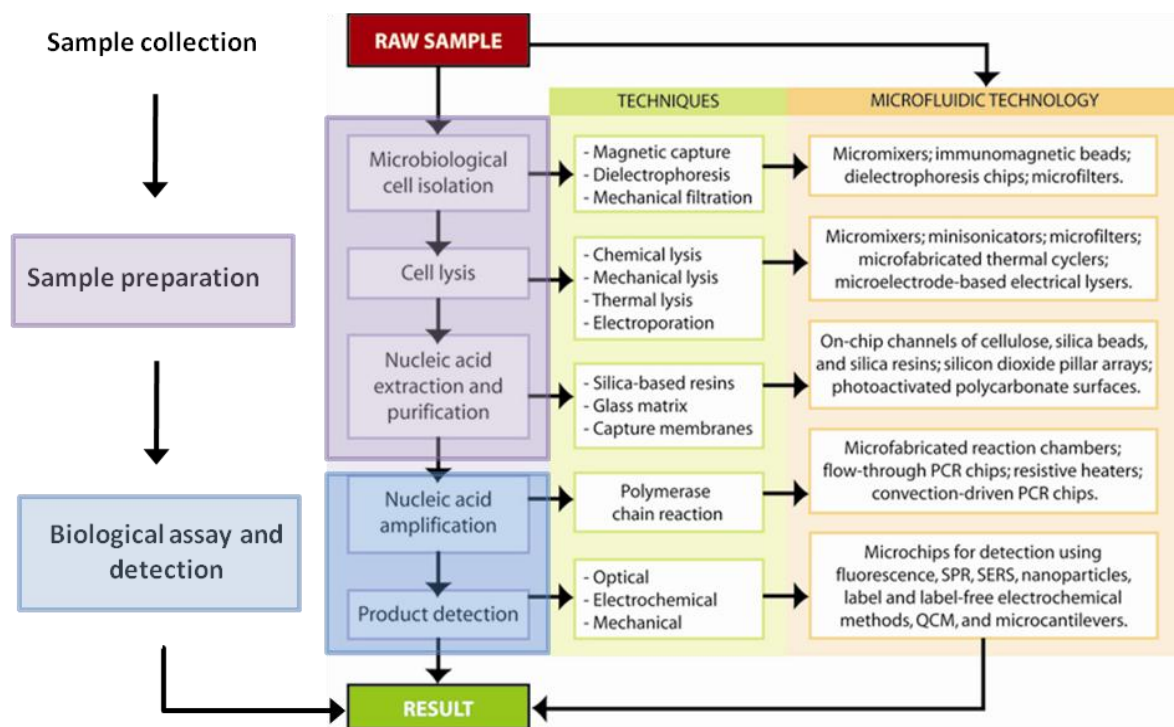


Figure 4 Overview of nucleic acid analysis, techniques and microfluidic technology, adapted from Lui et al. Surface-enhanced Raman scattering (SERS) and surface plasma resonance (SPR) are optical detection methods (Lui, Cady et al. 2009).

In the following chapters, two sample preparation devices and one amplification system are presented using the different techniques and technologies shown in the Figure 4:

- Chapter 2 Describes a *Cell lysis microdevice*, with cell isolation using dielectrophoresis and electrical cell lysis using a microelectrode base microchip.
- Chapter 3 Describes a *RNA sample preparation microdevice*, with cell isolation using a mechanical (nanoporous aluminium oxide) filter, chemical lysis, and nucleic acid extraction and purification using the same filter as used for mechanical filtering.
- Finally, Chapter 4 Describes *RNA amplification on-chip* with nucleic acid amplification using the NASBA technique and a thermo-regulated microchip. Detection is achieved using a laser induced fluorescence detection system.

The section below briefly introduces the transcription-based amplification technology. Following this, Section 1.3 (page 39) discusses different nucleic acid amplification-based lab-on-a-chip devices with “sample-in” to “answer-out” capability which have been developed in other research groups, and their potential suitability for phytoplankton monitoring applications.

1.2.1. Introduction to PCR and NASBA

Highly conserved target nucleic acid sequences isolated from the few cells typically present in environmental samples are very difficult to detect straight after sample preparation (i.e. the typical amount of total RNA in a cell is 30 pg (Alberts, Bray et al. 1986)). Amplification based nucleic acid assays make detection at low concentrations possible by amplifying a detectable product prior to quantification. PCR is the most used nucleic acid amplification technique and was first described by Mullis and Saiki in 1985 (Saiki, Scharf et al. 1985). Knowledge of the DNA segment to be amplified is used to design two synthetic DNA oligonucleotides which are known as primers. One primer is complementary to the sequence on one strand of the DNA double helix, and one is complementary to the sequence on the other strand, but at the opposite end of the region to be amplified. These primers serve for selective in vitro DNA synthesis which is performed by a DNA polymerase. In brief, short oligonucleotide primers are annealed to denatured DNA using hybridization conditions ensuring that only primers with desired sequences will anneal. Two primers are complementary to the two 3' ends of DNA segment to be amplified (polarity in a nucleic acid chain is indicated by referring to one end as 3' end and the other as the 5' end, see NASBA paragraph on the next page). Primers are extended using a DNA polymerase and the 4-deoxynucleotide triphosphates. A 3-step cycle is used that includes melting of DNA, annealing of primers and elongation of primers. This cycle is repeated more than 20 times to create a sufficient amount of the desired DNA³ (see Figure 5a). RT-PCR is a variant of PCR which enables measurement of an RNA target. It uses the reverse transcriptase enzyme to transcribe RNA into its DNA complement. This complementary DNA (cDNA) is synthesized with DNA

³ <http://users.ugent.be/~avierstr/principles/pcr.html>

polymerase. Using PCR the cDNA is then amplified; the number of molecules doubles with each step, and therefore it requires approximately 20 cycles to produce one million-fold amplification. The main product of this reaction is double stranded DNA (dsDNA). Both PCR and RT-PCR suffer from the inconvenience of DNA interference during amplification (i.e. mismatched hybridization between primers and non targeted nucleic acids material), and can be less selective than other amplification methods (Burchill, Perebolte et al. 2002). A thermo-cycler is also required to produce the temperature cycles to induce denaturation (~94-98 °C), annealing (~50-65 °C) and elongation (~70-80 °C). The need for temperature cycling in PCR has made it challenging to build low-cost and simple devices suitable for on-site testing. An exciting development that removes the need for thermocycling is isothermal nucleic acid amplification (see section 1.1.1.b, page 24).

NASBA is an alternative to PCR which has been developed for RNA sequence amplification through the simultaneous use of the activities of the three enzymes; avian myeloblastosis virus reverse transcriptase (AMV-RT), *Escherichia coli* ribonuclease H (RNase H) and phage T7 RNA polymerase (RNA polymerase from the T7 bacteriophage that catalyzes the formation of RNA in the 5'→ 3' direction (Tabor and Richardson 1992)). This technique was developed by J. Compton in 1991 (Compton 1991). The function of each enzyme and the sequence of the process are discussed in the following paragraph. Although RNA can also be amplified by RT-PCR, NASBA has the advantage that it is an isothermal method. Single-stranded RNA amplicons are produced by NASBA which can be used directly in succeeding rounds of amplification or probed for direct detection without the need for denaturation or strand separation. Moreover with NASBA, 10-100 copies of RNA are generated in each transcription step, so fewer amplification steps are necessary to achieve similar amplification to PCR (Compton 1991). Consequently, both the total incubation time and the overall error frequencies are reduced with NASBA (Keightley, Sillekens et al. 2005; Schneider, Wolters et al. 2005). Errors that are inherent in some enzymatic reactions (for example, reverse transcriptase) are cumulative, and therefore fewer cycles should reduce such errors. NASBA has been shown to be a highly reproducible assay in a very controlled environment. Chantratita et al. presented results showing a coefficient of variation of the assay of lower than 10 (Chantratita, Pongtanapisit et al. 2004). Moore et al. reported that the NASBA method is 10 to 100 fold more sensitive than RT-PCR under the same experimental conditions (Moore, Clark et al. 2004; Houde, Leblanc et al. 2006).

The NASBA reaction principle is as follows: the core of the amplification process consists of a cyclic process of primer annealing, formation of a double-stranded DNA with a T7-promoter, and the transcription of multiple antisense copies of the target sequences (amplicons) with the help of the T7-RNA-polymerase (Böhmer, Schildgen et al. 2009). The T7-promoter is a specific DNA sequence that directs T7-RNA polymerase to bind to DNA and to begin synthesizing an RNA molecule (amplicons). Sense (or positive (+) sense) and antisense (or negative (-) sense) are concepts used to compare the polarity of nucleic acid molecules. The way in which the nucleotide subunits are linked together gives

each nucleic acid strand a chemical polarity. This polarity in a nucleic acid chain is indicated by referring to one end as 3' end and the other as the 5' end. A sense strand is the segment of double stranded nucleic acid running from 5' to 3' that is complementary to the antisense strand 3' to 5'. "The direction of RNA polymerase movement determines which of the two DNA strands is to serve as a template for the synthesis of RNA. Polymerase direction is determined by the orientation of the promoter sequence, the site at which the RNA polymerase begins transcription" (Alberts, Bray et al. 1986). In the NASBA assay the T7-promoter indicates a sense (DNA(+)) direction, therefore the T7-RNA polymerase binds to the dsDNA and makes RNA using the sense DNA strand as a template.

The NASBA process (see Figure 5b) is initiated with denaturation of the targeted RNA (+) and the annealing of the Primer A (which contains the antisense T7 promoter sequence and is complementary to the RNA (+)) to the target at 65 °C over a short incubation. AMV RT extends the Primer A, producing cDNA (complementary DNA) as the transcribed product (see Figure 5b) and results in the formation of a cDNA-RNA (+) heteroduplex which is a double-stranded single nucleic acid molecule. The RNA (+) of the heteroduplex is then degraded by RNaseH and this enables the second primer B (complementary to RNA (-)) to anneal to the remaining single stranded cDNA. The primer B is then elongated by the AMV-RT, resulting in a double-stranded DNA intermediate containing the T7-RNA-polymerase-promoter (sense) sequence. The sense polymerase promoter will then be used by the T7-RNA-polymerase to initiate production of many new RNA molecules that are complementary to the target RNA. Following this non cyclic phase, NASBA now enters the amplification (cyclic) phase. The antisense RNA (RNA (-)) produced during the non cyclic phase is then amplified in the cyclic phase of the reaction (see Figure 5). At this step, the amplification process starts with primer B and the RNA (-) produced during the non cyclic phase (see Figure 5). AMV RT extends the Primer B producing DNA (+)-RNA (-) heteroduplex. The heteroduplex is then degraded by RNaseH and this enables the second primer A to anneal to the remaining single stranded DNA (+). The sense polymerase promoter will then be used by the T7-RNA-polymerase to initiate production of new RNA (-) molecules. The amplification can be monitored in real-time via molecular beacons which are complementary single-stranded oligonucleotides that possess a stem-and-loop, and generate under light excitation a fluorescence signal related to the number of molecular beacons-target duplexes (see below details on beacons technology).

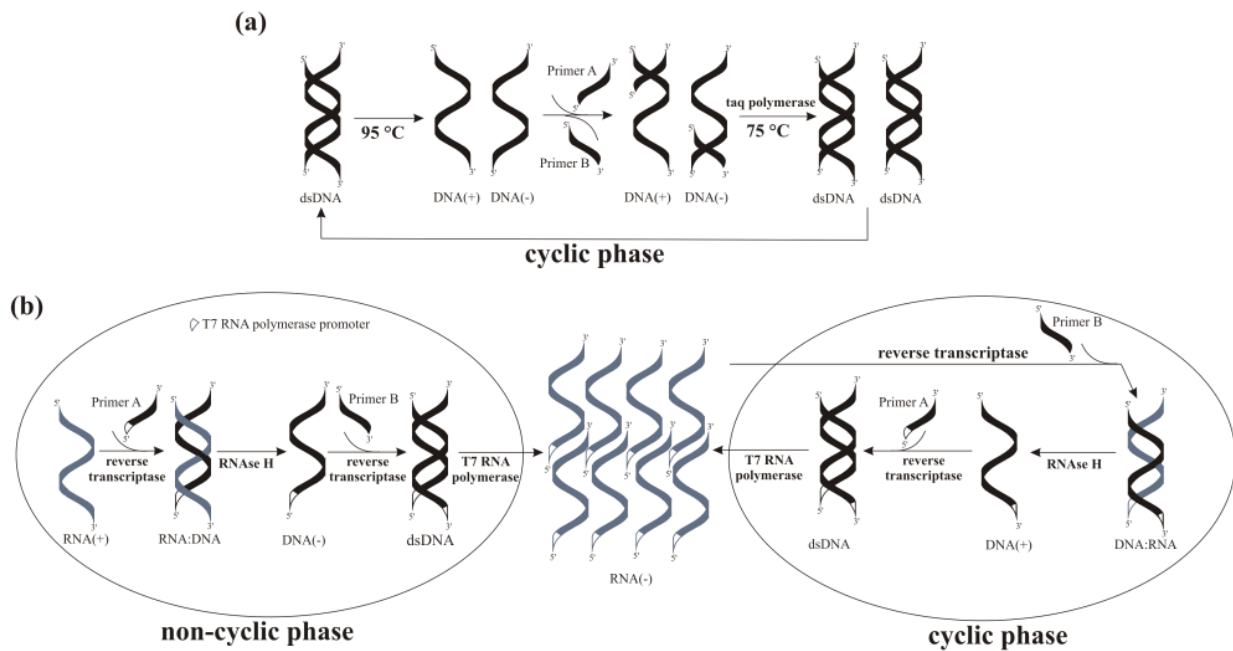


Figure 5 Schematic diagrams of the (a) PCR and (b) NASBA reactions. In PCR, DNA is first denatured at 95 C and then primers anneal to the single DNA strands at 50–60 C, depending on the target. Finally, taq DNA polymerase catalyses the synthesis of 2n–2n double stranded DNA molecules, where n is the number of amplification cycles. Typically, 20 cycles, at 5 min per cycle, are required for one million fold amplification.

NASBA is a complex process which amplifies mRNA using T7 RNA polymerase, reverse transcriptase and RNase H. NASBA needs approximately five cycles at an isothermal temperature of 41 C, to yield one million antisense single RNA copies, since 10–100 copies are produced in each transcription step. (Tsaloglou, Bahi et al. 2011)

NASBA is primer dependent at each step resulting in a higher level of discrimination than PCR. The reaction is rarely affected by dsDNA contamination as the production of dsDNA with a T7-promoter site allows selective production of RNA using T7-polymerase.

NASBA has been used in many applications such as phytoplankton environmental monitoring (Casper, Paul et al. 2004; Patterson, Casper et al. 2005; Casper, Patterson et al. 2007), human diagnostics (Polstra, Goudsmit et al. 2002), plant pathology for direct detection of viable *Ralstonia solanacearum* in potatoes (Bentsink, Leone et al. 2002), food microbiology (Cook 2003) and a diverse range of environmental and clinical samples (Birch, Dawson et al. 2001; Cook 2003). Its application in both pathogen detection and assessment of cell viability have been reviewed (Rodriguez-Lazaro, Hernandez et al. 2006). Consequently this assay was selected based on its outstanding advantages, (i) it has already been shown that RNA amplification with NASBA is particularly suitable for early detection and quantification of harmful microalga *K. brevis* (ii) NASBA is ideal for lab-on-a-chip applications because of its simple temperature control requirement.

Fluorescence labelling, combined with a suitable optical instrument, is a sensitive and quantitative method that is broadly used in molecular biology (Lakowicz 1999). Fluorescence detection offers various advantages: fluorescence molecules can have low toxicity and can be stored for long periods (Lakowicz 1999). Typically, the detection is done by illumination using an optical excitation source

which excites electrons in the molecule, and after few nanoseconds (the fluorescence lifetime is $10^{-9} \sim 10^{-7}$ seconds approximately) electrons release energy as light with a Stokes shift to longer wavelengths than the excitation light. The Stokes shift is the wavelength difference between the positions of the band maxima of the absorption and emission spectra. The fluorescence at longer wavelengths is separated from the excitation light geometrically (Fu, Fang et al. 2006) and with optical filters (Dandin, Abshire et al. 2007) and detected by a photo-detector. Detectors typically have a linear response over a wide range of fluorophore concentrations. The relation between dye concentration and fluorescence intensity ($\Phi_{F(\lambda_{em})}$) is given by the modified Beer Lambert law (Lakowicz 1999):

$$\phi_{F(\lambda_{em})} \approx Q_y \cdot \phi_{o(\lambda_{ex})} (1 - e^{-\varepsilon(\lambda_{ex}) \cdot l \cdot c})$$

Equation 1

where $\phi_{o(\lambda_{ex})}$ is the excitation light source optical power, c the fluorescent molecule concentration, l the optical light path, $\varepsilon_{(\lambda_{ex})}$ the fluorophores molar extinction coefficient and Q_y the fluorescent molecule quantum yield.

Fluorescence resonance energy transfer (FRET) is a mechanism describing energy transfer between two chromophores commonly used in fluorescent assays. A donor fluorescence chromophore, initially in its electronic excited state, transfers energy to an acceptor chromophore through non-radiative dipole–dipole coupling (Lakowicz 1999). FRET is the basic mechanism for various real-time PCR methods employing a variety of probe design tactics, including TaqMan™ probes, molecular beacons, Scorpion probes and SYBR green probes. TaqMan™ probes are short single stranded molecules that have a fluorescent reporter dye attached to the 5' end and a quencher coupled to the 3' end. The probe is designed to hybridize an internal region of the target during annealing steps. The proximity of the fluorophore and the quench molecules prevents the detection of fluorescent signal from the probe when it is in solution, and when initially hybridized. Following hybridisation and during the elongation step the polymerase cleaves the probe, increasing the distance between quench and fluorophore molecules and FRET no longer occurs. Thus, fluorescence increases in each cycle, proportional to the amount of probe cleavage and hence number of DNA copies.

Molecular beacons are single stranded nucleic acid molecules that possess a stem-and-loop. The loop portion is a probe sequence complementary to the target (Tyagi and Kramer 1996). The stem is formed by the annealing of two sequences complementary to each other at the terminal ends of the sequence forming the probe (see Figure 6). The stem sequences are designed to be unrelated to the target. A fluorophore and a quencher are attached, one on the terminal end of each arm. In the loop configuration the fluorophore and quencher are brought close together forming a non-fluorescent hairpin structure. When a molecular beacon encounters a target, the loop sequence hybridizes with the target sequence with sufficient energy to cause the stem to disassociate. Thus the fluorophore and

quencher separate, allowing for fluorescence. Unlike TaqMan™ probes, molecular beacons are designed to remain intact during the amplification reaction.

The first two detection methods reported for NASBA assay were electro-chemi-luminescence (Lanciotti and Kerst 2001) and enzyme linked gel assay (Loens, Ursi et al. 2005), which are both endpoint analyses. In the electro-chemi-luminescence method amplicons are hybridized to target-specific probes (an electrochemiluminescent (ECL) probe and a second probe coupled to paramagnetic beads). Following hybridization, the bead/amplicon/ECL probe complexes are captured at the magnet electrode of the automated ECL reader (Lanciotti and Kerst 2001). Enzyme linked gel assay is a electrophoresis based technique, where the electrophoresis of the hybridization reaction discriminates between free probes and probes that have specifically hybridized to the NASBA product, because the latter will migrate slower into the gel than the unbound probe (Loens, Ursi et al. 2005). Nowadays, the most widely used probes are fluorescent molecular beacons (Leone, van Gemen et al. 1998; Casper, Paul et al. 2004; Vet and Marras 2005). A real-time detection system is generated using molecular beacons with the NASBA amplification. Molecular beacons are single stranded hairpin shaped oligonucleotide probes. In solution with their targets molecular beacons can exist in three different states: bound to a target, free in the form of a hairpin structure, and free in the form of a random coil. For incubation temperatures above 50 °C molecular beacons form a random coil, in which the fluorophore and quencher are separated, and hence energy transfer does not occur and a significant fluorescence background is generated.

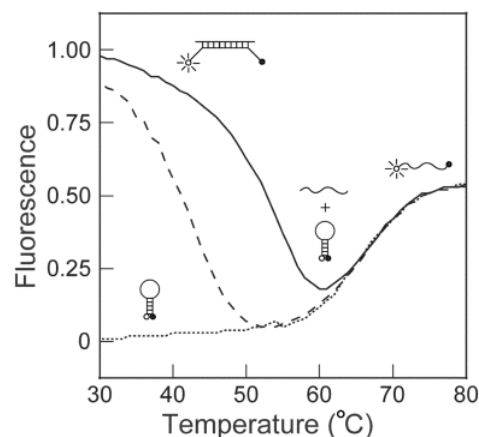


Figure 6 “Phase transitions in solutions containing molecular beacons. Schematic representation of the phases.

As the temperature is raised, the fluorescent probe–target duplex (phase 1) dissociates into a nonfluorescent molecular beacon in a closed conformation and a randomly coiled target oligonucleotide (phase 2). As the temperature is raised even higher, the hairpin stem of the molecular beacon unravels into a fluorescent randomly coiled oligonucleotide (phase 3).” Taken from (Bonnet, Tyagi et al. 1999; Vet and Marras 2005).

The strategy commonly employed to analyse the results obtained by real-time NASBA is the “Time-To-Positivity” (TTP) method. TTP is defined as the time in minutes when the fluorescence signal is above the amplification background: the threshold of detection (TOD) which is arbitrarily chosen (de

Baar, van Dooren et al. 2001; Niesters 2001). The TTP value is a function of how much initial target RNA is in the sample, this is the equivalent of the cycle threshold in PCR. Using the TTP method the amount of cells present in unknown samples can be calculated using a standard curve that indicated the relation between TTP value and input amount. Standard response curves are generated from serial dilutions with known cell concentration usually in the range from $10^1 - 10^6$ cells/mL. Finally, results from the NASBA assay are compared with the cells concentration expected from serial dilutions analysis, the number of cells per sample can be extrapolated from the standard curve. However the TTP method relies on the TOD and does not take into account the enzyme kinetics, chip to chip or instrumentation variability (i.e. time to reach incubation temperature) which makes batch-to-batch comparison difficult. For a better and a stronger approach a mathematical model was developed by the bioMérieux labs which describes the amplification curves, takes into account the enzyme and hybridization kinetics and removes the error due to batch-to-batch variations in reagents or degradation during storage. (Weusten, Carpay et al. 2002). This model allows to extract key parameters (i.e. amplification slope parameters) that are function to the initial amount of RNA. When NASBA curves are fitted to Equation 2 using non linear regression methods, the quantitation variable ($k_1\alpha_1\alpha_2^2$) can be used to create a standard curve (similarly to the TTP method) and the number of cells per sample can be extrapolated from this standard curve.

$$Y(t) = \lambda Y_0 - (\lambda - 1)Y_0 \exp\left\{-\frac{1}{2}k_1\alpha_1 [\ln(1 + e^{\alpha_2(t-\alpha_3)})]^2\right\}$$

Equation 2

$Y(t)$ is the fluorescence signal as a function of time t , Y_0 the initial or background fluorescence extrapolated to $t=0$, λY_0 the maximal fluorescence, $\alpha_1\alpha_2^2$ the transcription rate and α_3 is the time point at which the amplification begins of the linear phase (or time to primer depletion).

However, the requirement for three separate enzymes in NASBA combined with instrument and sample matrix variability (i.e. inhibitors) often results in a greater variability between replicate samples (Patterson, Casper et al. 2005). As a result the sample to sample amplification kinetics can be inconsistent, which could make quantitative and comparative analysis very challenging. Therefore without internal control this model cannot be used as a method for quantitative analysis but can be use as a semi-quantitative method for different samples using the same enzyme batch. In this case, curves fitting a linear relation can be obtained between the natural logarithm of ($k_1\alpha_1\alpha_2^2$) against the logarithm of cell equivalents (i.e. $\ln(\text{cell equivalents})$). The incorporation of a fixed amount of internal calibrator can serve as an internal quantification standard. Internal amplification controls or internal control (IC) that are co-purified and co-amplified with the target nucleic acid can be used as an indicator for kinetic variability and therefore can address the issue of analytical variability (Pasloske, Walkerpeach et al. 1998; Isaac 2009). The IC is usually designed (synthetic nucleic acid) to include the exact base composition as the amplicon of the targeted gene (Patterson, Casper et al. 2005) with the exception

that the original beacon site is replaced with a different sequence. This allows specific hybridization with a sequence specific molecular beacon (different from the target specific molecular beacon) and serves as a competitor RNA for assay quantification (Weusten, Carpay et al. 2002). In brief, both types of RNA are converted into cDNA (see section 1.2.1, page 32), so that there is competition between the RNA types for the primer pool, and the relative amounts of RNA that were originally present in the sample determine the relative amounts of cDNA formed. As the amount of cDNA formed determines the RNA production rate in the transcriptional phase, the relative rates of RNA formation in this phase directly reflect the relative concentrations of target RNA and IC RNA in the sample. As the concentration of IC is known, the target RNA level can be computed (Weusten, Carpay et al. 2002). When NASBA curves are fitted to Equation 2 using non linear regression methods, wild type concentrations can be determined using the transcription rates ratio ($(k_1\alpha_1\alpha_2^2)$ for wild type : $(k_1\alpha_1\alpha_2^2)$ for IC) and IC concentration. In such an assay two different molecular beacons with different fluorophores are used to allow multiplexed detection of the IC and wild type (target). When using an IC-based NASBA assay, quantification can be performed using the TTP method to compare IC against wild type (i.e. target).

1.3. Current nucleic acid amplification-based lab-on-a-chip devices with “sample-in” to “answer-out” capability

This section is structured around the current nucleic acid techniques and microfluidic technologies highlighted in Figure 4. Different nucleic acid amplification-based lab-on-a-chip devices with “sample-in” to “answer-out” capability that have been developed by other research groups, and their potential suitability for phytoplankton monitoring applications are evaluated. First, the sample preparation techniques used in these devices are discussed (see section 1.3.1, page 41) then, following this, biological assay, the level of integration in these devices and overall performance are examined (see section 1.3.2, page 46) and summarized (see Table 2, page 53).

Lab-on-a-chip devices for biological diagnostics have been widely reported in the literature (Chin, Linder et al. 2007; Myers and Lee 2008; Chin, Linder et al. 2012). Most of them are focused on either sample preparation (Tian, Hühmer et al. 2000; Price, Leslie et al. 2009) or on-chip PCR amplification (Zhang, Xu et al. 2006; Agrawal, Hassan et al. 2007) with occasional built-in microvalves (Marcus, Anderson et al. 2006). Despite impressive advances, the integration of sample purification and molecular analysis and detection remains a major challenge for portable diagnostic devices (Myers and Lee 2008; Pennathur 2008). For example Fukuba et al. developed an integrated *in situ* analyzer for microbial gene detection. The device performed cell lysis, DNA purification, PCR and optical detection (Fukuba, Miyaji et al. 2011). The core functional element of the system was a microfluidic device. The system was able to continuously introduce seawater samples into a sample coil. An important requirement for seawater sampling is to prevent cross contamination or carry over

between samples. To address this the sample coil was rinsed using a fresh sample of seawater, and the microfluidic device cleaned and treated with 100 mL of DNA Away® prior to each sample preparation procedure. Subsequently cells were lysed using guanidium thiocyanate, then the DNA was adsorbed onto the glass beads packed into the microfluidic device (similar to Dimov et al., see section 1.3.1.a below). Following to the washing process, purified DNA was eluted for PCR amplification. Although they demonstrated the use of the lab-on-a-chip technology for oceanographic applications, the system could not perform long term monitoring (the system allows only 4 to 5 measurements per dive) and uses macro scale elements such as pumps and valves, off-chip optical sensors etc. Moreover the detection limit of the system was 1×10^4 cells/mL of *Methylosinus trichosporium*. This limits the use of the system for the detection of low concentrations of phytoplankton (i.e. in early bloom conditions where cell concentration is similar to 1 cell/mL (Blasco, Levasseur et al. 2003; Chang 2011)). It should be noted that the system does not incorporate an integrated cell filtration/concentration strategy which is essential for detecting low cell numbers. However it is a great demonstration of an *in situ* system using a microfluidic device tested in actual deep-sea environments.

Several integrated devices with “sample-in” to “answer-out” capability, integrating the different functionalities (as see in Figure 4, i.e. (i) DNA/RNA sample preparation, (ii) nucleic acid amplification, and (iii) detection of amplified nucleic acid) needed for nucleic acid-based molecular analysis have been presented. These lab-on-a-chip devices use various techniques to achieve successful sample preparation including chemical lysis associated with silica particle-based extraction (see section 1.3.1.a, page 41) (Cady, Stelick et al. 2005; Dimov, Garcia-Cordero et al. 2008; Sauer-Budge, Mirer et al. 2009; Hagan, Reedy et al. 2011; Shaw, Joyce et al. 2011), antibody-conjugated magnetic microbeads for cancer cell capture combining with thermal lysis (see section 1.3.1.b, page 45) (Lien, Chuang et al. 2010), and mechanical filtering and membrane-based nucleic acid capture (see section 1.3.1.c, page 45) (Baier, Hansen-Hagge et al. 2009; Gulliksen and Hansen-Hagge 2012). For the biological assay step, PCR remains the most popular method integrated in lab-on-a-chip devices with “sample-in” to “answer-out” capability (see section 1.3.2.a, page 46), although isothermal approach (i.e. NASBA) have also been reported (see section 1.3.2.b, page 50) (Dimov, Garcia-Cordero et al. 2008; Gulliksen and Hansen-Hagge 2012).

As mentioned above, the different functionalities and related techniques specifically used in systems with “sample-in” to “answer-out” capability are presented below. Sample preparation functions, biological assay used and level of integration of these devices are discussed. For both sample preparation and biological assay, strengths, weaknesses and their potential suitability for phytoplankton monitoring applications are discussed at the end of each sub-section.

1.3.1. Sample preparation techniques in lab-on-a-chip with potential “sample-in” to “answer-out” capability

1.3.1.a Silica-based extraction techniques

For a fully integrated portable nucleic acid device with “sample-in” to “answer-out” capability, all the steps needed for the analysis (including sample preparation) must be performed in a lab-on-a-chip. Several integrated devices with “sample-in” to “answer-out” capability have been presented incorporating different strategies for the sample preparation step. Groups have employed multiple techniques including chemical lysis methods combining to silica coated channels technique. Cady et al. developed a suitcase format, fully automated, PCR-based system, incorporating a solid phase extraction (SPE) based sample preparation (details on the SPE technique can be find section, 3.2.1, page 89) (Cady, Stelick et al. 2005). Cell lysis was then achieved by mixing 90 μL of lysis buffer with 10 μL of sample containing *Listeria monocytogenes* cells (concentration of 10^5 cells/mL) and incubating at room temperature for 5 minutes. This mixture was pumped into the chip for DNA capture and purification using a silica coated microchannel. After channel washing, distilled water was pumped into the purification region to recover DNA for amplification in the PCR chamber (see Figure 7). Cady et al. were then able to purify DNA and detect between 10^7 and 10^4 *Listeria monocytogenes* cells with real-time PCR.

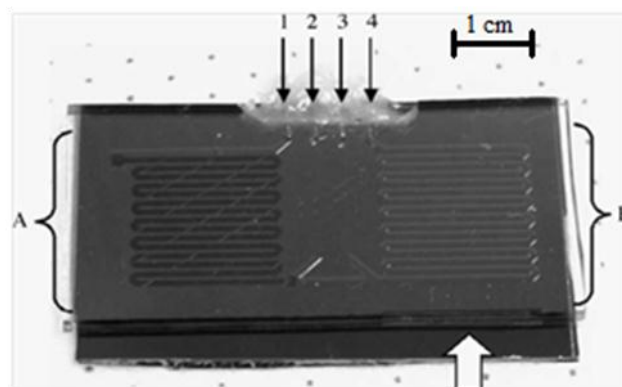


Figure 7 “An optical micrograph of the DNA purification/real-time PCR microchip is shown. The nucleic acid purification region is shown in (A) while the real-time PCR region is shown in (B). The fluid connections are (1) sample input, (2) waste outlet, (3) PCR reagent input, and (4) reaction outlet. The large white arrow denotes the lateral path for fluorescent excitation for real-time PCR.” Taken from (Cady, Stelick et al. 2005).

Shaw et al. developed a laboratory system (see Figure 8) using a glass chip to perform sample extraction, PCR amplification using electro-osmotic pumping fluidic control and thermocycling using a Peltier element (Shaw, Joyce et al. 2011). All reagents for performing DNA extraction and amplification were encapsulated in 1.5% (w/v) low-melting temperature agarose gel into the glass chip and could be stored on-chip for up to 8 weeks. They showed a simple reagent storage method that can be easily tested and adapted for seawater monitoring devices. Buccal swab samples were manually added to a chaotropic binding/lysis solution pre-loaded into the glass chip. Buccal swab DNA present

in the binding/lysis solution (20 μL of lysate) was dispensed into the chip. The released DNA was then adsorbed onto a silica monolith contained within the DNA extraction chamber. They reported DNA extraction efficiencies of approximately 52 % (limit of capture efficiency of pure DNA on-chip) resulting in a DNA concentration extract of 0.57 ng/ μL . The system was based on the use of electro-osmotic pumping for fluidic control. Although this chemical technique can simply be adapted and integrated into lab-on-a-chip devices, electrodes can only be integrated onto glass-based lab-on-a-chip. Moreover glass is an expensive material (\$500 to \$4,000 m^{-2}) (Chin, Linder et al. 2007), and electrode fabrication relies on laborious fabrication processes. In addition, electrokinetic-based actuation of fluids requires a charged surface for electro-osmotic flow (which limits the type of material that can be used), buffer compatibility and a high voltage supply. Finally this method often produces slow flow rates which have a direct impact on the analysis time of the device.

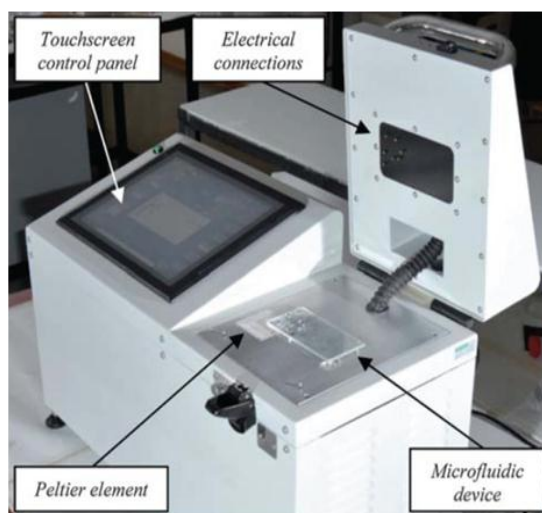


Figure 8 Photograph of the bench top instrument using a microfluidic chip, Peltier element, electrical connections and touch screen control panel. Taken from (Shaw, Joyce et al. 2011).

Dimov et al. were the first to demonstrate a system incorporating RNA purification and NASBA assay on a single chip. RNA purification was performed using the SPE method by silica bead immobilisation on a 40 μL purification chamber surface (see Figure 9). A pre-mixed sample solution of 10 μL containing 100 *Escherichia coli* cells (sample concentration of 1×10^4 cells/mL) mixed with 90 μL of lysis/binding buffer was then pumped through the extraction chamber at 5 $\mu\text{L}/\text{min}$. The system achieved a detection limit of 100 *Escherichia coli* cells, this means that positive NASBA was observed for a sample containing 100 *Escherichia coli* (no indication on the system extraction efficiency was provided) (Dimov, Garcia-Cordero et al. 2008).

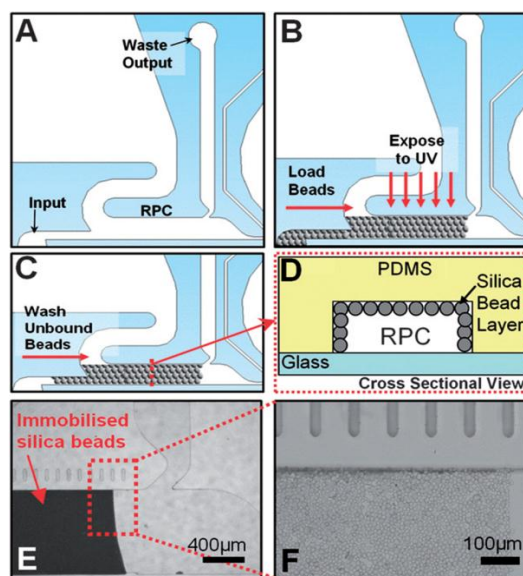


Figure 9 “Method for silica bead immobilisation on PDMS surface. (A) Before loading the beads, all ports are sealed except for the Input and Waste Output. (B) 3 mL of plain silica bead solution flows into the input, left to dry, and exposed to UV-ozone for bonding. (C) Unbound beads are washed away with dH₂O, leaving a (D) layer of silica beads bonded to the walls of the RPC (E–F) Bright-field micrographs of the immobilised 10 mm silica beads on the PDMS walls of the RNA purification chamber.” Taken from (Dimov, Garcia-Cordero et al. 2008).

Silica coated microchannels could offer poor performances. To achieve efficient extraction, high surface area is needed to effectively capture nucleic acids which can lead to complex microfluidic design (Cady, Stelick et al. 2003). Moreover, significant volumes for elution are necessary in the implementation presented above due to the long channels necessary to achieve a sufficient surface area to effectively capture DNA. This could be an issue for low nucleic acid concentration samples but can be mitigated by the use of smaller channels with textured surfaces. A fully integrated and automated system for the detection of bacteria incorporating sample preparation steps based on a particle packed column has been developed by Sauer-Budge et al. (Sauer-Budge, Mirer et al. 2009). This system performed chemical lysis, silica-based technique DNA purification (see Figure 10), PCR amplification and fluorescence readout function. A porous polymer monoliths solution with embedded silica particles was polymerised in the microfluidic channel for the creation of a “SPE column”. 50-400 µL of fresh sample (concentration of 3.1×10^6 cells/mL) was mixed on-chip with guanidium thiocyanate, and this mixture then pumped at a flow rate of 0.18 µL/s into the “SPE column” for further DNA capture, purification and elution. They observed subsequent positive amplification and detection for a concentration of 1.25×10^6 *Bacillus subtilis* cells. This system could only perform and detect successfully a high concentration of *Bacillus subtilis* cells. This species is a gram positive bacterium that is known for having a thick peptidoglycan cell wall which makes it more difficult to lyse (Sauer-Budge, Mirer et al. 2009).

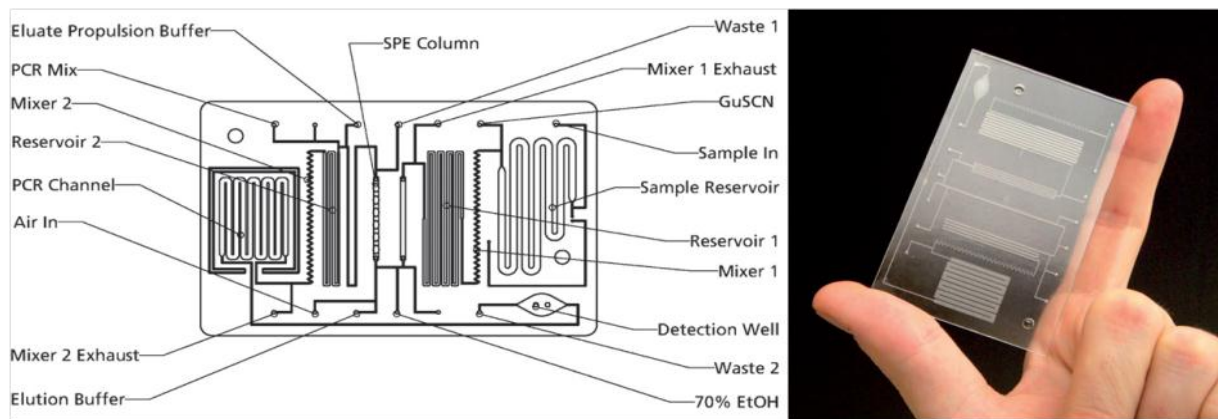


Figure 10 Photograph of Left: Final chip design with fluid inputs and outputs and functional regions labelled. Right: Picture of a chip prototype demonstrating its credit card-like size.(Sauer-Budge, Mirer et al. 2009)

This method relies on slow dispensing of the lysate into the silica packed microfluidic channel to enable nucleic acids capture, limiting fast sample preparation time. In addition Preston et al. highlighted that column nucleic acid extraction efficiency could decrease with repeated use (Preston, Harris et al. 2011). Finally, it is worth noting that the devices above do not incorporate cell filtration strategies which are essential in low cell number sample conditions for on-site phytoplankton monitoring applications.

A device for sample extraction and purification, and RT-PCR amplification for the identification and detection of influenza A was presented by Hagan et al. (Hagan, Reedy et al. 2011). The sample extraction and purification step was based on SPE using chitosan-based technique, a pH control technique, avoiding the PCR inhibitory effects of guanidine and isopropanol used in traditional silica-based extraction methods. The pH-controlled approach, which promotes nucleic acid binding to and releasing the chitosan phase based on a change in buffer pH, is exploited for nucleic acid purification in a Borofloat glass microfluidic device. A channel was filled with new chitosan-coated silica beads prior to each extraction. A 75 μ L sample containing a nasal swab was loaded into the microchip for nucleic acids extraction. They demonstrated successful extraction of 0.2 ng of viral RNA. This system takes the advantage of its small channel volume for high nucleic acid concentration into a small elution volume. This example is a good demonstration of a chemical method suitable for successful subsequent nucleic acid amplification. However this technique involves the use of new silica beads prior each extraction which will make the adaptation of this technique for on-site phytoplankton monitoring applications difficult and could require complex design. For phytoplankton monitoring applications fully autonomous devices are required and extensive manual handling for sample preparation is therefore not suitable.

1.3.1.b Antibodies-conjugated magnetic microbeads for cancer cells capture and nucleic acids extraction

Lien et al. developed an automatic one-step RT-PCR diagnosis system that integrates a sample purification step using antibody-conjugated magnetic microbeads for cancer cell capture (Lien, Chuang et al. 2010). The 3D integrated system could perform the whole process automatically with the aid of integrated heaters, micropumps and microvalves. 1 mL of sample containing cancer cells was loaded into the 3D incubation chamber with pre-loaded magnetic beads. A swirling effect was generated within the 3D chamber using a pneumatic-driven PDMS membrane running at 1.5 Hz for the rapid isolation of cancer cells. The purified magnetic complexes were then re-suspended and further transported into a chamber for thermal cell lysis. These systems achieved a detection limit of 50 cancer cells/mL. Antibodies are globulin proteins (immunoglobulins) that react specifically with the antigen and that are present in the blood of immunised animals or plants. Although the antibodies-based technique can allow capture and concentration of specific target, for some applications (i.e. phytoplankton work) antibodies are not always available on cells. Moreover antibody techniques use a complex sample matrix and therefore require elaborate device design. Although they have shown successful thermal lysis for cancer cells, for phytoplankton cells the literature shows that the use of thermal lysis only is usually not enough for efficient lysis. It is worth noting that combining functionalised beads (i.e. oligodeoxythymidylic acid dT (Oligo (dT)) beads to specifically capture mRNA – see section 3.3, page 97) with swirling mixing could offer a fast sample preparation process. This technique could be explored and adapted for phytoplankton monitoring applications (see Chapter 5 Discussion and further work).

1.3.1.c Mechanical filtering and membrane-based nucleic acid capture and extraction

The Institut für Mikrotechnik Mainz in collaboration with the University of Oslo developed a diagnostic platform for the detection of HPV E6/E7 mRNA (Baier, Hansen-Hagge et al. 2009; Gulliksen and Hansen-Hagge 2012). A standalone bench top system using microchips was finalised, where nucleic acid analysis is accomplished using different pieces of equipment. The automated platform was made of two on-bench systems using microchips, one for sample preparation and one for amplification and detection. All necessary reagents for cell lysis, washing, and elution are stored on-chip and the extraction is performed in 2 filter stages: one for cell pre concentration and the other for nucleic acid capture. The chip consists of COC (cyclic-olefin copolymer) sealed with COP (cyclic olefin polymer). The sample preparation system used two modified syringe pumps containing two syringes: one to pump 3mL of sample (16 cells/mL of HPV E6/E7) through the cell capture filter and a second one for fluid actuation and drying by pressurised air. The released nucleic acid was captured downstream onto a silica filter (Genomed GmbH, Germany), in the presence of a chaotropic salt and extracted by solid-phase extraction using a modified version of Boom's extraction method. Following extraction, downstream washing steps were performed to remove cellular debris. A heater below the

chip table elevates the temperature during lysis and for drying of the SPE filter before elution of nucleic acid. Gulliksen et al. showed a great demonstration of cell concentration and lysis using a first filter and subsequent nucleic acid capture using a second filter. This resulted in the development of a stand alone bench-top platform for sample preparation. In this thesis we report a RNA sample preparation microdevice (see Chapter 3, page 85), with cell isolation using a mechanical (nanoporous aluminium oxide) filter, chemical lysis, and nucleic acid extraction and purification using the same filter as used for mechanical filtering.

1.3.2. Biological assay and integration level in lab-on-a-chip devices with potential “sample-in” to “answer-out” capability

1.3.2.a PCR-based lab-on-a-chip devices with “sample-in” to “answer-out” capability

Many integrated devices with “sample-in” to “answer-out” capability have been presented, incorporating several strategies for the biological analysis step. Most of them are exploiting PCR amplification. Cady et al. developed a suitcase format, fully automated, PCR-based system (Cady, Stelick et al. 2005). After nucleic acid elution, the solution was pumped into the 50 μ L PCR chamber for DNA amplification. An entire 40 cycle reaction could be completed in 35 min. A microcontroller-based control system was built to automate fluid handling and control the thermal cycling operation. The control system drives an automatic syringe pump, a thermoelectric heater/cooler, a fluorescence excitation/emission module, and a pressure valve. Optical detection for real-time PCR was accomplished using a LED-induced fluorescence optical architecture, combining lenses and a photomultiplier tube (PMT) for detection. They were then able to purify DNA and detect with real-time PCR between 10^7 and 10^4 *Listeria monocytogenes* cells after 45 min.

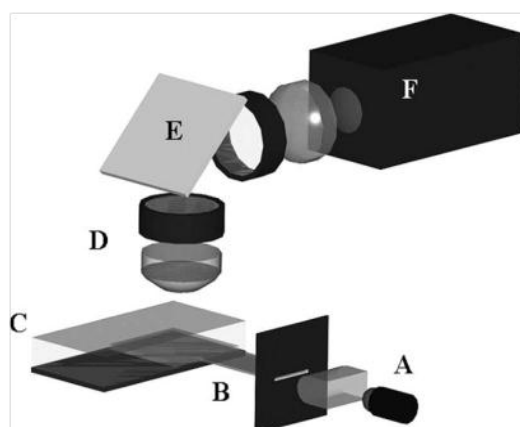


Figure 11 “The fluorescence excitation/detection system is shown. A 480 nm wavelength LED (A) is used to illuminate the PCR chamber of the microfluidic detection chip (C) through a chrome-plated glass waveguide (B). Upon fluorescence of the real-time PCR reaction.” Taken from (Cady, Stelick et al. 2005).

This suitcase format PCR-based system is a very good demonstration of the potential of field nucleic acid-based systems; however the detection system relies strongly on the careful alignment of the optical components (lenses, mirrors etc.). Unlike controlled research environments, devices for

phytoplankton monitoring applications will be subjected to a variety of environmental conditions such as vibrations, which makes the use of precise optical components unsuitable .

Sauer-Bugde et al. used PCR to conduct detection of the *Bacillus subtilis* bacteria. They used injection moulding strategy fabrication to create a Zeonex® plastic chip in a planar format without any active components. The associated on-bench instrument incorporated active components and was able to automate control of the fluids, temperature cycling, and optical detection. The PCR thermal cycling was performed with a ceramic heater and air cooling. The system used a commercial optical spectrometer for end-point fluorescence detection. An interface block aligns and ensures good contact of the chip to the temperature controlled region and the optics of the on-bench instrument, using o-rings and alignment pins. After sample preparation the eluted nucleic acids were mixed and pushed to the 50 µL PCR reaction channel using a “propulsion buffer”. After thermocycling the mixture was pushed to the detection chamber for optical read out. The system was able to detect 1.25×10^6 cells. All components for fluid actuation, temperature control and fluorescence detection were off-chip. A fully automated laboratory system was demonstrated with all assay steps performed on-chip. They estimated a limit of detection of less than 1 ng/mL of amplicon using a Taqman assay technology. Pneumatic dispensers were used for fluid handling. Although this solution results in low cost instrumentation it also generates a more complex system than using a solution with pumps. Moreover, pneumatic systems are usually bulky making the system difficult to transport. Even though this system has “sample-in” to “answer-out” capability and use the microfluidic technology, it is clear to see that it can only be used in a laboratory, therefore the system does not meet the requirements for on-site phytoplankton monitoring applications (see Figure 12).

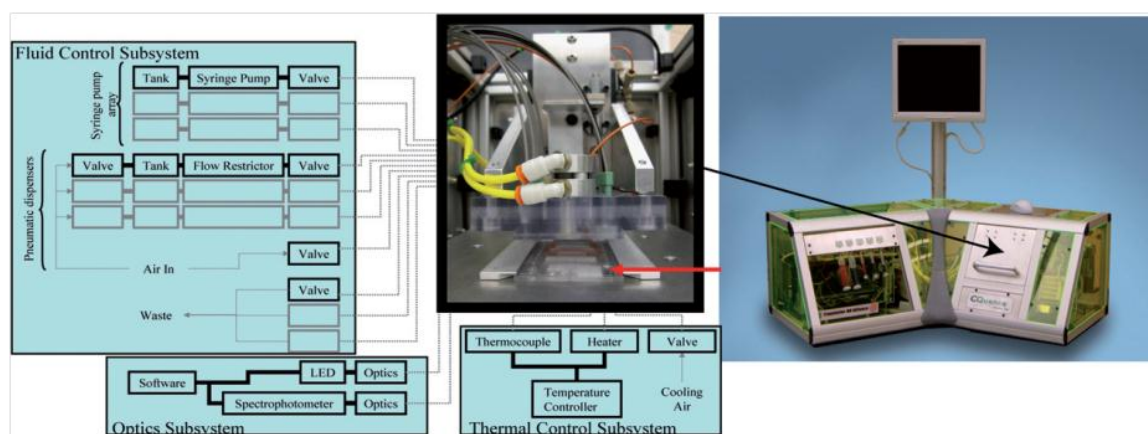


Figure 12 Photograph of “Left: Schematic of instrument functionality and photo of chip/instrument interface. The interface block is raised to show the position of the chip (red arrow). Right: Picture of instrument. The black arrow points to the door of the chip/in.” Taken from (Sauer-Bugde, Mirer et al. 2009).

Shaw et al. also developed a laboratory system using PCR for the detection of Buccal swab DNA (Shaw, Joyce et al. 2011). The internal glass surfaces of the PCR chamber were silanised to prevent DNA polymerase adsorption. Fluidic actuation was carried out using electro-osmotic pumping

technique. The actuation principle of the electrokinetic micropump is based on the movement of molecules in an electric field due to their charges. There are two components to electrokinetic flow: electrophoresis and electro-osmosis. Electro-osmosis leverages the surface charge that spontaneously develops when a liquid comes in contact with a solid (Iverson and Garimella 2008). This technique involves the integration of electrodes, and is therefore associated with laborious fabrication processes. Moreover electro-osmotic techniques are very dependent on the properties of the pumped liquid and the electrokinetic pumping effect could degrade over time (Brask, Kutter et al. 2005).

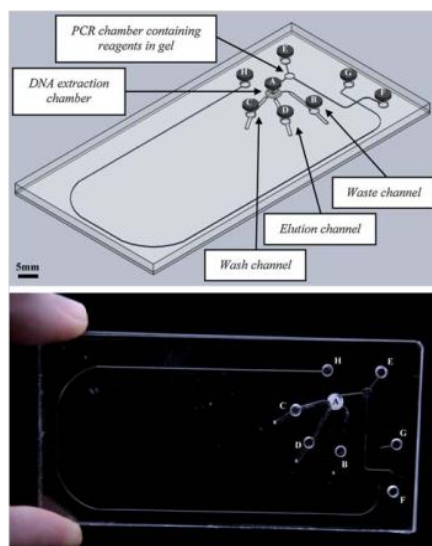


Figure 13 “Schematic (top) and photograph (bottom) of the microfluidic device, showing the thermally activated silica monolith (A) within the microfluidic device, the position of the carbon electrodes (B–H) and the locations of the gel encapsulated reagents. The additional channel between electrodes G and H provides the potential for future integration with capillary electrophoresis for detection of PCR products.” Taken from (Shaw, Joyce et al. 2011).

Hagan et al. used RT-PCR amplification for the identification and detection of influenza A. A single 500 nL chamber was used for RT-PCR reaction. Prior to biological assay the borosilica glass chip was passivated with SigmaCote[®] to avoid enzyme adsorption (see section 1.4.2, page 55). An additional chamber was used as a reference chamber for thermocouple insertion to allow temperature monitoring during infrared mediated heating. They used a non contact infrared heating technique to perform RT-PCR thermocycling. The reaction chamber temperature was controlled using an infrared lamp. Following nucleic acid preparation the RT-PCR microchip was placed on a stage seated over an infrared lamp. Due to the faster temperature rate transitions of the non contact heating technique, the reaction time was reduced from 3.5 hours on a conventional thermal cycler to approximately 40 minutes simply by using the RT-PCR microchip. All RT-PCR products were analyzed via microchip gel electrophoresis on a Bioanalyzer 2100. After amplification the RT-PCR microchip was able to produce 2 ng of viral RNA. Thermocycling for RNA amplification was performed using infrared-mediated temperature control allowing a 5 fold decrease of RT-PCR analysis time. This allows the system to achieve more rapid heating and cooling rates than traditional heating techniques. The

infrared-mediated temperature control is a contactless technique allowing a fast cooling process; however this heating technique requires the use of a high power consumption infrared lamp and bulky equipment, which are difficult to integrate into a portable device.

Lien et al. developed an automatic RT-PCR diagnosis system for ovarian and lung cancer cell identification. The detection limit of the developed system was found to be 50 cells/mL for the target cancer cells. The microchip was made of PDMS and glass allowing array-type micro-heater integration for thermocycling functions. Fluidic actuation was based on a suction-based sample transportation technique. The sample transportation unit consisted of a circular air chamber and a fluidic reservoir with a normally-closed vacuum pump driven PDMS membrane (see Figure 14). Fluidic transport can be achieved when the normally-closed PDMS membranes are deflected upwards sequentially by the negative gauge pressure in the air chambers generated by the vacuum pump so that the fluidic sample can be drawn into the fluidic reservoirs underneath the PDMS membrane. This is followed by releasing all the PDMS membranes of the microfluidic control module to push the fluidic sample from the fluidic reservoirs into the reaction chambers. The maximum volume in the sample transportation unit is designed to be 20 μL and the maximum pumping rate is approximately 450 $\mu\text{L}/\text{min}$.

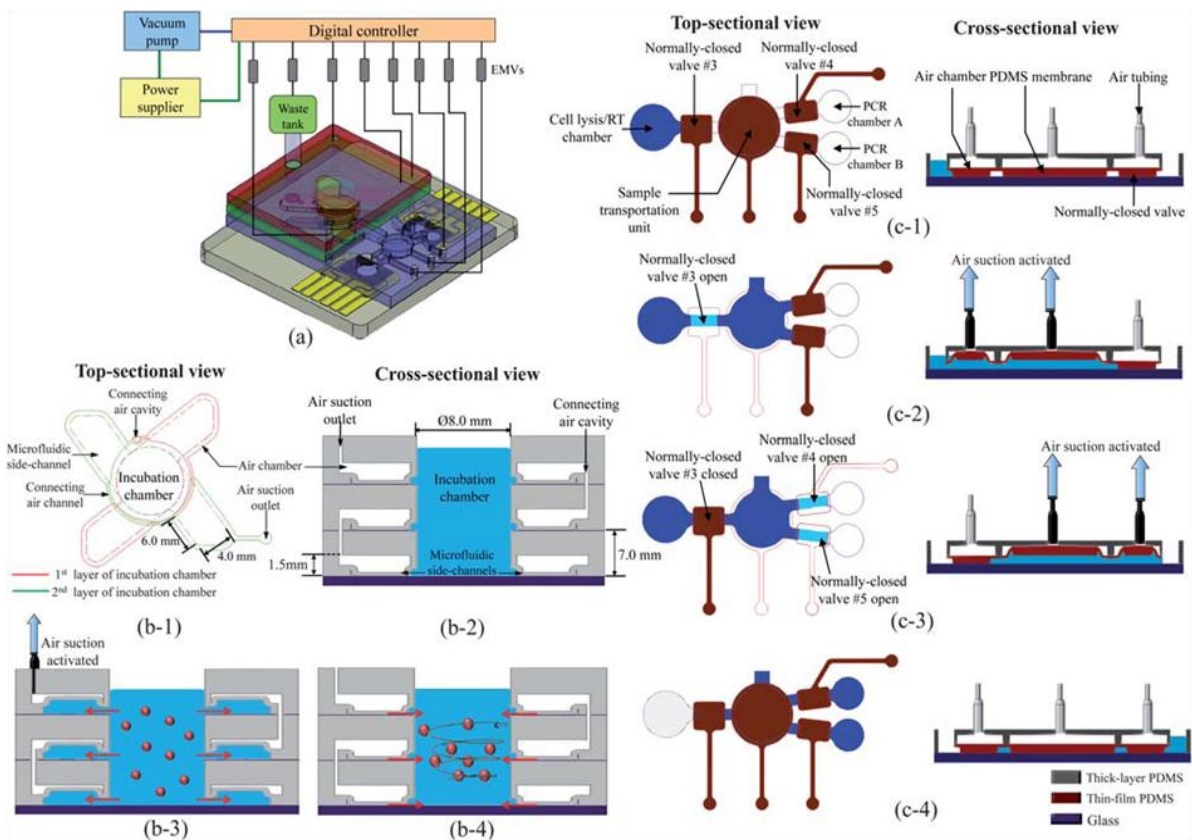


Figure 14 “(a) Experimental setup of the proposed 3D microfluidic system. (b) Schematic diagram and the designed parameters of the 3D microfluidic incubator in both top-sectional view (b-1), and cross-sectional view (b-2), during the membrane-deformation process (b-3) and during the membrane recovery process (b-4). (c) The working principle of the suction-based microfluidic control module.” Taken from (Lien, Chuang et al. 2010).

The microchip performed multiplex identification using two 10 μ L chambers for RT-PCR assay. The RT-PCR end products were visualised off-chip using gel electrophoresis separation. Complete nucleic acid analysis was performed in 1 h 40 min taking advantage of the fast sample preparation (~37 min) and high thermal ramping rate for RT-PCR. Although the RT-PCR reaction time was reduced compared to a conventional thermal cycler, Hagan et al. shown a faster reaction time using a contactless infrared heating technique (RT-PCR analysis time to only 39 min, ~5-fold reduction in time compared to conventional RT-PCR performed in a standard thermal cycler.) (Hagan, Reedy et al. 2011). Lien et al. have successfully integrated thermal management, fluidic valves and a mixer on-chip but no detection function was integrated and the amplification product was detected off-chip. Moreover vacuum-based fluidic actuations require the use of a bulky vacuum pump, and this technology is not satisfactory for transportable systems. However magnetic bead technology offers advantages including specific capture of target analyte and also allows beads to be separated from the lysate and transferred and captured (i.e. using a magnet) into a low volume elution chamber This technology needs to be explored for further improvements to our sample preparation microdevice (see Chapter 5).

1.3.2.b NASBA-based lab-on-a-chip devices with “sample-in” to “answer-out” capability

Alternative isothermal approaches have also been reported, NASBA amplification microdevices have been developed for the detection of human papilloma virus in SiHa human cells (Gulliksen, Solli et al. 2004; Gulliksen, Solli et al. 2005; Gulliksen and Hansen-Hagge 2012) and for *Escherichia coli* molecular diagnostics (Dimov, Garcia-Cordero et al. 2008).

The Institut fur Mikrotechnik Mainz in collaboration with the University of Oslo developed a diagnostic platform using NASBA. The operating microfluidic principles of the two chips are different. In the sample preparation chip, the sample is pushed through the chip by pressure driven flow, while for the NASBA chip, capillary forces and pneumatic pressure are the respective actuation principles. The NASBA chip consisted of a disposable microfluidic cartridge composed of injection moulded COC. Briefly, the chip had eight parallel 740 nL reaction channels and a waste chamber containing a highly absorbent filter paper acting as a capillary pump. The chip surface was coated with a hydrophilic surface coating using 0.5% polyethylene glycol (PEG) in methanol to avoid enzyme adsorption (see section 1.4.2, page 55). The NASBA chips contained freeze-dried enzyme and primer/probe mixes. Following sample preparation the NASBA master mix and purified nucleic acid sample were incubated together at 65 °C for 2 minutes off-chip. Subsequently, the mixture was loaded onto the NABSA chip containing the enzyme and primer/ probe mixes. Reaction chamber temperature control at 41°C was achieved by a Peltier element. Real-time fluorescence measurement was performed using a 2 channel LED induced fluorescence scanner for Carboxyfluorescein (FAM) and Carboxy-X-rhodamine (ROX) detection. The scanning function was performed mechanically by introducing an optical probe connected via flexible fibres to the illumination and detection source of

the optical system. A Multi-Pixel Photon Counter was used as detector of the fluorescent signal. The system came across systematic amplification inhibition issues showing that inhibition related to the polymer surface is a key challenge for on-chip nucleic acid amplification. These can be the result of enzyme adsorption (i.e. surface coating issues resulting in nonhydrophilic surface) (see detail on protein adsorption in section 1.4.2, page 55), salt contamination etc. Many studies including those describing lab-on-a-chip devices have highlighted the amplification problems associated with contaminating ethanol and salts. They also show incomplete filling of amplification channels, resulting in failure of capillary-based fluid progression through the microfluidic channel and clogging of the reaction channel at a number of critical stages in the chip assembly. The paper capillary-based fluidic handling technique limits the number of subsequent uses of the chip because of the decrease in efficiency of the paper absorption. Moreover this technique involves the use of new paper after a few experiments; this will make the adaptation of this technique for on-site phytoplankton monitoring applications difficult. For phytoplankton monitoring applications fully autonomous devices are required and extensive manual handling for sample preparation will be unsuitable. It is worth noting that this is the first study to comment on the performance of a microfluidic device which was developed on a number of clinical specimens.

Dimov et al. demonstrated a system incorporating RNA purification and NASBA assay on a single chip. Real-time detection was performed using a fluorescence microscope. Lysate and the binding buffer were loaded into the chip for RNA purification, and then the annealing and amplification steps were performed in a single chamber with a reaction volume of 2 μ L. The device was treated against adsorption using 1 mg/mL of bovine serum albumin (BSA). Fluid actuation was controlled with a manual valves system, and real-time amplification was monitored via a fluorescence imaging microscope. The system achieved a detection limit of as little as 100 *Escherichia coli* cells (Dimov, Garcia-Cordero et al. 2008). They demonstrate the first integrated microfluidic RNA purification and nucleic acid sequence-based amplification device, however sample collection and lysis were performed off-chip and real-time detection was performed using a fluorescence microscope. Further integration of the system is necessary in order to finalise a truly portable system.

These platforms all have both advantages and disadvantages, which make it difficult to select a single platform as ideal for all on-site applications. However none of them are fully ready for point-of-care analysis or on-site environmental deployment and further integration needs to be implemented. A microdevice for phytoplankton monitoring will require a combination of these techniques in conjunction with other necessary innovative technological development. In this thesis we have chosen to develop a microelectrode base microchip for cell isolation and lysis (see Chapter 2). We also explored an alternative technique based on filtering technology for sample concentration and nucleic acid extraction (Kim and Gale 2008; Baier, Hansen-Hagge et al. 2009), and developed a RNA sample preparation microdevice (see Chapter 3) with cell isolation using a mechanical (nanoporous

aluminium oxide) filter, chemical lysis, and nucleic acid extraction and purification using the same filter as used for mechanical filtering. However, some promising technology (e.g., functionalised magnetic beads) will require further study and this is discussed in Chapter 5. Finally, we developed a microchip with nucleic acid amplification using the NASBA technique and a thermo-regulated microchip (see Chapter 4). NASBA technology was chosen as the amplification method used in this thesis because it has already been shown that RNA amplification with NASBA is particularly suitable for early detection and quantification of harmful microalga *K. brevis* on a macro scale system (Casper, Patterson et al. 2007). NASBA is ideal for lab-on-a-chip applications because of its simple temperature control requirement (see section 1.1.1.b, page 24). Detection was achieved using a laser induced fluorescence detection laboratory system but further integration will be explored (see Chapter 5).

Summary of current nucleic acid amplification-based laboratory on-chip devices with “sample-in” to “answer-out” capability

References	Cells concentration/isolation	Sample volume and minimum concentration	Sample preparation			Biological assay				Reagent storage	Device Performance
			Lysis technique	Nucleic acids extraction technique	Sample preparation function performance	Chip and treatment	Amplification technique	Detection technique	Comments		
(Cady, Stelick et al. 2005)	None	90 µL lysis buffer + 10 µL of sample containing 10 ⁴ <i>Listeria monocytogenes</i> cells (10 ⁵ cells/mL)	Off-chip chemical lysis	Silica coated microchannel structures	DNA - Not given	PDMS chip treated with 10mg/mL BSA	PCR using a Peltier module	Fluorescence module, PMT and LED using optical components	50 µL PCR chamber for DNA amplification. Off-chip fluid actuators	Off-chip	10 ⁴ to 10 ⁷ <i>Listeria monocytogenes</i> cells (10 ⁵ cells/mL)
(Sauer-Budge, Mirer et al. 2009)	None	400 µL containing 1.25 x 10 ⁶ <i>Bacillus subtilis</i> cells (3.1 x 10 ⁶ cells/mL)	On-chip chemical lysis	Channel filled with silica particles	DNA - Not given	Zeonex® plastic	PCR using ceramic heater and air cooling	Commercial Optical spectrometer (Ocean optics)	50 µL PCR reaction channel. Bench top system	Off-chip	1.25 x 10 ⁶ <i>Bacillus subtilis</i> cells (3.1 x 10 ⁶ cells/mL)
(Shaw, Joyce et al. 2011)	None	Buccal swab in 20 µL lysis buffer	Off-chip Chemical lysis	Silica monolith coated microchannel	0.57 ng/µL of buccal swab DNA recovery	Glass microchip silanised	PCR using a Peltier element	Off-chip analysis	Use the electro-osmotic pumping technique	On-chip using argose gel	Demonstrated detection of buccal swab
(Hagan, Reedy et al. 2011)	None	75 µL of lysate containing nasal swab	Off-chip Chitosan based	Channel filled with Chitosan coated beads	Not given - 0.2 ng of viral total RNA	Borosilica glass, surface passivated with SigmaCote®.	RT-PCR using a contactless infrared heating technique.	Off-chip electrophoresis	500 nL RT-PCR chamber volume	Off-chip	Demonstrated detection of nasal swab
(Lien, Chuang et al. 2010)	Antibody-coated magnetic microbeads to capture cells	1 mL of sample containing 50 cancer cells (50 cells/mL)	On-chip thermal lysis using microheater	Antibody-coated magnetic microbeads	RNA - Positive RT-PCR was observed for a sample containing 50 cells/mL	Glass / PDMS	RT-PCR using a microheater.	Off-chip	20 µL RT-PCR chamber volume.	Off-chip	Positive RT-PCR was observed for a sample containing 50 cells/mL
(Gulliksen, Solli et al. 2004; Baier, Hansen-Hagge et al. 2009; Gulliksen and Hansen-Hagge 2012)	Mechanical filter	3 mL of sample (16 cells/mL)	On-chip chemical lysis	Silica-based filter	RNA - Positive NASBA amplification observed for a concentration of 16 cells/mL of HPV cells	COC and COP treated with PEG	NASBA using a Peltier element	On-chip detection using fibres for excitation and fluorescence collection, detection using photomultiplier	740 nL NASBA chamber	On-chip using PEG	Positive NASBA was observed for samples containing 20 cells/µL (20 ⁴ cells/mL) for the SiHa cell line (Gulliksen, Solli et al. 2004)
(Dimov, Garcia-Cordero et al. 2008)	None	10 µL sample containing 100 <i>Escherichia coli</i> + 90 µL lysis buffer (10 ⁴ cells/mL)	Off-chip chemical lysis	Channel surface coated with silica beads	RNA - Positive NASBA was observed for a sample containing 100 <i>Escherichia coli</i>	Glass / PDMS	NASBA using a Peltier element	Off-chip fluorescence reader	2 µL NASBA chamber	Off-chip	Positive NASBA was observed for a sample containing 100 <i>Escherichia coli</i> in 100 µL (10 ³ cells/mL)
Devices developed in this thesis (Chapter 3 and Chapter 4)	Mechanical filter (Aluminium oxide). Filter could theoretically accept a few hundred of mL depending on sample concentration	1 mL (2.5 x 10 ³ cells/mL for <i>K. brevis</i> and ~20 cells/mL for <i>Karenia mikimotoi</i>),	Chemical lysis	Aluminium oxide filter	RNA - Positive NASBA was observed for a sample containing 2500 <i>K. brevis</i> . Total RNA was detected using the Bioanalyzer for a concentration of ~20 cells/mL of <i>Karenia mikimotoi</i>	PMMA	NASBA using a Peltier element	Off-chip fluorescence reader	20 µL NASBA chamber	Off-chip	Positive NASBA was observed for a sample extracted on bench containing 10 cells/mL of <i>K. brevis</i>

Table 2 Summary of nucleic acid amplification-based laboratory on-chip devices with “sample-in” to “answer-out” capability.

1.4. Lab-on-a-chip systems challenges

Ideally lab-on-a-chip devices should integrate fluid actuation, sample pre-treatment, sample separation, signal amplification, and signal detection into a single robust and autonomous device. As they stand, these devices are not yet appropriate for on-site phytoplankton monitoring applications which could present extreme conditions and demanding requirements. Additionally there is a need for systems capable of performing repeated measurements, over a long period of time, which are fully autonomous with no necessary user intervention, with a low limit of detection and with potential easy technology transfer for mass production. For example, the miniaturization of detection systems involves a shorter optical path length through the sample which reduces the sensitivity of these devices, however research has shown that compact optical components can be integrated and detection systems can reach an acceptable sensitivity level (Pennathur 2008). Challenges also include interfacing submicrolitre volumes from the conventional laboratory to the chip. While lab-on-a-chip devices are powerful and offer advantages that include miniaturization, portability and reduced reagent consumption, many of the automation technologies are complex both in terms of initial design and operation. A fully-automated system is a clear challenge. Nonetheless lab-on-a-chip research holds substantial potential for fulfilling these challenges by automating complex biological assay procedures that are normally performed in a centralised laboratory into a hand-held microfluidic chip (Northrup, Benett et al. 1998). For example reagents have been incorporated into lab-on-a-chip devices, which avoids human intervention and labour (Hagan, Reedy et al. 2011). Many academic groups, along with a number of startup companies, have developed methods for fluid delivery and control, signal detection, and microfabrication that have potentially transformative capabilities (Chin, Linder et al. 2007).

1.4.1. Small volume and sample preparation challenges

A significant challenge arising directly from the adoption of small volume systems is to efficiently detect and prepare analyte molecules. Generally for nucleic acid analysis, preparation sample volumes are on the order of hundreds of micro-litres to ensure sufficient quantity of target analytes in the sample. This makes the process problematic for some miniaturized microfluidic applications (see illustration Figure 15). Many genes or species of interest may be relatively rare, requiring sample volumes greater than hundreds of millilitre to ensure the presence of the target analyte in the sample in sufficient numbers to be detected. Moreover non-targeted analyte can be relatively abundant and could interact negatively and mask detection of the target analyte. Generally lab-on-a-chip research has historically focused on the “more exciting challenge” of developing the last two steps of nucleic acid assays: nucleic acid amplification and detection. Very few (Crevillén, Hervás et al. 2007) address the issue of the sample collection, cell isolation, cell lysis and nucleic acid extraction and purification from a complex sample matrix.

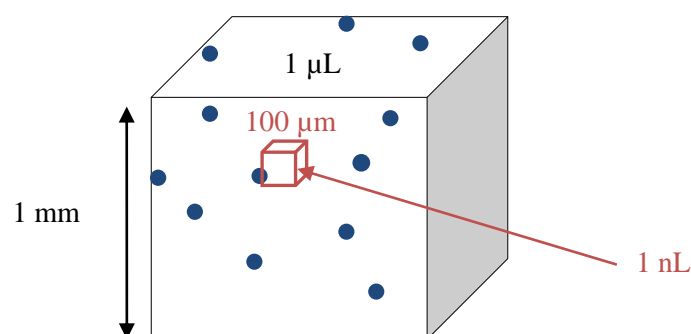


Figure 15 Illustration of the relation between miniaturisation and analyte amount.

As shown in Figure 15, the reduction of volume in microsystems decreases the absolute number of molecules available for detection. Hence, the ‘lab-on-a-chip devices’ ability to manipulate small volumes of fluid is one of the strengths, but also a weakness, because low numbers of molecules are more difficult to capture and detect. Some processes including sample capture and biological assay could require the mixing of samples with different analytes and reagents for capture or amplification. For example, without a mixing function the target capture technique could be time-consuming as it may rely on the diffusion of sorbent (e.g. silica beads) and target molecules. Thus, in numerous applications micromixer could be essential to decrease the time of the overall biological assay (Squires and Quake 2005). Table 3 shows that a small protein would be expected to have a diffusion coefficient of approximately $40 \mu\text{m}^2/\text{s}$. Without mixing, the molecule will diffuse across a dimension of 1 mm in approximately 3.5 hours. If the dimension is reduced to $150 \mu\text{m}$ the diffusion time drops to about 5 minutes.

Particles	Typical size (nm)	Diffusion constant	Diffusion time in 1 mm
		($\mu\text{m}^2/\text{s}$)	(minutes)
Solute ion	0.1	$2 \cdot 10^{-3}$	4
Small protein	5	40	208
Virus	100	2	4,200
Bacterium	1,000	0.2	42,000
Mammalian cell	10,000	0.02	420,000

Table 3 Typical diffusivities for various species in water at room temperature, adapted from (Squires and Quake 2005).

1.4.2. Biocompatibility and surface adsorption challenges

Another important challenge for the lab-on-a-chip technology is the behaviour difference between biochemical bulk reactions and biochemical reactions in microfluidic channels. In contact with the inorganic materials and higher surface area-to-volume ratios encountered in microstructures, biochemical behaviours have been found to be quite different than in macroscopic reaction systems (Lionello, Josserand et al. 2005). Consequently, protein adsorption onto hydrophobic microfluidic

channel surfaces occurs (Shoffner, Cheng et al. 1996; Alcantar, Aydil et al. 2000). Most lab-on-a-chips are made from hydrophobic polymers such as PDMS and PMMA. These problems can be prevented by surface modification, or via the introduction of microdroplet technology (Shoffner, Cheng et al. 1996). Microdroplet technology has recently been utilized to perform PCR in droplets, which offers shorter thermal-cycling times, lower surface adsorption and offers great potential for single DNA molecule and single-cell amplification (Mohr, Zhang et al. 2007; Zhang and Ozdemir 2009; Hatch, Fisher et al. 2011).

To prevent protein absorption, the surface coating must be heavily hydrated, hydrophilic and neutral in terms of charge to avoid electrostatic interactions (Ratner 1995). Various strategies have been developed for surface passivation.

Surface passivation methods can be classified as static or dynamic (Shoffner, Cheng et al. 1996; Zhang, Xu et al. 2006; Christensen, Pedersen et al. 2007). Static passivation is where the surface is treated before performing the biochemical assay. Dynamic passivation is where agents are introduced into the reaction mixture (Lou, Panaro et al. 2004). Silanization (e.g. with SigmaCote[®]) is a widely used process to prevent adsorption in silicon/glass microchips (Shoffner, Cheng et al. 1996). SigmaCote[®] is a solution consisting of 2.5% chlorosiloxane ((SiCl₂C₄H₉)₂O) and 97.5% heptane that functionalizes the surface with short alkane chains (Krishnan, Mackay et al. 2007). The solution reacts with surface silanol groups on glass and forms a covalent, microscopically thin film on glass that repels water. Another approach is to block the surface with a suitable bio-molecule which is added in excess. For instance, the protein BSA adsorbs to nearly any surface, thus creating a passivation layer (Shoffner, Cheng et al. 1996; Christensen, Pedersen et al. 2007). When a protein solution is supplied to a solid surface, five major processes in the adsorption process can be distinguished: i) transport of proteins toward the surface; ii) actual attachment to the surface; iii) adsorption at higher surface coverage which is hindered due to lateral repulsion between proteins in solution and at the surface; iv) structural and/or orientation rearrangements in the adsorbed proteins; v) desorption of proteins from the surface (Buijs, van den Berg et al. 1996). Protein adsorption is a very complex process, which is driven by different protein-surface forces, including Van der Waals hydrophobic and electrostatic forces (Norde 1994; Nakanishi, Sakiyama et al. 2001; Roach, Farrar et al. 2005). A different method of surface passivation is to use polymers such as PEG (Bell, Brody et al. 1998; Choi 2003; Panaro, Lou et al. 2004; Bi, Meng et al. 2006; Zhang and Xing 2007; Furuberg, Mielnik et al. 2008; Zhang, Feng et al. 2010). PEG is a linear polymer with repeat unit -CH₂-CH₂-O-. For example, a group developed an environmental friendly surface modification method for PDMS microchips to prevent protein adsorption. For surface modification, 3-glycidoxypropyltrimethoxysilane was first silanised on the PDMS surface. Since its glycidoxy group becomes reactive to amino groups in basic solutions, modified PEG-NH₂ was readily covalently attached to GPTMS on PDMS (see Figure 16) (Zhang, Feng et al. 2009).

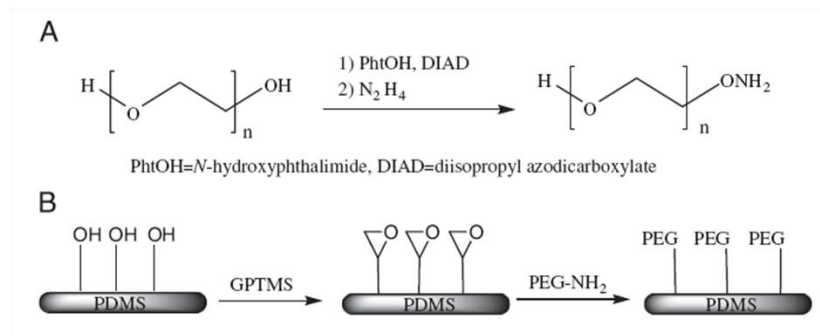


Figure 16 “Synthesis of PEG-NH₂ (A) and the two-step surface modification procedure (B).” Taken from (Zhang, Feng et al. 2009)

Coating surfaces with PEG is one of the most efficient methods for creating resistance to protein adsorption. Proteins and other bio-molecules are forced away from approaching a PEG-coated surface because of an enhanced steric stabilization force. Steric stabilization is achieved by polymer molecules (e.g. PEG) attaching to the surface and forming a coating which creates a repulsive force counterbalancing the attractive Van der Waals force acting on a particle approaching the surface (Napper 1983). First, when a protein gets close to a PEG-covered surface, the available volume for each polymer is reduced, and consequently, a repulsive force develops owing to loss of conformational freedom of the PEG chains (Andrade, Hlady et al. 1996; Bi, Meng et al. 2006).

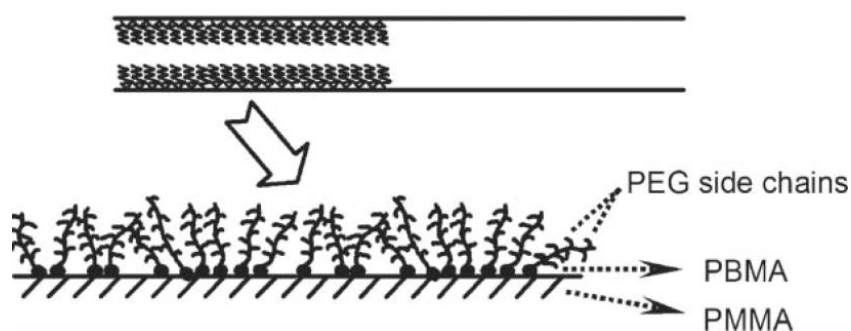


Figure 17 Illustration of biocompatibility, PMMA substrate coated with PEG, taken from (Bi, Meng et al. 2006).

Second, an osmotic interaction between the protein and the PEG-covered surface occurs. In this case, the number of available conformations of PEG segments is reduced owing to either compression or interpenetration of the protein chains, generating an osmotic repulsive force (Andrade, Hlady et al. 1996; Alcantar, Aydil et al. 2000). In dynamic passivation, BSA and PEG are included into reaction solutions to stabilize enzymes and to reduce undesired adsorption of the enzymes onto the surface. Proteins consist of amino acids which exhibit a wide variety of side chains which can have large variation in polarity. The major interactions that drive the interfacial activity and adsorption of proteins are i) the water structure-driven hydrophobic effect, ii) electrostatic interactions, and iii) strong hydrogen-bonding interactions characterized by cooperative, multiple hydrogen bonds (Alcantar, Aydil et al. 2000). It has been reported that hydrophobic surfaces adsorb more protein than hydrophilic ones, and that dehydration of hydrophobic surfaces promotes protein adsorption from

aqueous solution (Alcantar, Aydil et al. 2000). It is assumed that protein adsorption is related to the number and size of the hydrophobic patches on the protein's exterior and that the surface adsorption of proteins increases with hydrophobicity and size.

1.4.3. Reagent storage challenges

For long term environmental monitoring, long-term (i.e. 1 year – full seasonal cycle) stability of reagents is required to ensure device self-sufficiency. In order to be able to use lab-on-a-chip devices in the field, the reagents should be able to withstand low and high storage temperatures (Stevens, Petri et al. 2008). Moreover a critical issue can be the incompatibility of fabrication processes with reagents: generally dry reagents are encapsulated during fabrication processes using high temperatures. Therefore if temperature-sensitive reagents are pre-stored, compatibility of the bonding technique must be investigated (Focke, Kosse et al. 2010). However, by investigating protectants, the reagents could be stable during the fabrication process. It is worth noting that in most cases, long-term stability of enzymes is obtained by freeze-drying⁴ (Carpenter, Prestrelski et al. 1993; Prestrelski, Arakawa et al. 1993; Roy and Gupta 2004; Seetharam, Wada et al. 2006; Gulliksen, Marek. et al. 2007), and that nucleic acid amplification technology has never been tested for long term (over 6 months) exposure to a pressurized environment.

1.4.4. Detection techniques challenges

Nucleic Acid detection on lab-on-a-chip devices can be achieved by a variety of methods, including optically and electrochemically. The electrochemical method can be influenced by temperature variations, chemical factors and electrode surface deterioration. Thus, optical detection remains the preferred technique for quantitative proteomic or genomic diagnostics (Myers and Lee 2008). It offers high sensitivity and selectivity with usually no degradation of analytes. Optical detection is quite straightforward in a laboratory environment where bulky optical detection systems are precisely arranged and aligned. However, miniaturization of these systems involves a shorter optical path length through the sample which reduces sensitivity. Usually for devices with a path length range between 500 to 50 μm the limit of detection for common fluorophore molecules (e.g. Cyanine 3, Fluorescein) can reach the nanomole (Myers and Lee 2008; Ryu, Huang et al. 2011). Also, in order to obtain optimal detection conditions, stray light, scattering and auto-fluorescence need to be minimised. The optical architecture of lab-on-a-chip devices should be efficient in order to reach the maximum sensitivity for fluorescence. The main parameters are detector noise, external fluorescence, optical filtering efficiency and distance between the sample and the detection part. Lab-on-a-chip fluorescence is typically laser-induced by laser diodes, because the coherence and low divergence of a laser beam can easily be focused into a small detection region to obtain very high irradiation. Furthermore, laser

⁴ de Rosier. A, de la Cruz. B, and Wilkosz. K, (2001) Method and formulation for stabilization of enzymes, US patent <http://www.patentstorm.us/patents/6294365/description.html> (for NASBA)

diodes are inexpensive and can be easily integrated into a portable device. High-output LEDs are an alternative to laser diodes. Their small size, availability in a wide range of output wavelengths (including in the UV range) and low cost of production make them a promising solution for microfluidic devices and new applications. However, a serious drawback of on-chip fluorescence detection is the auto-fluorescence generated by polymer chips or non-specific bio-molecules in the sample (Pennathur 2008). Detector noise effect is intrinsic to the photodetector. The distance between the detection part and the sample depends on the capability to integrate the sensor inside the chip and depends also on the filter thickness (in the case of detection system without optical components). The separation efficiency between fluorescence light and excitation light seems to be an important parameter for increasing the sensitivity of fluorescence-based detection microsystems. There are various technologies for this approach such as interference-based filters, absorption-based filters (Dandin, Abshire et al. 2007) and wavelength selective detectors (Starikov, Benkabou et al. 2002). The most widely used technology is an interference-based filter, based on Bragg's law. Interference filters reject 'like a mirror' the unwanted light. These filters can have a significant rejection rate (around -40 dB) of the unwanted light, and could be customized in accordance with the spectrum rejection wanted (Dandin, Abshire et al. 2007). It is important to note that, unlike controlled research environments, devices for phytoplankton monitoring applications will be subjected to a variety of environmental conditions such as vibrations, and therefore detection systems that rely strongly on the careful alignment of optical components are not suitable for long term reliable measurements. The integration of microlenses into microfluidic devices is useful to improve fluorescence detection in microsystems by focusing the light into the channel to improve the excitation density power, without using off-chip optical components (e.g. glass lenses). Seo and Luck Lee developed a self-aligned 2D compound microlens for biochip applications. This microsystem has several advantages such as disposability, controllability of optical characteristics, self-alignment and a simplified fabrication process using PDMS (Seo and Lee 2003).

1.4.5. Nucleic acid analyse time versus high temporal resolution

As discussed in the criteria section (see section 1.1.1, page 23) monitoring for biochemical molecules in seawater requires reliable *in situ* sensors that can withstand long-term deployment, maintain accuracy and make measurements at high temporal and spatial resolutions (Prien 2007; Erickson, Hashemi et al. 2011). Molecular biology analyses are inherently slow compared to most chemical measurements. Nucleic acid assay time (usually around 1 to 2 hours) makes fast sampling to result very challenging. However lab-on-a-chip technology offers the advantage of parallel sample analyses and can be associated with sampling systems that store analyte's previous analysis.

1.4.6. Microfluidic interconnections standard challenges

Lab-on-a-chip development requires fluidic, mechanic, optical, and electronic interconnections. Complex engineering is necessary for efficient delivery of fluids into microfluidic systems, but the lack of an international lab-on-a-chip standard makes it difficult to produce fast prototypes, therefore the development relies on repeated creation of macro-to-micro interfaces (Whitesides 2011).

1.4.7. Fluidic automation and integration

For long-term phytoplankton monitoring applications the device should be fully autonomous. An ideal lab-on-a-chip device should be capable of automatically actuating the flow of fluids with reliable flow rates using inexpensive and compact instrumentation. The main components to handle fluids are pumps. There are two groups of micro pumps that can be used for a fully integrated and autonomous microdevice: mechanical micro pumps with moving parts, and non-mechanical micropumps without moving parts. There are many actuation principles for each group. These mechanical micropumps can be subdivided into quite a few categories: piezoelectric, pneumatic, electrostatic, thermal etc. The non-mechanical micropumps mainly include electrokinetic, magnetohydrodynamic, electrochemical and acoustic-wave techniques. Microvalves are also one of the most essential components for the realization of a totally integrated microfluidic system.

1.4.8. Fabrication challenges

In my view fabrication remains one of the greatest challenges. Lab-on-a-chip fabrication processes are still complex (especially when on-chip valves need to be integrated), time-consuming and difficult to translate for production scale-up. In addition polymers including PMMA can be degraded by long exposure to seawater⁵. Moreover, some current fabrication processes offer very poor reproducibility and different surface properties can lead to a chip-to-chip performance irreproducibility (Becker 2010). However the reproducibility issue can be addressed by integrating an internal reference into chemical or nucleic acid assay, for example a NASBA internal control (IC) (Hoorfar, Malorny et al. 2004; Rodríguez-Lazaro, D'Agostino et al. 2004). This is discussed in section 1.2.1, page 32 **Error! Bookmark not defined.**

⁵ <http://solutions-in-plastics.info/nl-be/datasheets/Transparante%20Kunststoffen/ERIKS%20-%20PMMA%20resistance%20to%20chemical.pdf>

Chapter 2 Cell lysis microchip

2.1. Cell lysis microchip summary

Objective

The phenomenon of electroporation of cell membranes, where an applied electric field leads to a pore or rupture of the cell membrane, has been known for several decades. Electroporation is used for molecular transport of molecules into (or out of) the cells subjected to electric field pulses, particularly as a means of introducing a range of drugs, DNA, antibodies and plasmids into cells (Prausnitz, Bose et al. 1993; Neumann, Kakorin et al. 1999; Weaver 2000). Electroporation of cell membranes can lead to a dramatic increase of permeability and if the electric field is high enough, it leads to irreversible mechanical breakdown of the membrane resulting in electrical cell lysis. Electric field-mediated lysis was observed by microscopy for yeast and plant protoplast cells (Lee and Tai 1999). As part of a complete bio-analysis microfluidic platform for RNA detection including the three key functions, cell lysis, RNA extraction and RNA amplification, we demonstrated a microchip for manipulation and electric field-mediated cell lysis of a phytoplankton species *K. brevis* using an array of interdigitated electrodes.

Background

Cell lysis (rupture of cellular membranes) is a key step in accessing RNA for molecular biology analysis. Current cell lysis methods applied to nucleic acid extraction are primarily chemical agent-based, these methods are slow, time consuming, necessitate handling of hazardous chemicals and requires human intervention (Price, Leslie et al. 2009). To obtain all sub-cellular materials without the complications of chemical and mechanical lysis, irreversible electric field induced breakdown of cell membranes can be used to obtain subcellular materials for nucleic acid extraction for further DNA or RNA amplification and analysis (see page 72, 2.2.3 Electroporation Theory)

Method & Results

Matlab™ simulations, experiments and results for a prototype lysis microchip are presented in this chapter. The microchip demonstrated the ability to lyse cells and release RNA from the nucleus of target cells. Dielectrophoresis (see page 66, 2.2.2 Dielectrophoresis background) was demonstrated. Cell membrane deformation and destruction was observed with bright field microscopy images, electroporation phenomenon was observed with fluorescence microscopy technique. Finally microchip lysis performance was validated against bench-top lysis using a commercial buffer using NASBA.

Features highlight

- Dielectrophoresis at 1V_{pp}, 200 kHz for 10 s duration was used to concentrate cells from suspension onto electrodes
- Total membrane destruction was observed at a voltage of 45 V, 600 kHz for 60 seconds duration.
- Optimal lysis conditions were found to be, 1 V, 120 s, and 30 V, 1 s
- The total amount of RNA extracted from each cell was

Conclusions

This work represents the first demonstration of electrical lysis for RNA extraction from phytoplankton cells. Lysis efficiency results were comparable to commercial bench top lysis methods, the amount of total RNA extracted from cells using electric field-mediated cell lysis was around 15 pg (well within the expected range of 10–30 pg for typical cells). However for on-site preparation (i.e. seawater medium), cells are in seawater which is a high conductive medium. This means that only negative DEP occurs and this is with a force weaker than positive DEP (real Clausius-Mossotti factor has a maximum value of 0.5 for negative DEP, see Figure 22). Moreover subsequent high electric field mediated lysis cannot be performed after negative DEP, as cells are attracted to low electric field zones. Therefore for on-site application cells need to be re-suspended or transferred into a non-conductive medium in order to enable positive DEP and high electric field mediated lysis. This could result in the implementation of a complex sample preparation technique. Please see published manuscript in the Journal of the Royal Society Interface, entitled “*Electroporation and lysis of marine microalga *Karenia brevis* for RNA extraction and amplification*” by M. M. Bahi, M.-N. Tsaloglou, M. Mowlem and H. Morgan (Bahi, Tsaloglou et al. 2010).

2.2. An introduction to dielectrophoresis and electroporation

Dielectrophoresis (DEP) occurs when a force is exerted on a polarisable particle, (e.g. a biological cell) when it is exposed to a non-uniform electric field (Li 2008). Electroporation is a phenomenon during which exposure of a cell to high voltage electric pulses results in a significant increase in its membrane permeability. For controlled use of the method in all applications, the basic mechanisms of electroporation need to be known. Different cell types and having different electrical properties can significantly affect the effectiveness of the dielectrophoresis and electroporation phenomenon. Understanding the phenomenon of electroporation, its mechanisms and optimization of all the parameters that affect electroporation is a prerequisite for successful treatment. Thus, electroporation parameters need to be specifically optimized for different cell types. In the section below theory is studied and optimal conditions are identified.

2.2.1. Electrostatic concept and polarisation effect

An electric charge can come in two types regarding the electron balance, positive charge (shortage of electrons) or negative charge (excess of electrons). Positively charged and negatively charged objects experience a Coulomb force in presence of an electric field:

$$F = QE$$

Equation 3

Where Q is the electric charge on the particle, E the external electric field vector and F the force induced by the external electric field. The surrounding electrical field E can also be given by:

$$E = \frac{1}{4\pi\epsilon} \frac{Q}{r^2} \hat{r}$$

Equation 4

Where r is the position vector to where the field is calculated, \hat{r} is the unit vector from the particle centre to the measurement location and ϵ is the electrical permittivity⁶. The force results in the displacement of charged particles, this phenomenon is called electrophoresis. Biological particles (e.g. cells) generally have a fixed surface charge density (usually negative) and observation of the movement of these particles in a uniform electric field (Electrophoresis) is commonly used in laboratory both to characterise and separate particles. Over a certain size range, the migration of linear biological particles varies with the logarithm of their molecular weights. Consequently particles sizes can be estimated by monitoring their migration relative to standard of known molecular weights. If

⁶ $\epsilon_0 = 8.854 \times 10^{-12}$ Farads m⁻¹

now we consider two charges, $-Q_1$ at a distance r from $+Q_2$ (i.e. dipole) the force⁷ between the two particles is:

$$F_{12} = \frac{Q_1 Q_2}{4\pi\epsilon r^2} \hat{r}_{12}$$

Equation 5

Dielectric particles are electrical insulators and can form an equivalent dipole (see Figure 18), under the influence of an external electric field. Their charge is neutral from a macroscopic point of view, but they locally show positive and negative charges. A permanent external electric field applied to a dielectric material makes charges reorganize, creating an internal electric field, due to the newly created dipoles. This is the polarization effect.

2.2.2. Dielectrophoresis background

When a dielectric is placed in an electric field, electric charges do not flow through the material, as in a conductor, but only slightly shift from their average equilibrium positions causing dielectric polarization. When a dielectric sphere is suspended in a dielectric liquid, under an uniform electric field the charges at the surface of the sphere attract counter charges (i.e. oppositely charged) from the liquid. This results to the formation of an induced equivalent dipole with no net force (see Figure 18).

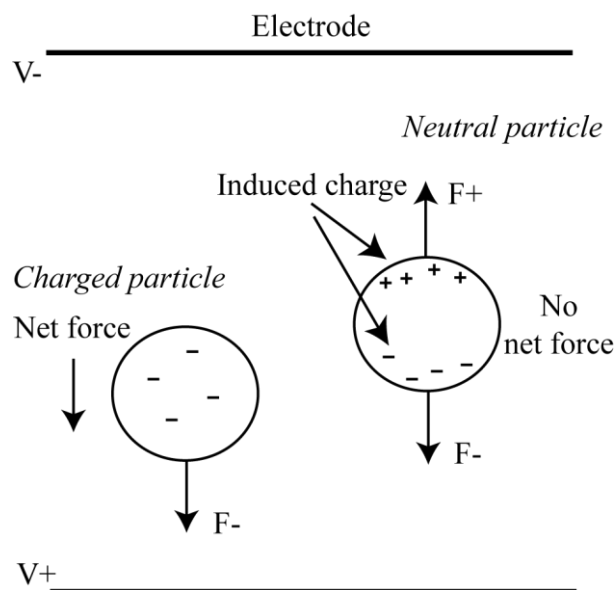


Figure 18 Particles under uniform field, the net force on the dipole is zero because an equal and opposite force acts on each half of the dipole.

⁷ The force is attractive if the two charges are opposite in sign and repulsive if they have the same sign. The force resulting from the action of Q_2 on Q_1 is equal and opposite.

If the same dielectric sphere is placed in a non uniform electric field, the two halves of the induced dipole experience a different force magnitude and thus a net force is produced. This is the dielectrophoretic force (see Figure 19).

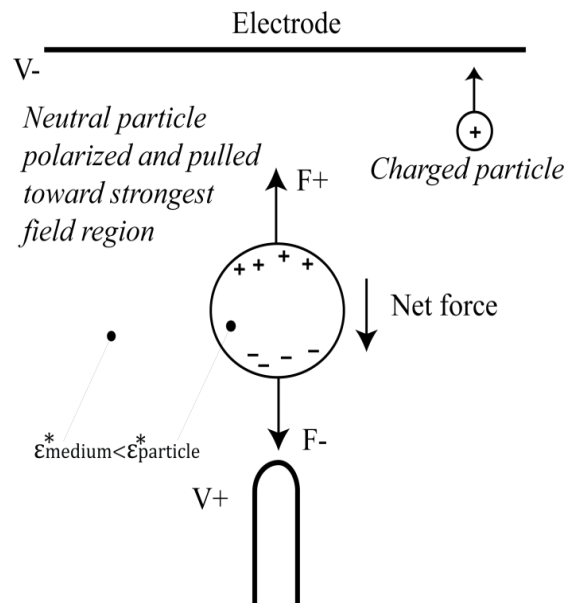


Figure 19 In non uniform field, the electrostatic force on each half of the sphere will be different, resulting in a net force on it.

The DEP force direction can be described by the Clausius-Mossotti factor, and depends on the relationship between the polarisability of the particle and the polarisability of the medium (Equation 7). For a spherical dielectric particle, the time averaged force is given by:

$$\langle F_{DEP} \rangle = \pi a^3 \epsilon_{\text{medium}} \text{Re}(f_{CM}) \nabla |E|^2$$

Equation 6

where a is the particle radius, ϵ_{medium} is the permittivity of the suspending medium, $\text{Re}(f_{CM})$ is the real part of the Clausius-Mossotti factor for the particle and the surrounding media and E is the peak value of the electric field vector. It is clear to see from the Equation 6 that the dissymmetry of the external electric field (i.e. need a gradient for DEP to occur - ∇E) is necessary to obtain the DEP force. The Clausius-Mossotti factor (f_{CM}) describes the frequency dependence of the effective polarisability and for a spherical, homogeneous particle is:

$$f_{CM} = \frac{\epsilon_{\text{particle}}^* - \epsilon_{\text{medium}}^*}{\epsilon_{\text{particle}}^* + 2\epsilon_{\text{medium}}^*}$$

Equation 7

Where $\epsilon_{\text{particle}}$ is the complex permittivity of the particle, and ϵ_{medium} is the complex permittivity of the medium. The Clausius-Mossotti factor gives the frequency (ω) dependence of the force, and its sign determines whether the particle experiences positive or negative DEP. The complex permittivity can be calculated from the electrical properties of a material with:

$$\epsilon^* = \epsilon - j \frac{\sigma}{\omega}$$

Equation 8

Where ϵ is the bulk permittivity of the material, σ is the conductivity, ω is the angular frequency of the applied electric field and j is the imaginary vector. If the particle is more polarisable than the surrounding media, then $\text{Re}(f_{\text{CM}})$ is positive and the DEP force directs the particle towards regions of high electric field strength (see Figure 19), the particle experience positive dielectrophoresis. Conversely, if the medium is more polarisable than the particle, $\text{Re}(f_{\text{CM}})$ is negative and the DEP force directs the particle towards regions of low electric field strength (generally away from the electrodes), the particle experience negative dielectrophoresis. It is important to recognise that for investigations into the spatial and frequency dependencies of the DEP force on spherical particles, one only needs to examine the Clausius-Mossotti factor and the radius of the particle. The direction of the DEP force is independent of the polarity of the applied voltage; different polarity does not change the direction of the DEP force. Thus DEP works equally well with both direct current (DC) alternating current and (AC) fields.

Therefore depending on the frequency, particles move either towards an electrode under positive DEP or away from an electrode under negative DEP.⁸ At a particular frequency the cross-over frequency (f_0) the DEP force will be zero and the particle will remain stationary, f_0 is given by (Jones and Kraybill 1986):

$$f_0 = \frac{1}{2\pi} \sqrt{-\frac{(\sigma_{\text{particle}} - \sigma_{\text{medium}})(\sigma_{\text{particle}} + 2\sigma_{\text{medium}})}{(\epsilon_{\text{particle}} - \epsilon_{\text{medium}})(\epsilon_{\text{particle}} + 2\epsilon_{\text{medium}})}}$$

Equation 9

It is worth noting that if we apply an electric field E with an alternative frequency, negative DEP or positive DEP can be observed. Above sufficiently high frequencies, none of the dipole polarisation mechanisms are able to switch rapidly enough to remain in step with the field. The dipole no longer possesses the ability to polarise. Figure 20a illustrates the dependency of the Clausius-Mossotti factor resulting in sign force modification (i.e. from positive DEP to negative DEP).

⁸ This occurs when the real part of the effective polarisability of the particle is exactly equal to that of the suspending medium (the point at which $\text{Re}(f_{\text{CM}}) = 0$)

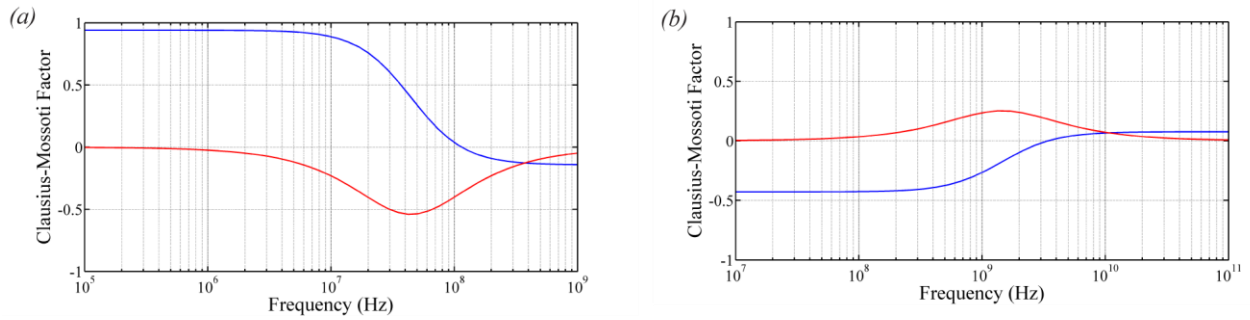


Figure 20 (a) Plot of the Clausius-Mossotti factor for a *K. brevis* cell (simple model) in low conductive medium, calculated using Equation 6 and the parameters in Table 4. In red $\text{Re}(f_{\text{CM}})$, in bleu $\text{Im}(f_{\text{CM}})$ (imaginary part of the Clausius-Mossotti factor), positive DEP occurs until 100 Mhz. (b) Plot of the Clausius-Mossotti factor for a *K. brevis* cell (simple model) in seawater, in red $\text{Re}(f_{\text{CM}})$, in bleu $\text{Im}(f_{\text{CM}})$. Weak positive DEP occurs from 3 GHz for *K. brevis* cells in seawater.

Characteristic	Symbol	Value	Note
Cell radius	A	10 μm	
Cell conductivity	σ_{cell}	0.5 mS/m	1
Cell permittivity	ϵ_{cell}	50	1
Medium conductivity	σ_{medium}	10.4 mS/m	2
Medium permittivity	ϵ_{medium}	80	3
Seawater conductivity	σ_{seawater}	5 S/m	
Seawater permittivity	$\epsilon_{\text{seawater}}$	40	

Table 4 Parameters used for the simulation of Clausius-Mossotti factor for *K. brevis* cells in low conductivity medium and seawater.

Notes:

1. Taken from Müller et al. 1998, snow algae dielectric parameters (Muller, Schnelle et al. 1998).
2. Measurement using Hanna EC215 Conductivity
3. calculated from σ_{medium}

2.2.2.a Cells parameters for dielectrophoresis:

Cells have a complicated internal structure and this result in complicated electrical properties. Shell models are typically derived from the cells physical structure, the most commonly used has a single shell representing the cell membrane with the rest of the internal volume representing the cytosol and cell interior, this is concentric multi-shell model (Irimajiri, Hanai et al. 1979; Gimsa, Marszalek et al. 1991). This results in a strongly frequency-dependent DEP for biological cells.

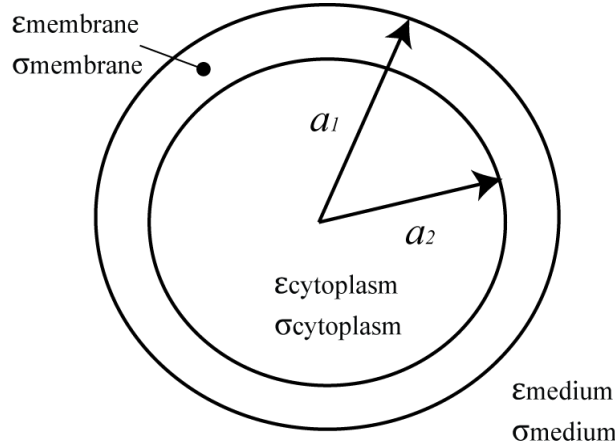


Figure 21 A single concentric shell model, typically used for modelling biological cells.

When a cell and its environment are separated into three phases, namely, the internal, the membrane and the external phases, as shown in Figure 21, the Clausius-Mossotti factor for the particle/medium system together (Equation 12 - $f_{CM \text{ cell}}$) can be calculated by determining first the Clausius-Mossotti factor for the particle itself (Equation 10 - $f_{CM \text{ cytoplasm-membrane}}$) and the equivalent complex permittivity for the particle (Equation 11 - $\epsilon_{\text{cytoplasm-membrane}}$) as shown by Huang et al. (Huang, Holzel et al. 1992) :

$$f_{CM \text{ cytoplasm-membrane}} = \frac{\epsilon_{\text{membrane}}^* - \epsilon_{\text{cytoplasm}}^*}{\epsilon_{\text{membrane}}^* + 2\epsilon_{\text{cytoplasm}}^*}$$

Equation 10

$$\epsilon_{\text{cytoplasm-membrane}} = \epsilon_{\text{membrane}}^* \frac{(a_2/a_1)^3 + 2f_{CM \text{ cytoplasm-membrane}}}{(a_2/a_1)^3 - f_{CM \text{ cytoplasm-membrane}}}$$

Equation 11

$$f_{CM \text{ cell}} = \frac{\epsilon_{\text{cytoplasm-membrane}}^* - \epsilon_{\text{medium}}^*}{\epsilon_{\text{cytoplasm-membrane}}^* + 2\epsilon_{\text{medium}}^*}$$

Equation 12

It is worth noting that the multi-shell model shows that cells exhibit a different frequency dependent behaviour to that predicted by single sphere simplistic models (see Figure 20a for the simple model

simulation and Figure 22 for the multi-shell model simulation). Figure 22 shows the real part of the Clausius-Mossotti factor changing from approximately 0.5 to 1 and then positive to negative as the frequency is raised.

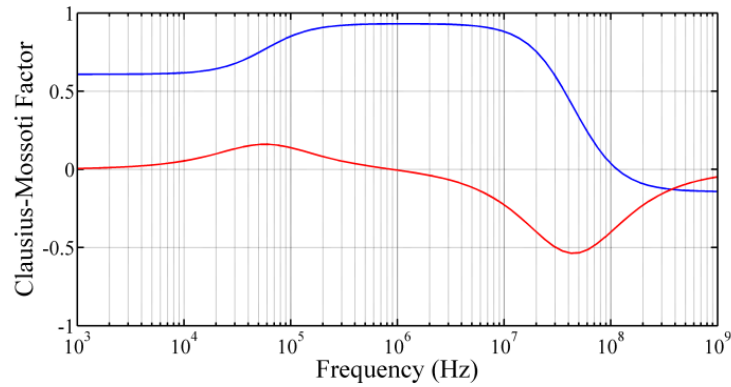


Figure 22 Plot of the Clausius-Mossotti factor for *K. brevis* cells, calculated using Equation 12 and the parameters in Table 5. In bleu $\text{Re}(f_{\text{CM}})$, in red $\text{Im}(f_{\text{CM}})$.

Characteristic	Symbol	Value	Note
Cell radius	a_1	10 μm	
Membrane conductivity	σ_{cell}	0.5 mS/m	1
Membrane permittivity	ϵ_{cell}	50	1
Cytoplasm conductivity	σ_{medium}	10.4 mS/m	1
Cytoplasm permittivity	ϵ_{medium}	80	1
Membrane thickness	$a_1 - a_2$	6 nm	1
Medium conductivity	σ_{medium}	10.4 mS/m	2
Medium permittivity	ϵ_{medium}	80	3

Table 5 Parameters used for the simulation of Clausius-Mossotti factor using the multi-shell model for *K. brevis* cells in low conductivity medium.

Notes:

1. Taken from Müller et al. 1998, snow algae dielectric parameters (Muller, Schnelle et al. 1998).
2. Measurement using Hanna EC215 Conductivity.
3. calculated from σ_{medium} .

2.2.3. Electroporation Theory

The phenomenon of electroporation of cell membranes, where an applied electric field leads to a pore or rupture of the cell membrane, has been known for several decades. Electroporation is used for molecular transport of molecules into (or out of) the cells subjected to electric field pulses, particularly as a means of introducing a range of drugs, DNA, antibodies and plasmids into cells (Prausnitz, Bose et al. 1993; Neumann, Kakorin et al. 1999; Weaver 2000). Electroporation of cell membranes can lead to a dramatic increase of permeability and if the electric field is high enough, it leads to irreversible mechanical breakdown of the membrane resulting in electrical cell lysis.

The key parameter for successful cell electroporation and electrical lysis is the induced critical transmembrane voltage (Zimmermann 1982; Tsong 1991; Weaver and Chizmadzhev 1996). Under normal conditions, the phospholipid bilayer in the cell membrane is a poor conducting medium, and it can mimic a capacitor. When the transmembrane voltage induced by an external electric field exceeds a certain threshold (normally 0.2–1 V), a rearrangement of the molecular structure of the membrane occurs, leading to pore formation in the membrane and a considerable increase in the cell membrane permeability to ions, molecules and even macromolecules (Teissie and Tsong 1981). Literature suggests that hydrophobic pores are enlarged by the presence of an electric field and thus rendered hydrophilic by an energetically more favourable reorientation of the bilipids of the membrane (Figure 23).

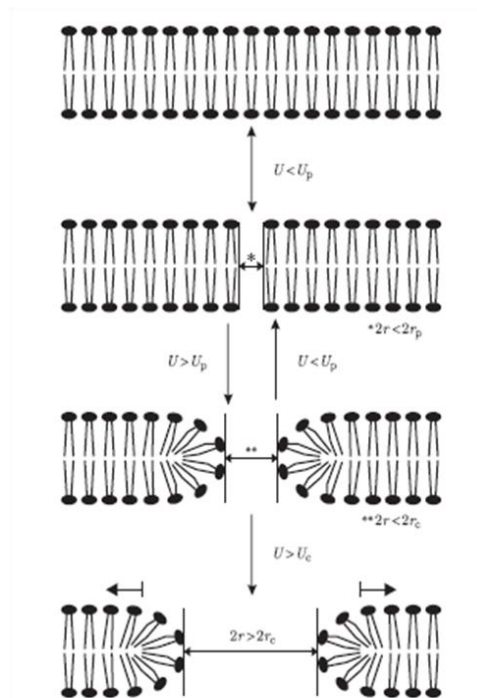


Figure 23 “Formation of an aqueous pore according to the model of electroporation. From top to bottom: the intact bilayer; the formation of a hydrophobic pore; the transition to a hydrophilic pore and a limited expansion of the pore radius corresponding to a reversible breakdown; unlimited expansion of the pore radius corresponding to an irreversible breakdown.” Taken from (Pavlin, Kotnik et al. 2008).

The transmembrane potential is usually measured by staining the cell membrane with a voltage-sensitive fluorescent dye. Under an electric field pulse, the spatial distribution of the induced potential is recorded using digital video microscopy at a submicrosecond time resolution (Gross, Loew et al. 1986). If the transmembrane voltage is higher than the critical threshold it also can lead to irreversible rupture and damage of the cell membrane resulting in molecular sub materials release and electrical lysis (Weaver 1993; Pethig and Markx 1997; Sedgwick, Caron et al. 2008). Transmembrane voltage is generated by an external electric field due to the difference in the electric properties of the cell membrane, external medium and cytoplasm. The transmembrane potential $\Delta\psi$ generated by an applied DC field may be calculated according the Maxwell relationship:

$$\Delta\psi = 1.5 * a * E_{\text{appl}} \cos \theta$$

Equation 13

Where E_{appl} is the applied field strength and θ is the angle between the field line and a normal from the centre of the sphere to a point of interest on the cell membrane.⁹ The electroporation of the cell membrane can be reversible or irreversible depending on the electric field strength and duration. The irreversible breakdown of the membrane causes cell membranes to burst open. The primary use of irreversible electroporation is to induce the death of undesirable cells without causing excessive heating. It can also be employed as a technique to electrically lyse cells for nucleic acids extraction prior further analyses (Coster 1965; Lee and Tai 1999; Brown and Audet 2008; de la Rosa, Tilley et al. 2008; Kim, Johnson et al. 2009).

If DC voltages are applied the large electric fields required to achieve lysis would result in bubbles (hydrogen and oxygen gases), as well as extreme pH conditions near the electrodes. To avoid such limitations AC electric fields can be employed (Lu, Schmidt et al. 2005). When an AC field is used, the situation becomes more complex, the imposed fields can exist across the cell membrane or the cytoplasm. Consequently, the induced transmembrane potential module becomes strongly dependent on the frequency of the applied field (Grosse and Schwan 1992):

$$\Delta\psi = \frac{1.5 * a * E_{\text{appl}} * \cos \theta}{1 + a * (G_{\text{membrane}} + i\omega C_{\text{membrane}}) * (\rho_{\text{int}} + \frac{\rho_{\text{ext}}}{2})}$$

Equation 14

Where C_{membrane} is the membrane capacitance and ρ_{int} and ρ_{ext} are the resistivities of the internal and external spaces. The model predicts (see Figure 24) that the transmembrane voltage decreases rapidly,

⁹ The conditions for Equation 13 to be valid are the following: a cell of the spherical shape, a much higher resistivity of the membrane than those of the internal and the external media, and a thin membrane compared with the radius of the cell. Moreover It is important to flag that Equation 13 is not anymore valid as the dielectric breakdown of the cell membrane occurs Chen, C., S. W. Smye, et al. (2006). "Membrane electroporation theories: a review." *Medical and Biological Engineering and Computing* **44**(1): 5-14..

owing to the decrease in membrane capacitive impedance, once a certain frequency is reached, and also predicts that applied field strength of 3×10^6 V/m (60 V applied) at 600 kHz will produce a transmembrane voltage of 1.53 V which can be sufficient to cause electrical lysis as this is significantly above the critical transmembrane threshold (estimated in the literature to be between 0.2 to 1 V).

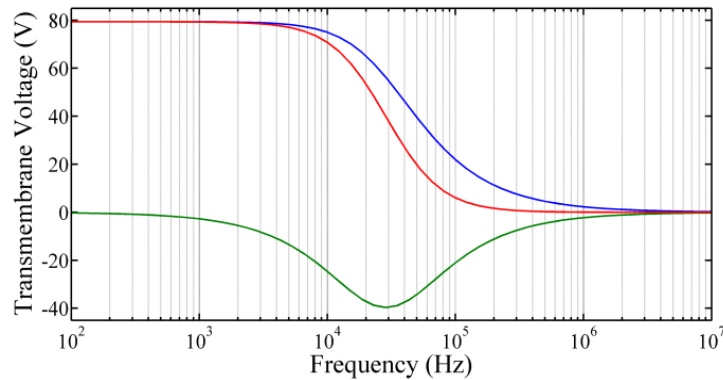


Figure 24 Plot of the approximate transmembrane potential induced on a *K. brevis* cell. The calculation is based on the Equation 14 using parameters in Table 6 . In bleu the absolute value of the transmembrane potential, in red its real part and green its imaginary part.

Characteristic	Symbol	Value	Note
Cell radius	A	10 μ m	
Membrane capacitance	C_{membrane}	8 mF/m ²	1
Membrane conductance	G_{membrane}	170 S/m ²	1
Resistivity of the cell interior	ρ_{int}	3.8 Ω m	2
Resistivity of the medium	ρ_{ext}	71 Ω m	3
Electric field	E_{appl}	3×10^6 V/m	4

Table 6 Parameters used for the calculation of transmembrane potential on *K. brevis* cells.

Notes:

1. The parameters extracted from the literature for similar marine alga, taken from Wang et al. and Müller et al. (Wang, Sukhorukov et al. 1997; Muller, Schnelle et al. 1998).
2. Taken from Wang et al., an internal cytosol conductivity of 0.26 S/m (Wang, Sukhorukov et al. 1997).
3. Calculated from Conductivity $\sigma_{\text{medium}} = 10.4$ mS/m at 20°C
4. Based on and estimated from Green et al. for a voltage of 60 V (Green and Morgan 1997).

The induced transmembrane voltage is a function of the applied field magnitude and frequency as shown in Figure 24 .The electrical potential that drops across the cell membrane can be calculated provided the cell dielectric properties are known (Grosse and Schwan 1992). There is very little literature describing the dielectric properties of marine organisms, and we did not specifically measure the properties of *K. brevis*. However, estimation of the transmembrane potential can be performed

using values typically found for most cells and marine organisms that have been studied previously, e.g. microalga *Chlorella protothecoides*, giant marine alga *Valonia utricularis* (Wang, Sukhorukov et al. 1997) and red/green snow algae (Muller, Schnelle et al. 1998). From the simulation, the transmembrane potential at 600 kHz is of the order of 3.06 V for an electric field of 3×10^6 V/m (60 V applied), 1.53 V for an electric field of 1.5×10^6 V/m (30 V applied) and 0.06 V for an electric field of 4×10^5 V/m (1 V applied). At 60 and 30 V the trans-membrane voltage seems to be sufficient to cause dielectric breakdown of the membrane and complete cell lysis (Weaver 1993; Pethig and Markx 1997). In our work positive DEP was performed using 1 V at 200 kHz generating a transmembrane voltage of the order of 0.16 V (from simulation) which is in the order of the critical transmembrane voltage (0.2 to 1 V) and could lead to cell permeability, however the transmembrane voltage induced might not be enough for complete electrical cell lysis. It is worth noting that positive DEP generates a higher trans-membrane voltage than the lysis configuration using 1 V at 600 kHz, this configuration was used to assess the impact of positive DEP on the cell lysis performance.

2.3. State of art of electroporation for cell lysis on-chip

Cell lysis is defined as disrupting cells by physical, chemical, mechanical, thermal or enzymatic means in order to obtain intracellular materials (Li 2008). Physical means include osmotic shock or pressure while mechanical lysis relies on mechanical breakdown of the cell membrane by shear and wear. In a recent study, a miniaturized mechanical lysis system based on a microfluidic filter region with nanostructured barbs achieving high lysis efficiency was demonstrated (Carlo, Jeong et al. 2003; Yun, Yoon et al. 2010). Detergents, solvents and antibiotics are used for the chemical method in order to solubilize the lipid membranes. The chemical lysis method is the most commonly used in laboratories, with well-established bench-top protocols (Sambrook and Russell 2001). A combined physical (using high pH level for osmotic shock) and chemical lysis device employing electrochemically generated hydroxide ions acting as alkaline lytic agents has been shown (Lee, Kim et al. 2010). Thermal lysis denatures proteins but leaves nucleic acids intact, and the Motorola Laboratories (USA) have developed a fully integrated chip using this method (Liu, Yang et al. 2004). The state-of-the-art in lysis microfluidic devices has been recently reviewed (Kim, Johnson et al. 2009) as well as single cell lysis on-chip (Sims and Allbritton 2007; Brown and Audet 2008) and general micro-electromechanical systems that include lysis steps (Huang, Mather et al. 2002; Lagally and Soh 2005) and electrical-based lysis microdevices for environmental applications (Jesús-Pérez and Lapizco-Encinas 2011).

Electroporation of cell membranes was first presented in 1965 (Coster 1965), since then several microdevices have been developed for electroporation. Electric field-mediated lysis was observed by microscopy for yeast and plant protoplast cells (Lee and Tai 1999). Human hepatocellular carcinoma cells transfected with green fluorescent protein genes were lysed on-chip by electroporation in a continuous flow microchip (Lin, Jen et al. 2001). Single-cell electroporation of human prostate

adenocarcinoma cells, reported by infiltration of YOYO-1 nucleic acid stain that cannot pass through intact cell membranes, has been demonstrated on-chip (Huang and Rubinsky 2003). A micro-electroporation device was used to lyse human colon carcinoma cells, confirming lysis with a vital stain of acridine orange and propidium iodide (PI) (Lu, Schmidt et al. 2005). Single plant protoplast cells as large as 85 μm were captured and lysed using two pairs of electrodes inside a pinched microchannel by applying an alternating voltage (Ikeda, Tanaka et al. 2007). Pulsed discontinuous current lysed *Bordella pertussis* bacteria and lysis was validated by DNA recovery using real-time PCR (de la Rosa, Tilley et al. 2008). Most recently, a similar device was described for the isolation and electroporation of A431 human epithelial carcinoma cells (Sedgwick, Caron et al. 2008). To our knowledge, no previous work has used electric field-mediated cell lysis-based microdevice for RNA analysis of phytoplankton species.

To obtain all sub-cellular materials without the complications of chemical and mechanical lysis, irreversible electric field induced breakdown (see section 2.2.3, page 72) of cell membranes can be used to obtain subcellular materials for Nucleic Acid extraction for further DNA or RNA amplification and analysis. We developed a microfluidic device for manipulation and cell lysis of a phytoplankton species *K. brevis* using AC electric field. We demonstrated concentration and electric field-mediated cell lysis of the phytoplankton *K. brevis* followed by extraction and amplification of RNA using bench-top NASBA methods. The electroporation lysis microdevice could be incorporated within a complete microfluidic RNA extraction and amplification system.

2.4. Electroporation and lysis of the phytoplankton *Karenia brevis* for RNA extraction and amplification

2.4.1. Materials and methods

An array of interdigitated electrodes was used to both concentrate cells by positive DEP (Lapizco-Encinas and Rito-Palomares 2007) and subsequently perform electric field-mediated cell lysis. We developed a simple electric field-based cell concentration and lysis method that could be incorporated within a complete microfluidic RNA extraction and amplification system. The micro-electrode chip consisted of a 3 mm \times 4 mm (length \times width) array of castellated interdigitated electrodes patterned on a 1 cm \times 1 cm piece of glass (see Figure 25). The electrodes were made of platinum with a thickness of 200 nm. The width and gap of micro-electrodes¹⁰ were 20 μm . *K. brevis* cells were attracted and trapped to the electrodes by positive DEP using an AC single phase of variable voltage and frequency. Lysis was performed using a high voltage, amplified with a Trimate AC generator (Model 1000A, Engler Engineering, USA). A miniaturized 3 x 4 x 3.5 mm (length \times

¹⁰ Electrodes were made from layers of titanium and platinum, patterned using photolithography and ion beam milling. (Philips Cambridge)

width x height) chamber was made from PMMA and glued to the microchip to hold the cell suspension.

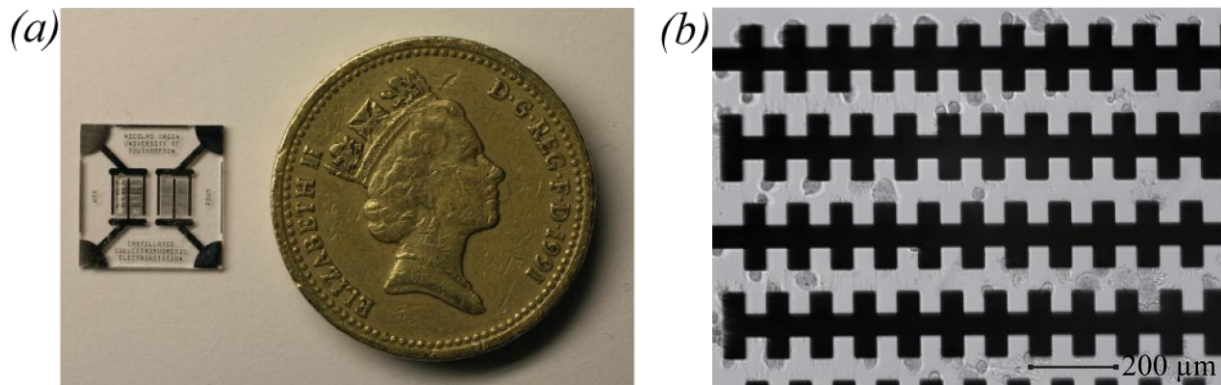


Figure 25 (a) Image of microchip using a UK pound coin for size reference. (b) Light microscopy image (20 magnification) of *K. brevis* cells captured on the micro-electrodes upon the application of 1 V at 200 kHz for 10 s.

2.4.1.a Cell culture

The *K. brevis* cell strain was kindly donated by the Purdie laboratory at the National Oceanography Centre (Southampton, UK). The cells were grown in L1 Aquil* artificial seawater media at 20°C with 12 L : 12 D at high irradiance. Cell samples were harvested during exponential cell growth. Cell growth was monitored by counting 1 mL culture aliquots fixed in 1 per cent Lugol's solution (Sigma–Aldrich, UK) in a Sedgwick-Rafter counting chamber (Fisher Scientific, UK).

2.4.1.b Sample preparation

For the device characterization cells were resuspended into a low conductivity medium. The sequential resuspension was performed in order to remove the presence of salt from the artificial seawater medium in which the cells were grown. Without resuspension, positive DEP and electroporation would not have been possible due to the high conductivity of seawater (add simulation with sea water Clausius-Mossotti). 1 mL aliquot of the cell culture was centrifuged at 20 000g for 1 min and the supernatant was discarded. The cell pellet was re-suspended in 1 mL of iso-osmotic low-conductivity buffer (280 mM mannose, 0.5% Tween, 10.5 mS m⁻¹ at room temperature). The sample was centrifuged and re-suspended three times. The supernatant was discarded without mixing and the pellet was dissolved in 250 μL iso-osmotic low-conductivity buffer to a final cell density of approximately 300,000 cells mL⁻¹. An aliquot of 42 μL of the iso-osmotic cell suspension was loaded into the PMMA chamber and cells were captured on the micro-electrodes by positive DEP (0.2 MHz, 1 V, 10 s). After the cells were trapped, the voltage and frequency was changed to perform cell lysis. The lysate was collected with a pipette and kept on ice. The process was repeated a further five times to process the 250 μL volume. The lysate was stored at -20°C for the NASBA process. To evaluate the efficiency of this method, the technique was compared with a commercial lysis protocol, which used lysis buffer and chemical extraction described in the Results section 2.4.2 (see page 78).

2.4.1.c Electroporation experimental

Given that cell disruption by electroporation requires the application of high electric fields, this device was designed to capture cells in the electroporation region by positive dielectrophoresis (DEP, 1Vpp 0.2MHz) before electroporation was conducted. The dielectrophoresis step was performed during 20 seconds before lysis. This condition was used before all lysis steps. Lysis conditions were optimized by observing the uptake of Propidium Iodide into the cells (Lu, Schmidt et al. 2005). PI was purchased from Sigma-Adrich, UK, has an excitation wavelength at 535 nm with emission at 617 nm, when DNA is bound to the dye and it was used to examine the effect of the electroporation on cell populations. Optimal voltage and frequency conditions were selected based on the accessibility of nucleic acids to PI under a fluorescence microscope by qualitative examination of fluorescence images. The PI solution at 50 mM was mixed into the iso-osmotic buffer and the cells observed with a fluorescence microscope during electroporation. Bright field observation of the cells was also conducted to image membrane damage.

The microchip lysis efficiency was validated against bench-top lysis using a commercial buffer containing chaotropic agent guanidine thiocyanate (Nuclisens Lysis Buffer, bioMérieux, The Netherlands). The experimental protocol RNA extraction kit was followed according to the manufacture's guideline. RNA from the cell lysate for both method microchip cell lysis and chemical lysis were purified using magnetic beads (Nuclisens miniMAG, bioMérieux, The Netherlands). The quality of the pure RNA extract was detected using a Nanodrop UV-VIS spectrophotometer (Thermo Fisher, UK). The pure RNA extract was amplified and measured with a bench-top NASBA instrument (EasyQ analyser, bioMérieux, Netherlands). Conditions for NASBA reaction have been previously described (Bahi, Tsaloglou et al. 2010). Cell cultures were lysed and analysed by NASBA on the same day to avoid degradation of RNA.

2.4.2. Results

Cells were concentrated onto the electrodes using an AC voltage of 1 Vpp and a frequency of 200 kHz, applied for 10 s. It is important to flag that only viable cells were captured as the DEP behaviour of non-viable cells is completely different to viable cells (Huang, Holzel et al. 1992), moreover non-viable cells would not have any RNA suitable for subsequent NASBA analysis. Figure 25 shows an image of the phytoplankton cells collecting at the electrode tips by positive DEP in iso-osmotic low-conductivity buffer. Positive DEP was observed for these cells from 70 to 600 kHz in accordance with the CM factor simulation (see real part of the Clausius-Mossotti factor in the Figure 22). Below 70 kHz, the cells did not move which might be due to the weaker DEP force at these frequencies range (see real part of the Clausius-Mossotti factor in the Figure 22); frequencies higher than 600 kHz could not be used because of the limited bandwidth of the amplifiers used in this work.

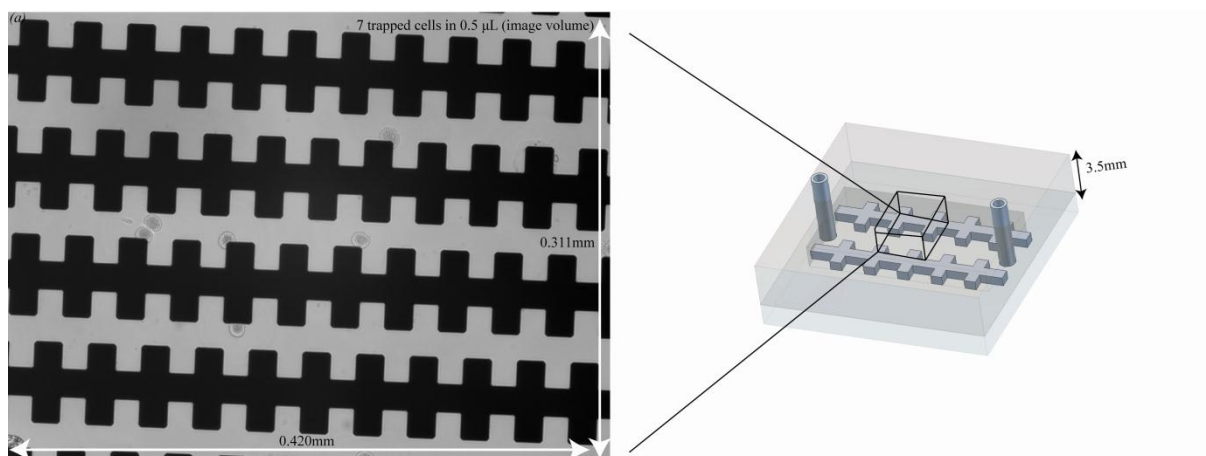


Figure 26 Estimation of the capture efficiency.

An estimation of the percentage trapped cells has been performed. For this estimation, 42 μL of cell suspension containing 585 cells was loaded onto the electrodes. A typical image of the electrode (see Figure 26) has a volume of 0.5 μL , which on average should contain 6.9 cells. A typical image contains between up to 10 cells (~7 cells on this image) indicating an efficiency of capture of nearly 100%. This does not take into account any cells losses during manipulation e.g. by adhesion to pipette tip walls.

The experimental conditions used for cell lysis were selected to maximise the applied voltage dropped across the cell membrane. If the frequency is too high, the field is no longer dropped across the membrane, while at low frequency the transmembrane voltage is significantly higher and can damage irreversibly bio-molecules and microchip electrodes. For this reason and in accordance with the transmembrane voltage simulation (see Figure 24), a frequency in the region of 600 kHz was used.

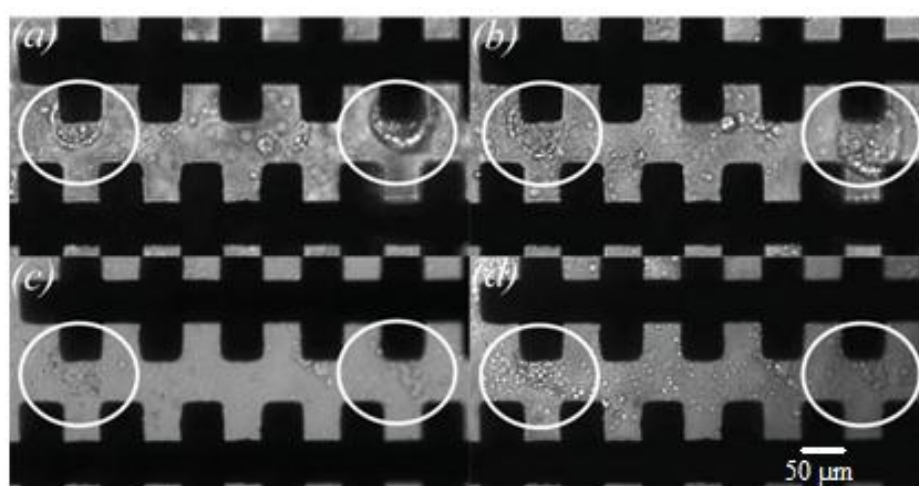


Figure 27 Membrane deformation and pore formation of *K. brevis* cells: (a) pre-electroporation under cell trapping of 1 V field at 200 kHz for 20 s. Two distinct cells, encircled white, can be observed trapped on the micro-electrodes. (b) Post-electroporation of 60 V field at 600 kHz for 5 s. Membranes of the encircled cells are becoming disrupted owing to the formation of pores by the continued application of an electric field. (c) Post-electroporation of 60 V at 600 kHz for 10 s. Poration of the encircled cells is so extensive that intracellular

material is escaping into the iso-osmotic low-conductivity buffer. (d) Post-electroporation of 60 V at 600 kHz for 15 s, the encircled cells have become completely disrupted and no distinct cell membranes can be observed.

After collecting the cells, the frequency and voltage was changed to induce electroporation. Figure 27 shows that upon application of 60 V at 600 kHz, the cells deform and undergo morphological changes, as shown by the sequence of images (see Figure 27). Two cells are shown (ringed), immediately after DEP trapping and then 15 s after application of a higher voltage. The figure shows that the cell membranes have been destroyed and the cytoplasm has leaked into the medium. In many occasions, a slight elongation of cells along the field lines was observed.

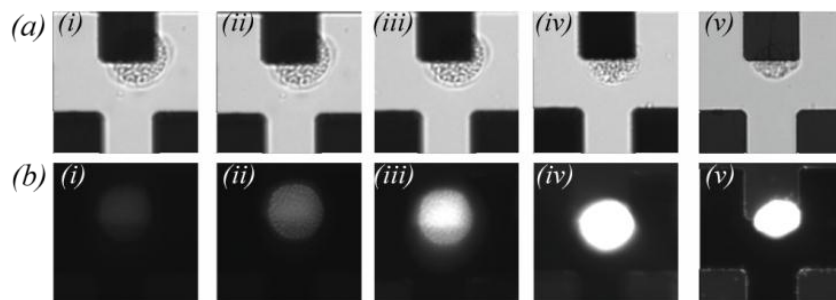


Figure 28 Micrographs showing the process of single-cell electroporation of *K. brevis* temporary cysts. (a) Bright-field images on the application of 45 V at 600 kHz captured at (i) 0 s (ii) 30 s (iii) 1 min (iv) 1.5 min and (v) 2 min. (b) Epi-fluorescence images collected simultaneously at an excitation of 536 nm and emission of 593 nm.

Further confirmation of cell electroporation was obtained by examining the uptake of PI in Figure 28. This molecule is weakly fluorescent in solution but its excitation maximum increases 20-fold when bound to DNA. It is membrane impermeant and is a good indicator of cell plasma membrane damage. Fluorescence images were acquired before and after electroporation at a frequency of 600 kHz and voltage of 45 V. This lower voltage was used to increase the time taken to achieve electroporation to 15 s because at 60 V electroporation was too fast to image. The PI was incorporated into the cells indicating that the membranes are electroporated. We could observe the scatter of the fluorescence across the chip, which could be the result of the DNA materials diffusing outside the lysed cells.

After qualitative selection of the optimal lysis condition by observing the PI fluorescence, lysis on microchip followed by RNA detection using NASBA were performed to establish the optimal microchip lysis conditions suitable for subsequent RNA extraction and amplification. Cells were captured and then lysed by high electric field using different voltages and times, in order to evaluate the yield and purity given by the different voltage/time combinations (at 600 kHz, 1, 30, and 60 Vpp, 1, 30, 60 and 120 seconds). Data summarised in Figure 29 show the yield and purity, they are expressed normalized to control experiments with RNA extracted using the commercial lysis buffer (for the same cell concentration). A negative control experiment indicated that some RNA was always present in the sample, but the amount was small and highly variable. The initial assumption was that no RNA would be released at low voltage (1V) since the transmembrane potential is quite low (i.e. 0.16 during DEP

and 0.06 V during lysis). However, there appears to be damage that is sufficient to release measurable amounts of RNA. The RNA release at this low voltage is slow, but does indicate that at even these low voltages, DEP manipulation of cells produces enough damage to release RNA. Figure 29a shows data for electric field mediated cell lysis at 1 V and indicates that RNA yield increases with time of exposure. Increasing the voltage to 30 V or 60 V gives the data in Figure 29b, c. The RNA yield is high and comparable to that obtained after 120 s at 1 V (Figure 29a). However, for the 30 V data, the yield is approximately twice that obtained using the commercial buffer but diminishes with time. At 60 V, yield is also better than the commercial buffer but the RNA degrades with time. Electroporation for longer than 60 s caused boiling at the electrodes and loss of the sample.

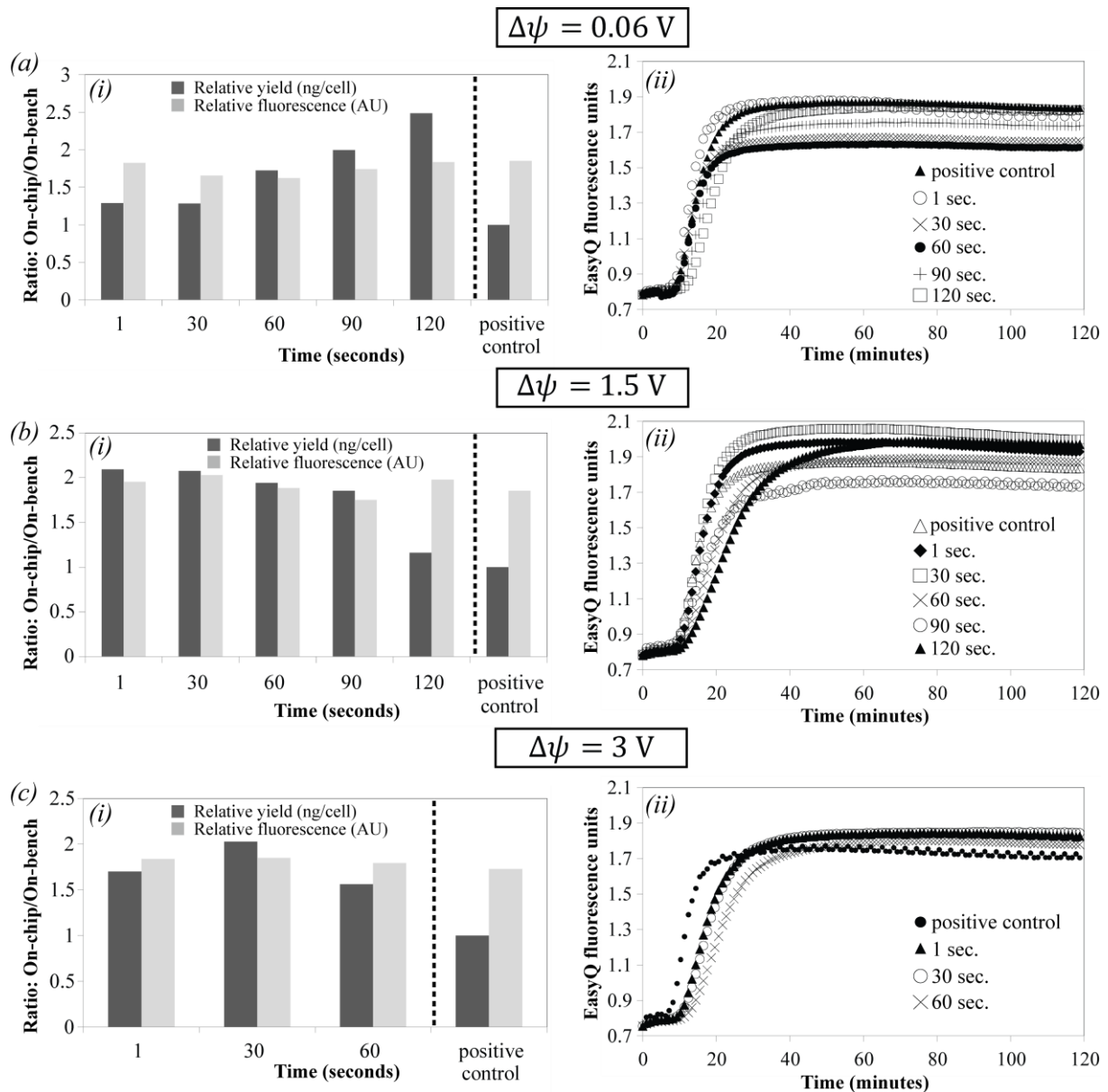


Figure 29 Identification of optimal electroporation conditions: (a) On-chip lysis using a 1 V field for five different time intervals: (i) yield and purity results (black bars, relative yield; grey bars, relative fluorescence) and (ii) NASBA amplification data. Triangles, positive control; white circles, 1 s; crosses, 30 s; black circles, 60 s; plus symbols, 90 s; squares, 120 s. Increasing duration of electroporation led to increased yield of RNA extracted from the cell lysate. (b) On-chip lysis using a 30 V field for five different time intervals: (i) Yield and purity results (black bars, relative yield; grey bars, relative fluorescence) and (ii) NASBA amplification data. White triangles, positive control; diamonds, 1 s; squares, 30 s; crosses, 60 s; circles, 90 s; black triangles, 120 s. Electroporation that lasted longer than 60 s caused the yield of RNA extracted from the cell lysate to decrease. (c) On-chip lysis using a 60 V field for different time intervals: (i) Yield and purity results (black-filled bars, relative yield; grey-filled bars, relative fluorescence) and (ii) NASBA amplification data. Black circles, positive control; triangles, 1 s; white circles, 30 s; crosses, 60 s. Data show that electroporation of 60 V was more effective than the bench-top alternative but appeared to degrade the quality of extracted RNA from the lysate.¹¹

¹¹ Normalisation was performed by dividing the RNA yield (from NASBA) of the on-chip electroporated cells to the value measure using the commercial buffer for the same number of cells.

2.5. Discussion and conclusion

This work has demonstrated dielectrophoretic concentration and electric field-mediated cell lysis of the marine microalga *K. brevis*. We used phytoplankton cells, which are non-mammalian targets chosen for their environmental relevance (they are a harmful algal bloom species) and the fact that they are difficult to break. The latter enabled us to produce a device suitable for robust cells. For the same reasons, other laboratories have used bacterial spores of *Bacillus subtilis* and *Bacillus thuringiensis*, non-pathogenic simulants of anthrax (Belgrader, Young et al. 2000; Lapizco-Encinas, Davalos et al. 2005) and *Bacillus subtilis* var. *Bacillus niger* (Hoettges, Hughes et al. 2003). Electric field-mediated cell lysis produced a high yield of RNA and in most cases pure RNA with amplification efficiency that was comparable with the commercial lysis buffer. High voltages did not interfere with the amplification and detection of the RNA target, but yield was diminished after long-term exposure to the field. In terms of developing a system for sensitive and accurate RNA extraction and amplification, the optimum conditions are either a long exposure of cells to a low voltage (120 s, 1 V) or short exposure at higher voltage (1 s, 30 V), both of which give the best quality and quantity of RNA. The amount of total RNA extracted from each cell using electric field-mediated cell lysis was around 15 pg, well within the expected range of 10–30 pg for typical cells (Alberts, Bray et al. 1986).

DEP does not require the particle to be charged in order to manipulate it; the particle must only differ electrically from the medium that it is in. DEP technique works with AC fields, whereas no net electrophoretic movement occurs in such a field. Large electric fields required to achieve lysis would create bubbles (hydrogen and oxygen gases), as well as extreme pH conditions near the electrodes in DC mode. To avoid such limitation AC electric fields could be employed which will minimise water electrolysis. Moreover, the use of AC fields reduces membrane charging of biological cells. As explained in section 2.2.3, the transmembrane potential, which can impact cell physiology, can be diminished by the application of high-frequency fields while cells are trapped. In contrast with electrophoretic forces, DEP forces increase with the square of the electric field (described in section 2.2.1, page 65), whereas electrophoretic forces increase linearly with the electric field. Furthermore the micro technology offers the possibility of creating micro-electrodes and therefore enables strong electric fields to be created with otherwise comparatively low voltages¹². Moreover mediated cell lysis is very versatile; lysis and electroporation can be effective with cells and species with different dielectric parameters.

However the microchip described above is not highly selective, the method does not enable cell sub-populations to be trapped and lysed selectively (i.e. cells size have to be consequently different to see selective DEP with this microchip). The use of electrodes often leads to using glass materials for chip

¹² Compare to macro scale lysis system, the microchip cell lysis device can reduce the voltage required for cell lysis because the electrode gap can be easily fabricated in a size comparable to the size of biological cells.

substrates, resulting in complicated and expensive fabrication processes (compare to plastic technology). For on-site preparation (i.e. seawater medium), cells are in seawater which is a high conductive medium. This means that only negative DEP occurs and this is with a force weaker than positive DEP (real Clausius-Mossotti factor has a maximum value of 0.5 for negative DEP, see in section 2.2.2, page 66). Moreover subsequent high electric field mediated lysis cannot be performed after negative DEP, as cells are attracted to low electric field zones. Therefore for on-site application cells need to be re-suspended or transfer into a non conductive medium in order to enable positive DEP and high electric field mediated lysis. A system could be developed where seawater samples containing cells are passed through a porous filter, if pores are smaller than cells size, cells would stay on the filter and could be washed away using a low conductivity medium. It should be noted that high electric field mediated lysis requires using high voltages and high frequency requiring instruments which are often bulky and difficult to integrate.

The work above is a unique example of phytoplankton electrical cell lysis followed by NASBA, showing compatibility with nucleic acid amplification technology. Although the microchip would be difficultly integrated in a system for on-site analysis of seawater-based samples, it has the potential for laboratory applications and to be part of a complete microfluidic system for sub-cellular analysis of RNA using NASBA. A typical lab-on-a-chip system would include RNA extraction and purification, and species-specific nucleic acid detection. In the next chapter we present an alternative technique that we developed for cell concentration, lysis and RNA extraction and purification.

Analysis of the cells lysis microchip	
Strengths	Weaknesses
<ul style="list-style-type: none"> • Non-hazardous method. • Microchip's performance comparable to commercial bench top lysis method. • Fast lysis technique (from 120 s to 1 s). • Versatile lysis method can be used for different cell species. (electric field can be adjusted regarding cells characteristics, see Equation 14). 	<ul style="list-style-type: none"> • Laborious sample preparation technique (i.e. need sample medium modification to allow dielectrophoresis). • Partial preparation step (only lysis step performed on-chip, no nucleic acids extraction and purification). • Expensive and complex fabrication process (i.e. glass chip). • Non selective method - cell sub-populations cannot be well distinguished (i.e. during dielectrophoresis). • Complex electronic full integration (i.e. high voltage and frequency electronic). • Stop flow method.
Opportunities	Threats
<ul style="list-style-type: none"> • Unique work on electrical lysis for phytoplankton. • NASBA compatibility - can be part of a "sample-in" "answer-out" system. 	<ul style="list-style-type: none"> • Phytoplankton species are especially difficult to lyse. • Technology limitations for possible improvement (i.e. medium modification technique). • Simpler alternative methods already available. (see page 41, 1.3.1)

Table 7 Analysis of the cells lysis microchip.

Chapter 3 RNA sample preparation microdevice

3.1. RNA sample preparation microdevice summary

Objective

For a complete bio-analysis microfluidic platform for RNA detection four key functions are required i.e. concentration, cell lysis, RNA extraction and RNA amplification. We demonstrate here and test a microchip that performs the first three of these functions i.e. cell concentration, cell lysis and RNA extraction. The device is based on the use of an aluminium oxide filter.

Background

For a fully integrated portable nucleic acid device with “sample-in” to “answer-out” capability, all the steps needed for the analysis including sample preparation must be performed. Cost and size reductions are best delivered using integrated a lab-on-a-chip technology. A challenge in sample preparation techniques for molecular detection assays is the complex nature of real environmental samples which might contain non-targeted molecules and microorganisms (i.e. bacteria, non-targeted cells species, pollutants, sediments) that may interfere, particularly when the targeted microorganism is present in lower concentrations. To ensure the presence of a sufficient quantity of targeted microorganism in the sample, bench-top sample preparation methods use large volumes of bio-sample (e.g. > 1mL) and concentration methods using bulky

Features highlight
<ul style="list-style-type: none">• At least 200,000 cells can concentrate onto the filter in microdevice.• The RNA binding efficiency of the microdevice method was 47.1%.• As few as 10 <i>Karenia mikimotoi</i> cells prepared on-chip gave sufficient RNA for Bioanalyzer detection.• The number of <i>K. brevis</i> cell necessary for obvious successful detection was 2,500 cells prepared using the microdevice.• A limit of performance of 1,000 <i>K. brevis</i> cells prepared on-chip was estimated for successful subsequent NASBA.

equipment. This presents a challenge for miniaturised microfluidic devices since the technology is based on the use of small volumes (e.g. > few μ L). These challenges can nonetheless be addressed by integrating concentration or enrichment/separation functions into a microfluidic platform to increase the amount of targeted microorganism during the sample preparation step.

Methods & Results

Experiments and analysis results are presented in this chapter. All steps in the sample preparation procedure are performed within a single disposable chip; cell pre-concentration, cell lysis, RNA extraction, and RNA purification. The concentration step was demonstrated using an aluminium oxide filter on-chip. The operating range (in terms of cell number) of the filtration / concentration system was assessed by measuring the pressure across the system. RNA capture efficiency was compared to a commercial bench top extraction system. Finally micro device extraction performance was validated against bench-top extraction system.

Conclusions

We have reported the first demonstration of a sample preparation micro device for phytoplankton *K. brevis* cells in complex sample matrix. The on-bench system demonstrated better performances in terms of RNA extraction efficiency, however the microdevice has the advantages of performing cell concentration and extraction providing better RNA quality, and could potentially be used for on-site sample preparation.

3.2. Nucleic acid preparation method and quantification

Prior to nucleic acid analysis, sample preparation is needed to isolate the specific compound, to remove substances that interfere with the assay and also sometimes to concentrate the analyte. Nucleic acid must be:

- 1) released from the cells (lysis step)
- 2) extracted from the lysate
- 3) concentrated
- 4) purified

Each of these four sample preparation steps and their implementation on-chip in the context of a field-deployable system is discussed below. Extraction and purification before nucleic acid analysis is necessary to remove endogenous contaminants found in cell lysate, or interfering substances from the sample matrix that can reduce amplification and detection efficiency. Nucleic acid extraction and purification is described as isolation, concentration and cleansing of nucleic acid from lysate for molecular analysis by chemical interaction.

3.2.1. Sample extraction methods

In early studies, nucleic acid was extracted using centrifugation-based density gradient methods (Price, Leslie et al. 2009). This method was based on nucleic acid migration across a caesium chloride (CsCl)/ethidium bromide (EtBr) gradient until reaching stabilisation point. Alternatively, the classic phenol chloroform phase separation method is a liquid-liquid extraction technique regularly used for nucleic acid extraction (Logemann, Schell et al. 1987). The lysate is dissolved in chloroform and phenol containing guanidinium thiocyanate (GuSCN) which also acts as a lysis buffer. This method relies on phase separation by centrifugation. Nearly all of the RNA is present in the aqueous phase, while DNA partitions in the interface (Brown 2001). Other methods use detergents like cetyl-trimethyl ammonium bromide (Murray and Thompson 1980) or alkaline buffers (Birnboim 1983). The latter was developed by Birnboim and Doly, and uses sodium dodecyl sulfate as a lysis buffer, followed by neutralization with a high concentration of low-pH potassium acetate. This generates selective precipitation of the nucleic acid and other high molecular weight cellular components. The nucleic acid remains in suspension and is precipitated with isopropanol. All the above methods exhibit many drawbacks: they are time-consuming, need bulky equipment (i.e. centrifuge) and use hazardous chemicals (Gjerde, Hoang et al. 2009).

Solid phase extraction (SPE) is the extraction technique most widely used in laboratories and is both fast and selective (Gjerde, Hoang et al. 2009). SPE is defined as the extraction of an analyte (e.g. nucleic acid) from a liquid sample matrix (e.g. lysate) onto a solid sorbent (e.g. silica column) using surface interactions chemistry between the analyte and the sorbent. SPE for nucleic acid can be

performed using different materials such as silica particles, glass particles, diatomaceous earth or anion-exchange materials (Elgort, Herrmann et al. 2004; Margraf, Page et al. 2004; Dames, Bromley et al. 2006; Tan and Yiap 2009). These methods utilise the binding interactions between the solid phase and nucleic acid, which, depending on functionalisation, can be either pH or salt-controlled.

Silica-based extraction methods are the most commonly used technique for nucleic acid SPE. In 1990, Boom and co-worker presented a simple extraction method to address previous difficulties with the traditional labour-intensive and hazardous-liquid-based isolation technique (Boom, Sol et al. 1990). The technique is based on the binding of nucleic acid in the presence of a chaotropic salt solution, such as guanidinium thiocyanate, to the surface of silica particles. Salts can have chaotropic properties by shielding charges and preventing the stabilization of salt bridges. Chaotropic salt solutions have the ability to disrupt the regular hydrogen bond structures in water. Hydrogen bonding profoundly affects the secondary structure of polymers such as DNA, RNA, and proteins. Thus chaotropic agents could unfold proteins, destabilize hydrophobic aggregates and increase the solubility of hydrophobes (Collins 1997). Guanidinium thiocyanate is used to lyse cells and virus particles during RNA and DNA extractions (Gjerde, Hoang et al. 2009). Its function is also to denature nuclei of (Deoxyribonuclease (Dnase) and Ribonuclease (RNase)), as they would otherwise damage the extracted solution (Meese and Blin 1987; Coombs, Pigott et al. 1990; Gjerde, Hoang et al. 2009).

Different theoretical mechanisms are proposed for nucleic acid-silica binding in chaotropic solutions. Melzak et al suggested that the DNA adsorption process is controlled by three competing effects: (i) weak electrostatic repulsion force, (ii) dehydration effects and (ii) hydrogen bond formation (Melzak, Sherwood et al. 1996).

- i. The phosphate diesters on the backbone of the nucleic acid are negatively charged, as are the molecules on the surface of the silica particles. At a low ionic strength the net electrostatic force will cause repulsion between the two molecules. Based on The Debye–Huckel theory, in high ionic strength solutions the negative potential of sorbent surface (silica) will tend to be reduced by counter ions condensation from the chaotropic solution, resulting in a reduction of the overall repulsion force between nucleic acid and silica particles.
- ii. In presence of chaotropic salts, water molecules are “captured” by salt molecules resulting in a decrease in the quantity of free water molecules in solution (Sposito 1989).¹³ The reduction of available free water molecules reduces the hydrophilic character of the silica hydroxyl (-OH) surface by adding high concentration salt solution. This process could drive the adsorption mechanism between the nucleic acid and silica sorbent (it is worth noting that dehydration effects are also the primary contribution to the driving force for protein adsorption).

¹³ In our device we used a filter aluminium oxide (Al_2O_3), when the surface is hydrated, water is chemisorbed to convert the top layer of oxide ions to a filled, square lattice of hydroxyl ions, hydroxyl groups might promote nucleic acid adsorption.

- iii. Intermolecular hydrogen bonding to protonated surface silanols ($\text{SiO}_3\text{-O}^-$) contributes slightly to the driving force for adsorption at neutral pH.

As a result, dehydration effects and intermolecular hydrogen bond formation over-compensate the net electrostatic repulsion and drive nucleic acid adsorption to the silica surface

Nguyen et al. proposed that nucleic acid-silica surface binding is driven by processes described by the Derjaguin-Landau-Verwey-Overbeek theory (Derjaguin and Landau 1941). In the presence of divalent cations such as Na^{2+} , the negative charges on the phosphate diesters on the backbone nucleic acid are screened (Na^{2+} ions of opposite charge to that of the nucleic acid tend to cluster nearby). This results in a decrease in the electrostatic energy barrier between the silica surface and the nucleic acid and an increase in adsorption rate by creation of a Na^{2+} ion bridge between the nucleic acid molecules and the silica surface as shown in Figure 30 (Nguyen and Elimelech 2007).

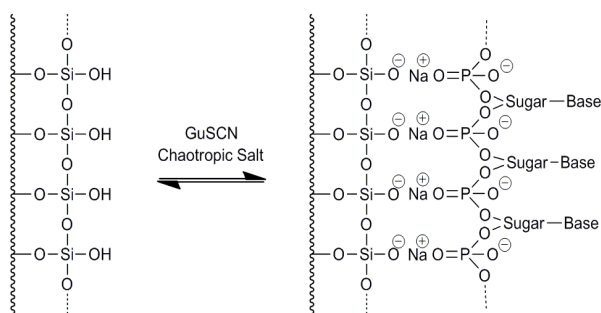


Figure 30 Principle of nucleic acid adsorption on silica substrate.

After nucleic acid binds onto silica particles, the solution is washed to remove sub-cellular materials, protein contamination, salt, and cellular debris while the nucleic acid remains bound. Then the nucleic acid is eluted in a low salt, aqueous buffer.

Many commercial kits based on solid phase silica extraction are available. These include GeneClean[®] (Q-BIOgene), QiaAmp[®] (Qiagen), NucleoSpin[™] (Macherey-Nagel), UltraClean[®] (MO BIO Laboratories), GenElute (Sigma Adrich, UK), easyMAG[®] (Biomérieux), and others. High throughput automated nucleic acid extraction systems have been designed for medium to large laboratories (Tan and Yiap 2009). These include the Qiagen Biorobot EZ1¹⁴, Beckman Coulter Biomek 3000¹⁵, Nuclisens[®] Easymag^{®16}, and QuickGene-810 systems¹⁷, and iPrep[™] Purification Instrument¹⁸ by Invitrogen[™]. The automation afforded by these systems is beneficial for a number of reasons, including the reduction of working time, decreased labour costs, increased worker safety, and

¹⁴ <http://www.qiagen.com/products/automation/instrumentservice/iqqservicesbiorobotez1.aspx>

¹⁵ http://www.beckmancoulter.com/products/instrument/automatedsolutions/biomek/biomek3000_inst_dcr.asp

¹⁶ http://www.biomerieux.fr/servlet/srt/bio/france/dynPage?doc=FRN_CLN_PRD_G_PRD_CLN_42

¹⁷ http://www.fujifilm.com/products/life_science_systems/nucleic_acid_isolation/qg810

¹⁸ <http://www.invitrogen.com/site/us/en/home/Products-and-Services/Applications/Nucleic-Acid-Purification-and-Analysis/Automated-Nucleic-Acid-Purification/iPrep-Purification-Instrument.html>

increased reproducibility and quality of results. Most silica-based techniques require the use of centrifugal equipment during extraction to concentrate the silica-nucleic acid complex during washing and processing. However this requirement can be eliminated by using silica coated magnetic beads which can be concentrated with a magnetic field (i.e. Nuclisens® Easymag®). SPE techniques are generally more appropriate than liquid-liquid extraction techniques for micro device applications, and the use of silica coated magnetic beads is also advantageous as then centrifugation is not required.

ChargeSwitch® technology (ChargeSwitch®, Invitrogen, UK) is another commercialised nucleic acid extraction technique based on an ion-exchange mechanism controlled by the pH of the solution. The beads bind nucleic acid at pH <6.5 and elute at pH >8.5 (Liu, Lien et al. 2009). Alternatively, Dynabeads (Dynabeads®, Invitrogen, UK) have also been developed for nucleic acid isolation based on the functionalization of magnetic beads. RNA can be extracted by introducing coated beads with an oligodeoxythymidylic acid dT (oligo (dT)). RNA with a polyadenylation-A (poly-A) tail attach to the oligo (dT) which minimizes the non specific binding of other nucleic acids and ensures the purity of mRNA (Hong, Studer et al. 2004; Lee, Jung et al. 2010).

3.2.2. Measurement of nucleic acid quantity and quality

3.2.2.a UV absorption methods

The efficiency of sample preparation methods can be assessed by measurement of the yield and purity of the nucleic acid extracted. Nucleic acid concentration and purity can be determined by UV spectrophotometric analysis. Measuring the UV absorption is the easiest and most rapid method for determining yield and purity (Gjerde, Hoang et al. 2009). The absorption of light at 260 nm is proportional to the concentration of nucleic acid. The ratio of the absorption at 260 nm (OD_{260}) and the absorption at 280 nm (OD_{280}) (i.e. OD_{260}/OD_{280}) gives a qualitative measure of nucleic acid purity. It is important to note that absorption in the region of 230 nm shows a strong correlation with other absorbing contaminants such as proteins, chaotropic salts (such as guanidinium isothiocyanate) and phenol and could therefore lead to an overestimation of nucleic acid concentration (Bustin, Benes et al. 2009; Price, Leslie et al. 2009). Commonly these contaminants are present in the sample or in the eluent derived from the standard SPE extraction method (Fleige and Pfaffl 2006). In addition the UV absorption method does not discriminate between single strand and double strand DNA. Generally UV absorption methods are not sensitive or accurate enough for quantitative analysis at low-concentrations (i.e. RNA) so quantification and purity assessment can only be taken as a rough indication (Bustin, Benes et al. 2009).

3.2.2.b Gel-electrophoresis methods

Nucleic acid purity can also be assessed by gel-electrophoresis. Gel-electrophoresis is a technique used to separate macromolecules that differ in charge and mass. The driving force for electrophoresis is the voltage applied to electrodes at either end of the gel (see section 2.2.1, page 65). As Nucleic

acids have a consistent negative charge imparted by their phosphate backbone, under an electric field they are forced to migrate toward the positive electrode (Coulomb's law). Microfluidic based gel electrophoresis techniques (Bioanalyzer 2100, Agilent, Germany) offer a great alternative to UV absorption methods. The advantage of the use of a Bioanalyzer 2100 system is the automatic calculation of the RNA integrity number and quantity, providing fast quantitative information about the general state of the RNA sample (Bustin, Benes et al. 2009). Historically, RNA integrity has been assessed using agarose gel electrophoresis. Typically, gel images show two bands comprising the 28S and 18S rRNA species, and other bands where smaller RNA species are located. RNA is considered of high quality when the concentration ratio of 28S:18S bands is about 2.0 and higher. But standard methods lack fast and accurate RNA quality control as they rely on human intervention and interpretation. Agilent developed a software algorithm for the Bioanalyzer 2100 that allows the accurate calculation of an RNA Integrity Number (Schroeder, Mueller et al. 2006). The algorithm at work behind the scenes takes the electropherogram output and calculates a RNA integrity number (RIN) of between 1 and 10, with 1 describing degraded RNA and 10 corresponding to intact RNA.

3.2.2.c Staining methods

Nucleic acid quantification can be done using intercalating dyes that bind to the nucleic acid in a fixed stoichiometric ratio. Suitable dyes include SYBR Green (which binds specifically to dsDNA) and Quant-iT™ (RiboGreen® for RNA, Picogreen® for dsDNA and OliGreen® for single-stranded DNA (ssDNA) - Molecular Probes, Invitrogen™, UK). Fluorescence measurement can be carried out using a fluorescence plate reader or a fluorescence microscope. The selectivity of the binding of each dye enables measurements which are selective between dsDNA, ssDNA and RNA. Due to the high sensitivity of these methods a small sample is needed for detection of sample concentrations as low as 100 pg/μL ((Invitrogen), Handbook Invitrogen™). Invitrogen™ commercialised a fluorometer (Qubit™) to perform fluorescence-based quantitation assays for DNA, RNA and protein using the Quant-iT™ assay kit. Other modern spectrometric methods use the NanoDrop™ 3300 (ND-3300, NanoDrop Technologies, USA) in combination with RNA RiboGreen dye, the absorbance of which can be measured using as the NanoDrop™ as a UV/VIS spectrophotometer for ultra sensitive quantification of RNA (limit of detection is around 5 ng/mL)¹⁹.

3.2.2.d Amplification methods

Quantitative amplification-based methods such as qPCR (Nolan, Hands et al. 2006) can be used for the evaluation of nucleic acid quality and quantity based on the assay kinetics. These amplification methods can also allow the detection and quantification of very low concentrations of nucleic acid. However, inhibitory components frequently found in biological samples can result in a reduction of

¹⁹ <http://www.nanodrop.com/Library/ND-3300-RiboGreen-Performance-Data.pdf>

the sensitivity of these methods²⁰ (Isaac 2009). Biological inhibitors and components of the lysis, purification and storage buffers such as ethanol, sodium dodecyl sulfate and guanidine thiocyanate may be carried through the extraction and purification processes and can interfere with amplification processes.

The integration of nucleic acid preparation technology into a lab-on-a-chip presents several technical challenges. Generally, genetic analysis requires sample volumes on the order of hundreds of micro-litres to ensure sufficient quantities of target analytes in the sample, however larger volumes are often required for seawater analysis (e.g. > 1 L). Consequently, an important challenge of the sample preparation process in microfluidic devices is to concentrate the target molecules in order to bridge the mismatch between the sample volume (from litre to hundreds of micro-litres range) and the microfluidic reaction chamber's volume (micro litre range). For *K. brevis* species monitoring applications, in extreme cases, early bloom can start at concentrations as low as 1 cell/L (Boesch 1997). If the assay limit of detection is 10 cells, the sample preparation step in microfluidic devices must provide nucleic acids from 10 cells, and therefore be able to filter 10 litres or more in a million-fold decreased volume without significant loss of cells and nucleic acids.

3.3. State-of-art of microdevices for nucleic acid extraction

For a fully integrated nucleic acid device with “sample-in” to “answer-out” capability, all the steps needed for the analysis including sample preparation must be performed in a lab-on-a-chip. However, performing nucleic acid preparation in these microdevices is very challenging. Common methods used in laboratories are difficult to reproduce in the micro-scale and cannot be integrated into microchips because of process incompatibilities such as centrifugation and human intervention. A challenge in sample preparation techniques for molecular detection assays is the complex nature of real environmental samples which might contain non-targeted molecules and microorganisms (i.e. bacteria, non-targeted cells species, pollutants, sediments) that may interfere with the accuracy and compatibility of the biological assays. These may also reduce the performance of the sample preparation step. In addition, very low concentrations of target cell species from environmental or clinical samples are very difficult to detect directly after nucleic acid extraction and purification, even with the subsequent use of nucleic acid amplification techniques. Most sample preparation techniques require bulky and expensive equipment for concentration using filtration, immuno-beads and centrifugation procedures, making this process labour-intensive and time consuming (Price, Leslie et al. 2009). Finally, to ensure the presence of a sufficient quantity of targeted microorganism in the sample, bench-top sample preparation methods use large volumes of bio-sample (e.g. > 1mL), a challenge for miniaturized microfluidic applications since the technology is based on the use of small

²⁰ Thermo Scientific Solaris RNA Spike Control Kit: Identifying Reaction Inhibition in the RT-qPCR Workflow
James Covino, Zaklina Strezoska, Melissa Kelley, Thermo Fisher Scientific, Lafayette, CO, USA

volumes (e.g. > few μL). These challenges can nonetheless be addressed by integrating concentration or enrichment/isolation functions into a microfluidic platform to increase the amount of targeted microorganism during the sample preparation step (Lien, Lin et al. 2007; Zheng, Lin et al. 2007; Baier, Hansen-Hagge et al. 2009; Lee, Lee et al. 2009; Lien, Chuang et al. 2010) (see details below and summary Table 8). Few sample preparation microdevices have been developed to overcome this issue by using filtration or specific concentration/isolation strategies.

In the Chapter 1 we reviewed a selection of current nucleic acid amplification-based lab-on-a-chip devices with “sample-in” to “answer-out” capability, with a focus on their sample preparation and nucleic acid assay step. The section below provides a short review of selected current single function sample preparation microchips that specifically incorporate a concentration step.

3.3.1.a Membrane technology

The Institut für Mikrotechnik in Mainz developed a sample preparation system with on-chip reagent storage to extract total RNA from CaSki, MS751 and HeLa cell lines (Baier, Hansen-Hagge et al. 2009). 3 mL of sample (with a concentration of approximately 16 cells/mL of *human papillomavirus* cells) was loaded into the instrument. Cells were first collected and concentrated on a nylon filter then subsequently lysed using the commercial BioMérieux NucliSens lysis buffer, combined with thermal lysis at 50 °C. Further downstream the nucleic acid was captured onto a silica membrane. Total RNA was eluted in 40 μL diethylpyrocarbonate in water. They showed that it is possible to observe a positive amplification and detect mRNA extracted from as little as 50 HPV-mRNA expressing cells (from 3 mL initial sample volume) using NASBA. In this article only the microdevice overall performance is given, they did not provide further characterisation of the microdevice extraction efficiency (i.e., mRNA concentration after elution).

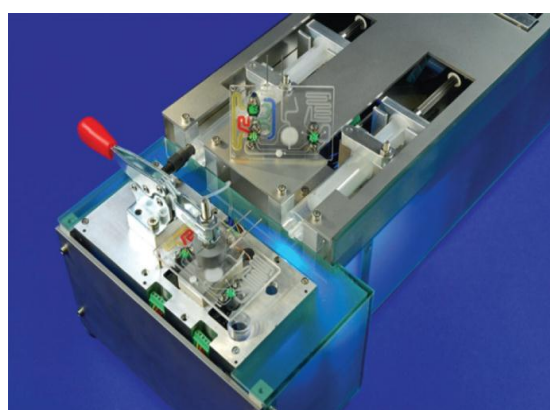


Figure 31 Institut für Mikrotechnik’s instrument for the sample preparation chip. Taken from (Baier, Hansen-Hagge et al. 2009).

Kim and Gale presented a DNA extraction device using an aluminium oxide membrane (AOM) as a sorbent, with pore sizes as small as 20 nm (Kim and Gale 2008). In this chapter we report a similar device based on AOM for RNA extraction with an assessment of the device’s performance in

simulated realistic conditions (i.e. complex sample matrix-mixed population)..100 μL of lysate (containing 5 μL of blood) samples were passed directly through the AOM and *human genomic* DNA was captured and eluted on-chip with 25 μL of Tris KCL buffer, however the cell lysis and concentration steps were performed off-chip. DNA was eluted at a yield of between 25 $\text{ng}/\mu\text{L}$ to 35 $\text{ng}/\mu\text{L}$ demonstrating a retention capacity of 75% (according to Kim and Gale blood contains about 38 $\text{ng}/\mu\text{L}$ of human genomic DNA). They also reported a micro device for RNA extraction from lysate with subsequent amplification on the AOM (Kim, Mauk et al. 2010), for which they reported a retention fraction of 34 %. Again their systems did not perform cell concentration and lysis steps on-chip. Recently an integrated device performing RNA extraction, amplification and detection from seasonal influenza A H1N1 has been presented by Xu et al (Xu, Hsieh et al. 2010). 0.1 $\text{ng}/\mu\text{L}$ of RNA in extraction mixture (approximately 800 μL) were loaded into a silica membrane chamber. RNA was adsorbed onto the silica surface using a chaotropic solution. This work was demonstrated with 200 μL of elution buffer. The system was able to extract, recover, and detect 0.1 $\text{ng}/\mu\text{L}$ of RNA after amplification.

3.3.1.b Antibody coated beads technology

Nucleic acid collection can be improved by continuously mixing the magnetic beads in solution in order to increase the probability/rate of bead-target interactions. Lien and co-workers developed a RT-PCR microdevice for viral RNA detection, using antibody coated magnetic beads to efficiently capture and concentrate Ovarian cancer cells from a large sample volume (approximately 1 mL). The cells were captured in 10 minutes by mixing 8×10^5 antibody coated magnetic beads in the fresh sample. The system needed 10 minutes mixing to achieve a binding ratio of 90%. The captured cells were re-suspended into a PBS solution with 0.1% (w/v) BSA with a volume of 20 μL , then the cells were thermally lysed (95 °C for 5 minutes). After lysis, 10 μL of PCR reagent was added into the lysis/RT-PCR chamber for RNA amplification. The systems achieved a detection limit of 50 cells/mL of cancer cells. No specific extraction performance of the microdevice was given. Again, although antibody-based techniques can allow capture and concentration of a specific target, for some applications (i.e. phytoplankton work) antibodies are not always available on cells. Cho et al. reported a compact disk format DNA extraction device for 100 μL sample volume containing 30 μL of plasma sample. Antibody coated magnetic beads were used to capture target cells, followed by a rapid cell lysis method using laser irradiation on magnetic particles. The plasma residual was then removed, leaving pure DNA (10 μL elution buffer) available for amplification.(Cho, Lee et al. 2007) They achieved a capture efficiency of about 90% for a concentration as low as 100 cells/ μL of *Escherichia coli*. However positive PCR was observed for concentrations of above 1,000 cells/ μL of *Escherichia coli*. Antibodies are globulin proteins (immunoglobulins) that react specifically with the antigen and that are present in the blood of immunised animals or plants. Although antibody-based techniques allow the capture and concentration of target cells, for some applications, including the detection of K.

brevis, antibodies are not available. In addition, using large sample volume techniques based on bead capture can be time consuming as each part of the lysate has to be subsequently incubated into a micro chamber or channel to enrich functionalized beads. As discussed in the section 1.3.1.b page 45, this technology offers a few challenges which include antibody availability and time consumption.

3.3.1.c Functionalized (oligo-dT) magnetic beads technology

An elegant approach is the use of silica coated or functionalized magnetic beads, which can be easily manipulated. Lee et al. demonstrated a micro reactor for mRNA extraction using oligo-dT coated magnetic beads. The principle of the X shaped reactor was to separate the beads from the lysate, combining fluidic flow and magnetic separation, resulting in a high speed extraction system (Lee, Jung et al. 2010). When an external magnetic field is applied, the inlaid ferromagnetic wire array generates a high-gradient magnetic field over the whole area of the microchannel. Then, magnetic beads passing over the wire experience magnetic force (see Figure 32). Human blood lysate was prepared from 50 μ L of finger-prick blood added to 175 μ L of lysis buffer and mixed with oligo-dT coated magnetic beads. 225 μ L of lysate was loaded into the microdevice for magnetic bead separation. Beads were directly used for downstream procedures (e.g., solid-phase cDNA synthesis). No quantitative result regarding the overall extraction process efficiency was given.

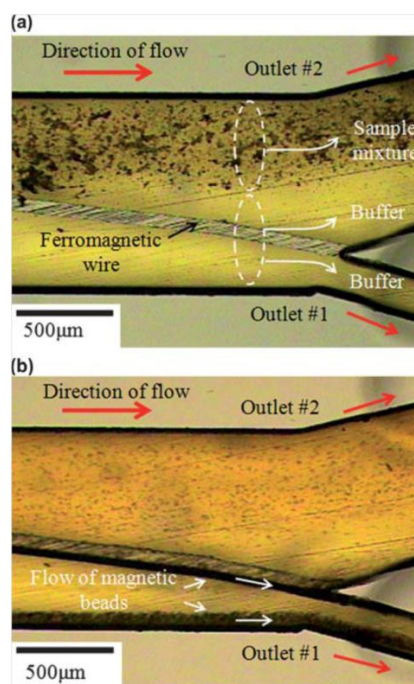


Figure 32 Photograph of “(A) Sample and buffer solutions pass through the microchannel of the RNA microextractor at sample and buffer flow rates of 15 mL/h, respectively, without an external magnetic field. In this case, the magnetic beads and other lysate components flow into outlet #2. (B) Sample and buffer solutions pass through the microchannel with an external magnetic flux of 0.14 T. The magnetic beads are laterally drawn and flow into outlet #1, while the other substances flow into outlet #2.” Taken from (Lee, Jung et al. 2010).

It is worth noting that some functionalized beads or silica particles / nucleic acid techniques are non-specific methods and can suffer from non-targeted nucleic acid contamination resulting in bead

saturation with non targeted nucleic acids. For example, silica particle-based extraction methods can have an estimated maximum nucleic acid binding capacity of around 100 µg (Boom, Sol et al. 1990). This suggests a maximum of 2 million cells that can be prepared using this method (if a mass of nucleic acids found in a single cell is 70 pg). Although the immuno-beads / cells technique relies on diffusion time and is complicated to develop, this method is cell target specific and could reduce sample contamination, as undesirable nucleic acid or protein from non-targeted species could be removed. Also mRNA can be specifically extracted by introducing coated beads with an oligo (dT). Although it ensures nucleic acid sample purity, non targeted mRNA (from other species) might also saturate and reduce the extraction efficiency. However this technique could offer a better level of discrimination when compared to total nucleic acid extraction techniques. Future improvement of our sample preparation device based on the functionalised bead technology is discussed in Chapter 5.

Summary of microdevices for nucleic acid extraction

Reference	Concentration / Isolation Step	Sample volume and concentration	Lysis technique	Extraction technique	Elution volume	Nucleic acid concentration after extraction
(Baier, Hansen-Hagge et al. 2009)	Cell concentration on a nylon filter	3 mL of sample at a concentration of 16 cells/mL of HPV cell	Combined chemical and thermal at 50 °C	RNA - Silica filter	40 µL	Not given but positive NABSA amplification observed for a concentration of 16 cells/mL of HPV cell
(Kim and Gale 2008)	DNA concentration and capture on an aluminium oxide membrane	100 µL of lysate containing 5 µL of blood	Lysis step was performed off-chip	RNA - Aluminium oxide membrane	25 µL	25 ng/µL to 35ng/µL of genomic DNA
(Xu, Hsieh et al. 2010)	RNA concentration and capture using silica membrane	Approximately 800 µL containing 10 µL of RNA (final concentration of 0.1ng/µL of RNA)	Lysis step was performed off-chip	RNA - Silica membrane	200 µL	Not given but positive RT-PCR amplification observed for an initial sample concentration of 0.1ng/µL of RNA
(Lien, Chuang et al. 2010)	Antibody coated magnetic beads	1 mL containing 50 cells (50 cells/mL)	Thermal lysis using Microheaters	Cells (RNA) - Antibody coated magnetic beads	20 µL	Not given but positive RT-PCR amplification observed for an initial sample concentration of 50 cells
(Cho, Lee et al. 2007)	Antibody coated magnetic beads	100 µL containing 1,000 cells of <i>Escherichia coli</i> (10×10^3 cells/mL)	Laser irradiation on magnetic particle	Cells (DNA) - Antibody coated magnetic beads	10 µL	Not given but positive PCR amplification observed for an initial sample concentration of 1,000 cells of <i>Escherichia coli</i>
(Lee, Jung et al. 2010)	Oligo-dT coated magnetic beads	175 µL of lysis buffer containing 50 µL of blood	Chemical lysis off-chip	mRNA - Oligo-dT coated magnetic beads	Beads with mRNA used directly for downstream procedures	Not given
Our sample preparation microdevice (Chapter 3)	Cell concentration on a mechanical filter (Aluminium oxide). Filter could theoretically accept a few hundred of mL depending on the sample concentration.	1 mL of sample (2,500 cells/mL for <i>K. brevis</i> and ~20 cells/mL for <i>Karenia mikimotoi</i>). All samples were mixed with 10,000 <i>Tetraselmis suecica</i> cells to simulate realistic conditions	Chemical lysis on-chip, 200 µL of lysis/binding buffer,	RNA - Aluminium oxide filter	40 µL	The amount of total RNA extracted from <i>K. brevis</i> cultures was on average 0.6 ± 0.3 pg-RNA/cell, whereas for <i>Karenia mikimotoi</i> cultures the amount was on average 23 ± 9.3 pg-RNA/cell. Positive NASBA was observed for a sample containing 2,500 <i>K. brevis</i> .

Table 8 Summary of microdevices for nucleic acid extraction.

3.4. A simple sample preparation platform for environmental applications

The extraction of high-quality RNA from biological samples is essential in order to obtain successful and efficient downstream RNA amplification. Although antibody-based techniques allow the capture and concentration of target cells, for some applications / species antibodies are not always available. Moreover, antibody techniques can be problematic when working with complex sample matrices. Consequently because of the assay complexity many systems do not use this technique and often suffer from the lack of a cell concentration step. Conventionally, cells of interest per unit volume can vary by many orders of magnitude. Concentrations of toxic phytoplankton species that can cause damage to marine life can be as low as 1,000 cells per litre (1 cell/mL) (Blasco, Levasseur et al. 2003; Chang 2011). It is clear to see that the volume reduction in microsystems (i.e. few μL) will decrease the absolute number of molecules available, and therefore the sample volume available in microsystems is unlikely to contain the targeted analyte or cell (see section 1.4.1, page 54). The nature of microfluidics devices therefore makes sample concentration a necessary task.

In this chapter, we describe a microdevice that rapidly produces purified and concentrated total RNA from large (over 1mL) volumes of environmental samples and show test results with mixed cell populations. The sample is collected and concentrated on a nanoporous aluminium oxide filter where it is subsequently chemically lysed and left for incubation. The total RNA is adsorbed onto the aluminium oxide filter with a method based on the Boom method. This uses commercial guanidine thiocyanate as a chaotropic and lysis agent and washing buffers (all from Nuclisens miniMAG© kit, bioMérieux, Netherlands). After several washing steps to remove sub-cellular materials, the purified RNA is eluted (Nuclisens miniMAG© elution buffer, bioMérieux, Netherlands). The eluent is the final product of this subsystem, which could be integrated with a RNA amplification and detection platform (see Chapter 4).

We present results showing the successful extraction of total RNA from *K. brevis* from various numbers of cells, mixed with a fixed quantity of a non-targeted species (*Tetraselmis suecica* cells). We demonstrated detection of total RNA using gel electrophoresis, and mRNA amplification and detection from phytoplankton cells using an on-bench NASBA instrument.

RNA degradation can occur for many reasons (i.e. inadequate sample handling, long storage, RNA digestion) and RNA may be degraded through cleavage by RNase enzymes. Moreover, the presence of inhibiting components during sample preparation such as salts, phenol, or other agents may also deteriorate results (Gjerde, Hoang et al. 2009). Therefore RNA integrity and purity assessment is essential before using RNA samples in downstream applications (i.e. amplification assays). However proper RNA quality control is lacking in a substantial number of studies. This is why we have tried, where possible, to follow the Minimum Information for Publication of Quantitative Real-Time PCR

Experiments (MIQE) (Bustin, Benes et al. 2009), as a guideline for the sample preparation microdevice characterisation, even though NASBA was used for mRNA detection and not RT-PCR. The MIQE's recommendation was also followed to ensure the reproducibility of the experimental and data.

3.4.1. Materials and methods

3.4.1.a Algal cultures

K. brevis (strain CMPP 2228, Bigelow Laboratory for Ocean Sciences, USA) cells were grown in L1 Aquil* artificial seawater media at 19 °C with 12 h: 12h light: dark at high irradiance. *Karenia mikimotoi* (strain PLY 4978, Marine Biological Association, Plymouth, UK) cells were grown in Keller's artificial seawater media at 19 °C with 12 h: 12h light: dark at high irradiance. *Tetraselmis suecica* (strain PLY 305, Marine Biological Association, Plymouth, UK) cells were grown in Erd Schreiber artificial seawater media at 19 °C with 12 h: 12h light: dark at high irradiance. Cell samples were harvested during exponential cell growth. Cell growth was monitored by counting 10 µL culture aliquots fixed in 1% Lugol's solution (Sigma Adrich, UK) in a hemocytometer (C-Chip, Digital Bio, Korea) counting chamber.

3.4.1.b Bench-top sample preparation and RNA purification

On-chip sample preparation performance was validated against a bench-top miniMAG® lysis-extraction system (Nuclisens miniMAG©, bioMérieux, Netherlands). RNA from the cell lysate was purified with a commercially available chaotropic technique based kit using silica coated magnetic beads (Nuclisens miniMAG© kit, bioMérieux, Netherlands). The experimental protocols for the RNA extraction kits were followed according to the manufacture's guidelines. For the sample preparation analytical step, *K. brevis* cell of 125, 250, 500, 2,500, and 5,000 cells were each mixed with 10,000 of *Tetraselmis suecica* to explore possible interferences (i.e. to test what might happen using real environmental samples). These were triplicated experiments, and the sample preparation steps were performed in parallel with both conventional and lab-on-a-chip apparatus. The results were then compared.

3.4.1.c Sample preparation microfluidic device

A rendering of the 3D CAD depicting the design of the microfluidic chip and thermo-regulated holder details are shown in Figure 33. The device consists of two PMMA chips that sandwich the aluminium oxide filter. The chip assembly consists of top and bottom chips with microfluidic channels, 8 mm diameter open chambers, and an aluminium oxide filter sandwiched between the two open chambers; sealed with double-sided tape on each side (see Figure 33, Figure 34 and Figure 35 for details). The polymer chips (83 mm x 38 mm) were manufactured from 1.5 mm PMMA substrate (layer 1 and 4 - Röhm, Darmstadt, Germany) with channels (see Figure 33), chambers and fluidic features created by micro-machining (Ogilvie, Sieben et al. 2010) (LPKF Protomat S100 micro-mill). To seal the fluidic

channels the chips were overlaid and solvent vapour bonded (Ogilvie, Sieben et al. 2010) to a 0.4 mm thick PMMA lid (layer 2 and 3 - 83 mm x 38 mm, Figure 33) with 8 mm diameter holes centred on the open chambers (see Figure 33, Figure 34 and Figure 35 for details).

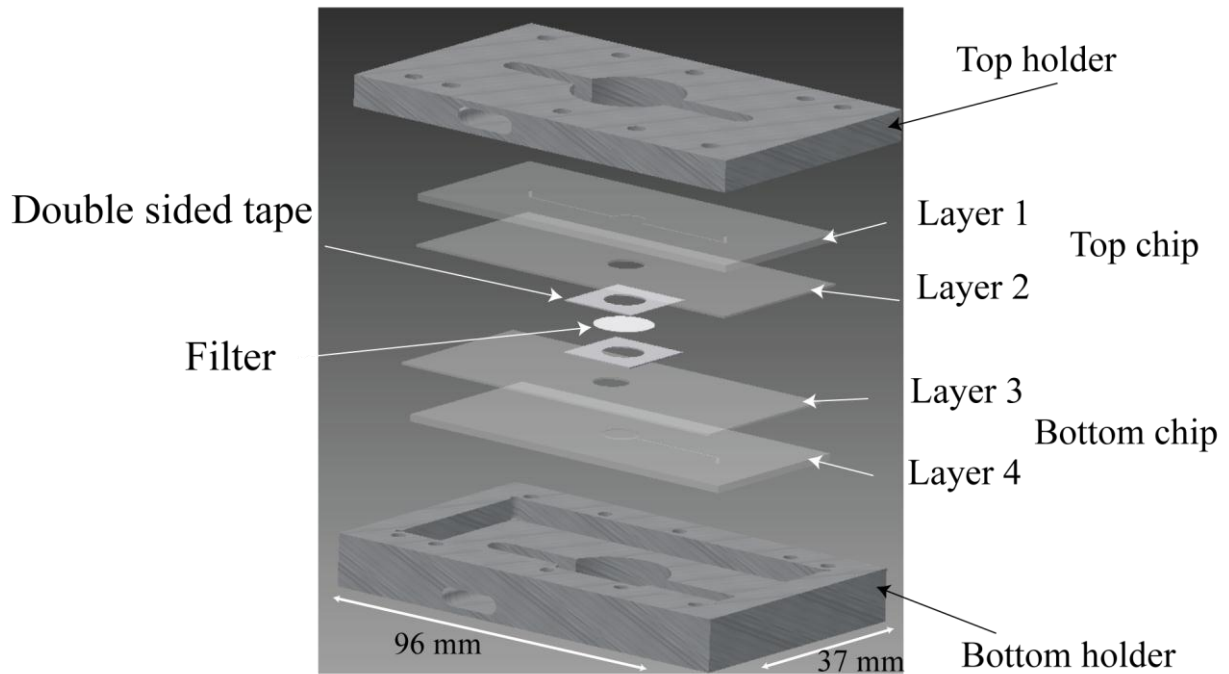


Figure 33 Sample preparation microdevice. (a) exploded view (95 mm long, 37 mm wide and 6 mm thick) with integrated aluminium oxide filter.

The top PMMA chip (layer 1 and 2) has one inlet (inlet 1 in Figure 34) and one outlet both formed by a vertical aperture (0.7 mm, outlet 1 Figure 34) and an open chamber above the aluminium oxide filter to enable cell concentration, lysis and RNA extraction.

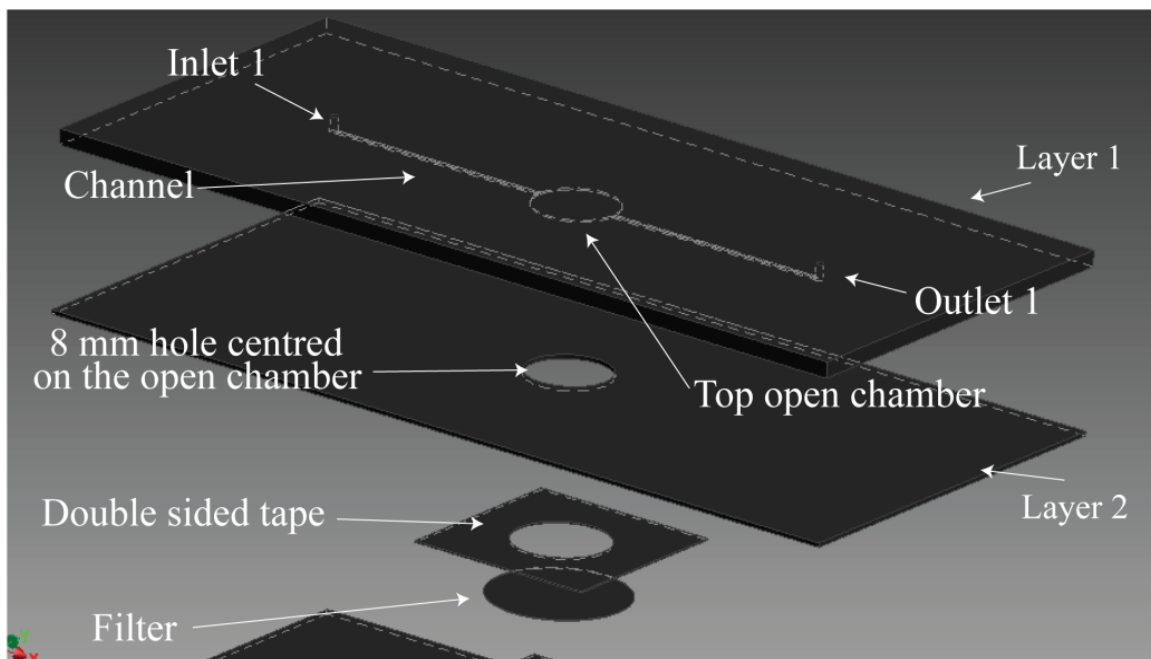


Figure 34 Sample preparation microdevice. Detailed exploded view of the microchip top part.

The bottom chip (layer 3 and 4) consists of one open chamber underneath the aluminium oxide filter and one outlet for used for waste (see Figure 35).

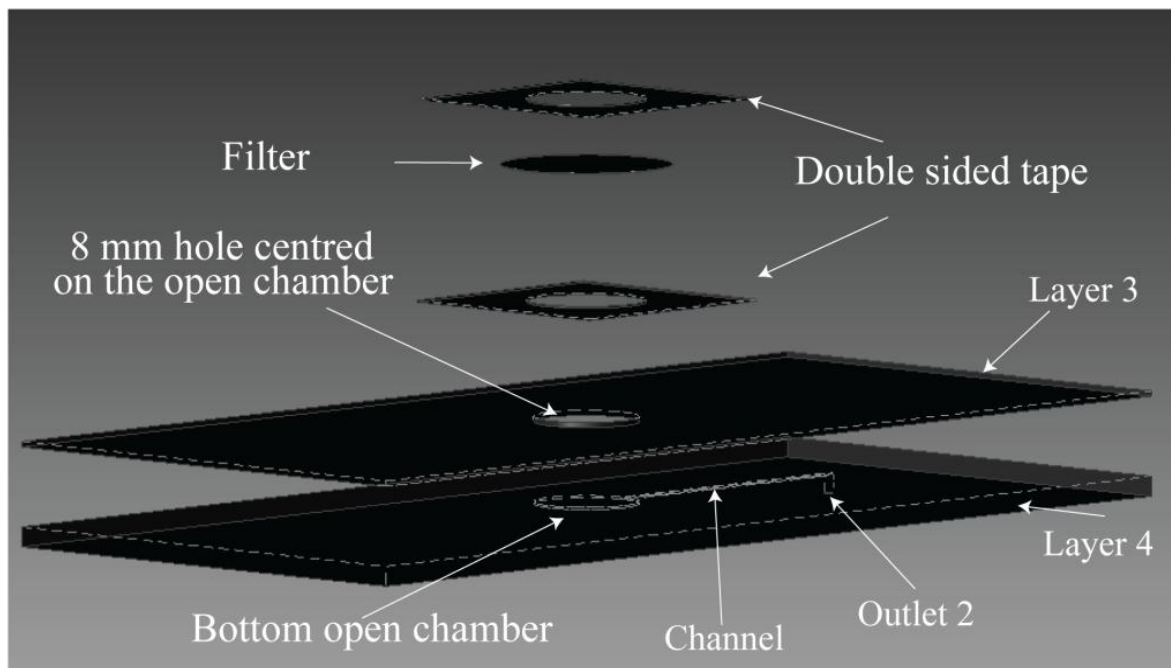


Figure 35 Sample preparation microdevice. Detailed exploded view of the microchip bottom part.

Hypodermic needles (222-222, RS, UK) were inserted into the inlet and outlets and used as fluidic connectors. Inlet 1 was connected to a syringe pump (Harvard Apparatus Nanomite, Kent, UK), outlets 1 and 2 were connected to a 3 way valve for output selection (see Figure 36). The channels have a cross section of $150\ \mu\text{m}$ by $150\ \mu\text{m}$, the dimensions of the $35\ \mu\text{L}$ top chamber (the extraction chamber) were approximately 8 mm diameter and 0.7 mm depth. Prior to assembly the aluminium oxide filter was sandwiched between two pieces of thin ($150\ \mu\text{m}$) double-sided tape (SecureSeal Imaging Spacers - 9 mm diameter hole, 654004, Grace Bio-Labs, USA) and then clamped between the two chips (see Figure 33).

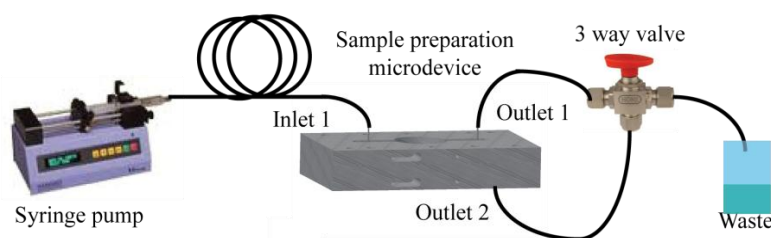


Figure 36 Sample preparation microdevice. Schematic of the microfluidic system setup, the sample is dispensed by a syringe pump, a manual 3 way valves allow switching between the two outputs. A personal computer running LabVIEW™ was used to control a National Instruments data acquisition card (NI-6281 USB), which control the holder temperature.

The assembled system was then connected to the microfluidic circuit, with outlets 1 and 2 connected to a three way manual valve for output selection. The same chip was used for all experiments. Before use the chip parts were washed sequentially with RNA Zap, 70 per cent (v/v) ethanol and RNase-free water. All chemicals were of RNase-free grade from Sigma Aldrich, UK.

3.4.1.d Sample preparation experimental procedure

The sample preparation microdevice operation can be divided into four steps (see Figure 37).

1. A sample containing cells is loaded using a syringe pump into the chip (through the filter) which concentrates cells on the surface of the filter,
2. lysis/binding buffer is dispensed using a syringe pump for cells lysis and RNA capture onto the filter
3. the filter and channels are washed by hand pipetting the commercial washing buffer 1, 2 and 3 (Nuclisens miniMAG© kit, bioMérieux, Netherlands)
4. 40 μ L of elution buffer is loaded by hand pipetting and the chip is thermo-regulated at 65 °C for 15 minutes for RNA elution.

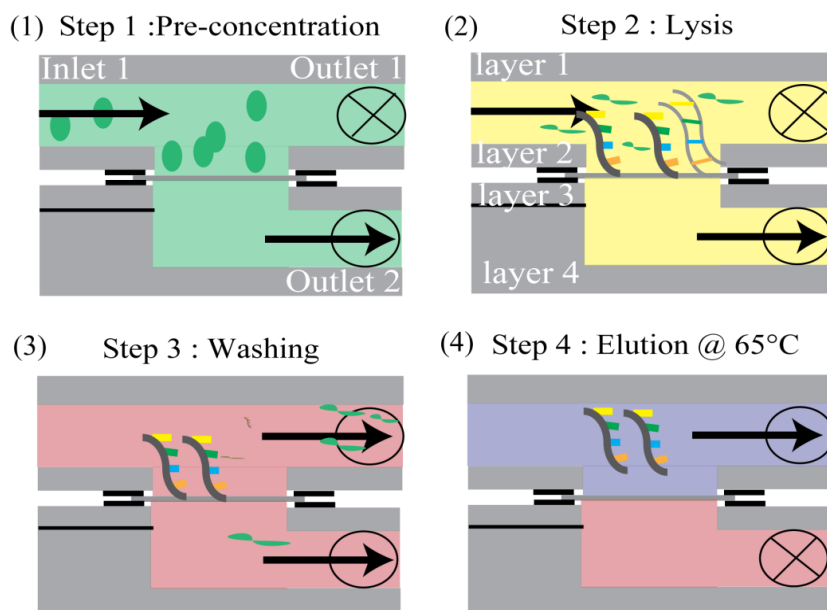


Figure 37 Sample preparation microdevice. Schematics of the microchip and illustration of the flow control and the operation process of the microdevice capable of performing RNA extraction,: (1) cells pre-concentration; (2) cells lysis and incubation process for total RNA binding with aluminium oxide filter; (3) washing and digestion of DNA by DNase washing buffer; and (4) RNA elution.

Inlet 1 was used for the loading of the sample containing cells for the pre-concentration step (see Figure 36), the commercial guanidine thiocyanate chaotropic lysis buffer and the washing buffers (Nuclisens miniMAG© kit, bioMérieux, Netherlands), respectively. Outlet 1 is used for washing waste and purified RNA / eluent collection. Outlet 2 was used for the filtrate of the sample / cell medium and

for washing waste (see Figure 36). Throughout the process described below the polymer assembly was housed in a holder (Figure 33, 100 mm x 60 mm, from 6013 Aluminium)

1 Cells pre-concentration

To extract RNA, a sample (1 mL) containing a single or mixed cell population was dispensed into the sample preparation microdevice using a syringe pump (Harvard Apparatus Nanomite, Kent, UK) driving pre-loaded 1 μ L disposable syringes (SZR-150-011Q, Fisher Scientific, UK) via inlet 1 to pass fluid through the filter at a flow rate of 200 μ L/min, and cells were concentrated on the top of the filter (see Figure 37(1)).

2 Lysis

Next, 100 μ L of commercial guanidine thiocyanate chaotropic lysis buffer was dispensed into the chip using the syringe pump via inlet 1 to pass fluid through the filter at a flow rate of 200 μ L/min. (see Figure 37(2)). The solution was left for 15-minutes to incubate at room temperature to allow RNA-filter binding.

3 Washing

The washing and elution steps were performed manually by hand pipetting the washing and elution buffers. 200 μ L aliquots of commercial washing buffer 1, 2 and 3 were then sequentially pipetted through the filter (Figure 37(3)).

4 Elution

Finally, 40 μ L of elution buffer was loaded (Figure 37(4)), and the chip thermo-regulated at $65\text{ }^{\circ}\text{C} \pm 0.1\text{ }^{\circ}\text{C}$ for 15 min to allow RNA release. The chip temperature was maintained at $65 \pm 0.1\text{ }^{\circ}\text{C}$ by an analogue proportional-integrative-derivative (PID) control loop system acting on heating resistors (LTO30 Power Resistor T/F 15R, Vishay Intertechnology, USA) and using a negative temperature coefficient thermistor for temperature feedback (B57540G0303J, Epcos, Germany). The temperature system unit was controlled with a custom-written LabVIEW™ (National Instruments, Austin, TX, USA) program, using a National Instruments card (NI-6281 USB, National Instruments, Austin, TX, USA). 35 μ L of RNA was collected and stored immediately after the purification process at $-10\text{ }^{\circ}\text{C}$. The sample preparation step was followed by analysis on a Bioanalyzer 2100 using electrophoretic separation on commercial microfabricated chips (RNA 6000 Pico LabChip®, Agilent, Germany), NASBA amplification and detection on-bench. To evaluate the performance of the sample preparation microdevice, the results were validated against a bench-top miniMAG® lysis-extraction system (Nuclisens miniMAG®, bioMérieux, Netherlands).

3.4.1.e Cell number filtration capacity

To evaluate the capacity of the filter and the device susceptibility to clogging due to cells and mucus content, the following measurements were made. High concentrations (100,000 cells/mL) of *Tetraselmis suecica* cells followed by cell free artificial seawater medium were sequentially passed through the sample preparation microdevice and the differential across the filter measured using an elementary pressure measurement circuit, as shown in Figure 38. Pressure was measured by an analogue sensor (26PCDF A6D, Honeywell differential pressure sensor, USA), and the signal acquired using a PCI-6289 data acquisition card (National Instruments, Texas, USA) logged and displayed using custom software (LabVIEW™). Cells were dispensed into Inlet 1 through the filter at a flow rate of 200 $\mu\text{L}/\text{min}$ with four syringe pumps driving four sequential 1 mL disposable syringes.

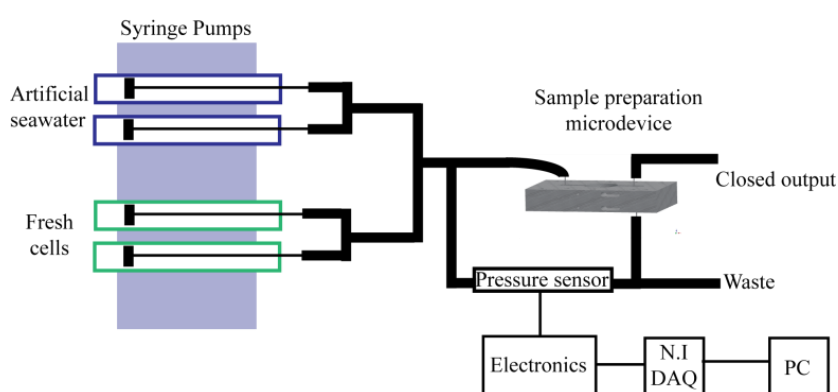


Figure 38 Schematics of the microfluidic setup for the pressure measurement. The pressure is monitored with a differential pressure sensor, its output signal is conditioned and acquired with a National Instruments data acquisition card (PCI-6289). The inlet was connected to 4 syringe pumps driving each 1 mL syringe (2 x fresh cells and 2 x artificial water) and 500 μL of each syringe (Artificial seawater then Fresh cells)was alternatively dispensed.

3.4.1.f RNA capture efficiency

The retention capacity for RNA and DNA molecules on aluminium oxide filters have been reported by others (Erali, Durtschi et al. 2004; Kim, Mauk et al. 2010) and these studies have shown different retention capacity rates depending on binding buffer composition. They reported, in the absence of any salt in the buffer, that the binding capacity for RNA was below 5%, and a binding capacity of 34% when the guanidine salt concentration was 4.5 M. Our experiment was carried out using the sample preparation device described above. Pure RNA from 1,000 *K. brevis* cells was extracted using the bench-top miniMAG® lysis-extraction system. To test the filter capture efficiency, RNA was mixed with the commercial guanidine thiocyanate chaotropic lysis buffer at a ratio of 1:4. The solution was dispensed into inlet 1 at a flow rate of 200 $\mu\text{L}/\text{min}$ with a syringe pump driving a 1 mL disposable syringe. This just filled the top chamber (actuation, Inlet 1 and Outlet 2 open). The mixture was incubated for 10 min in the 35 μL volume chamber at room temperature. Subsequently, 200 μL of washing buffer (Nuclisens miniMAG© kit, bioMérieux, Netherlands) 1,2 and 3 were dispensed to remove lysis /binding buffer residue (Nuclisens miniMAG© kit, bioMérieux, Netherlands). Finally, 40

µL of elution buffer (Nuclisens miniMAG© kit, bioMérieux, Netherlands) was injected to fully wash away the washing buffers, and the chip thermo-regulated at 65 °C for 15 min to promote RNA release. 35 µL (chamber volume) of pure RNA was collected and immediately transferred to storage at – 10 °C. The pure total RNA was analysed with the Bioanalyzer 2100 using electrophoretic separation on commercial microfabricated chips (RNA 6000 Pico LabChip©, Agilent, Germany). All reagents required to perform the RNA electrophoretic analysis were supplied as part of the Agilent RNA 6000 Pico Kit (Agilent, Germany). The experiment comparing RNA binding capacity was duplicated (n=2) on both the microdevice and the bench-top miniMAG® system (see 3.4.2, page 109).

3.4.1.g Sample preparation microdevice operation range

In order to determine the operational range of the device under idealised conditions (i.e. without the presence of non-target species), single species cultures were processed using the sample preparation microdevice. Samples of 10, 30, 50, 100, 250 and 1,000 *Karenia mikimotoi* cells (n=1, n represents the number of replicated experiments), and samples of 250 (n=1), 500 (n=1), 1000 (n=1), 12,000 (n=3, triplicate experiment only performed for this concentration of cells), 25,000 (n=1), 30,000 (n=1) and 120,000 (n=1) *K. brevis* cells were performed on-chip. See the section 3.4.1.d for the procedure. The pure total RNA extract was detected using the Bioanalyzer 2100.

3.4.1.h Sample preparation microfluidic performance assessment

In this section we try to follow the recommendations made by the standard for the Minimum Information for publication of Quantitative real-time PCR Experiments MIQE Guidelines (Bustin, Benes et al. 2009) for nucleic acid measurement after sample preparation. According to the MIQE guidelines, sample preparation steps should be characterised by providing key information including name of kit and details of any modifications, details of DNase or RNase treatment, contamination assessment (DNA or RNA), nucleic acid quantification (instrument and method, purity (A260/A280), yield), RNA integrity method/instrument and inhibition testing. However as our system is still in an early stage of development some points of the checklist were not studied (e.g. contamination assessment and inhibition testing). RNA purification quality and quantity from on-chip operation were compared with the bench-top RNA purification system. The efficiency of the sample preparation methods can be assessed by measurement of the yield and purity of the RNA extracted with the Nanodrop UV–VIS spectrophotometer (Thermo Fisher, UK). However the RNA quantity was not sufficient to reach reliable results using this method which could lead to an overestimation of RNA concentration (Bustin, Benes et al. 2009; Price, Leslie et al. 2009). To overcome this problem, NASBA and electrophoresis analysis (Agilent Bioanalyzer 2100) were performed with eluted samples to determine the amount and quality of RNA samples. *K. brevis* cells of 125, 250, 500, 2,500, and 5,000 cells were each mixed with 10,000 of *Tetraselmis suecica* to simulate environmental samples. These were triplicate experiments, and the sample preparation steps were performed in parallel with both conventional and lab-on-a-chip apparatus (see section 3.4.1.b, page 101).

3.4.1.i RNA quality assessment

Following the MIQE guidelines, after purification the RNA quality was assessed by determining the RIN from electrophoresis traces (see page 92, section 3.2.2.b). We used the Agilent Bioanalyzer 2100 using electrophoretic separation on commercial microfabricated chips. All reagents required to perform the RNA electrophoretic analysis were supplied as part of the Agilent RNA 6000 Pico Kit (Agilent, Germany). The experimental protocols were followed according to the manufacturer guidelines.

3.4.1.j RNA quantity assessment

The amount of pure RNA extracted from both on-chip and bench-top methods were determined using data and analysis from the Bioanalyzer 2100 software. NASBA was used to compare and assess qualitatively the performance of on-chip and on-bench extraction methods (i.e. the minimum number of cells detectable after sample preparation). In order to qualitatively compare both methods we used the mathematical model developed by the bioMérieux labs (Weusten, Carpay et al. 2002) (see section 1.2.1, page 32) to analyse the NASBA data. This takes into account the enzyme and hybridization kinetics and normalises for enzyme efficiency between different NASBA experiments (Weusten, Carpay et al. 2002). A Matlab™ program was written to calculate the quantitation variable $\ln(k_1\alpha_1\alpha_2^2)$, (see section 1.2.1) and a non-linear least squares algorithm was also used to compare the on-chip and on-bench results. RNA extract was amplified and measured using a bench-top NASBA instrument (EasyQ analyser, bioMérieux, Netherlands). Conditions for NASBA reactions are described in section 4.3.1.c (page 125). Oligonucleotides and beacons were purchased from Eurofins MWG Operon (Germany) and were of the highest purity. NASBA Basic EasyQ kits were from bioMérieux (UK).

3.4.1.k Suitability for subsequent amplification

NASBA was used to verify qualitatively if inhibition was occurring and to evaluate the efficiency of the on-chip RNA extraction protocol.

3.4.2. Results

3.4.2.a Cell number filtration capacity

We examined the device and filter strength in extreme cell concentration conditions to evaluate the pressure working range of the system. 200,000 *Tetraselmis suecica* cells were dispensed and pressure was measured in real-time. The pressure across the chip reached approximately 50 kPa after filtration of 200,000 cells (Figure 39), and the device did not show any leaks or pressure related failures. This result suggests that the microdevice could filter 200 mL of solution without failure for a sample concentration of 1,000 cells/mL (for cells of equivalent size).

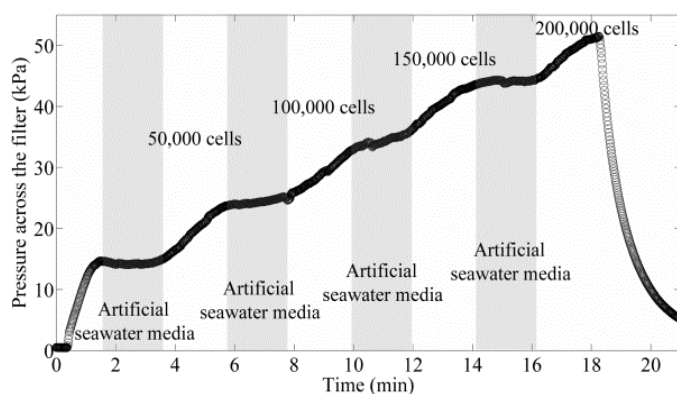


Figure 39 Pressure measured across the filter for on-chip concentration of *Tetraselmis suecica* cells. 2 mL of artificial seawater media (Erd Schreiber media) and fresh cells were dispensed alternately in 500 μ L aliquots at 200 μ L/min and pressure recorded every second.

3.4.2.b RNA capture efficiency

The results of RNA collection efficiency comparisons between the bench-top miniMAG® lysis-extraction system with the sample preparation microdevice are summarised in Figure 40, which shows the binding efficiency using both systems. The RNA binding efficiency of the aluminium oxide-based sample preparation microdevice was 47.1% with a range of 2.9% ($n=2$, n represents the number of replicated experiments) using the commercial guanidine thiocyanate chaotropic lysis buffer (guanidine salt concentration was approximately 6 M), while the miniMAG®'s binding recovery was approximately of 70% with a range of 8.6% ($n=2$).

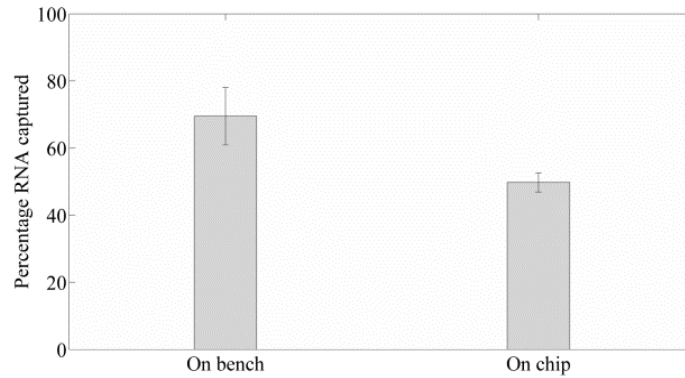


Figure 40 Comparison of extraction methods using bench-top and on-chip RNA extraction and purification techniques. These data were obtained from pure total RNA from 1,000 *K. brevis* cells previously extracted on-bench (n=2). The bar plot shows the percentage of total RNA recovery of the initial concentration, the error bars represent the standard deviation of the experiments.

3.4.2.c Sample preparation microdevice operation range

Using single species samples (*Karenia mikimotoi*), we examined the performance and operating range of the sample preparation microdevice by measuring the eluent with RNA electrophoresis analysis (Bioanalyzer 2100). This analysis was used to quantify the sample preparation efficiency by measuring the amount and purity (analysis of the ribosomal 18S (1.9-kb) and 28S (5-kb)) of extracted RNA from the *Karenia mikimotoi* cells. Figure 41a shows Bioanalyzer 2100 fluorescence data for different cell concentrations after sample preparation on-chip. For the lowest cell level of 10 cells (*Karenia mikimotoi*), the Bioanalyzer 2100 electropherogram trace shows a detectable amount of total RNA. *K. brevis* cells were also tested for on-chip sample preparation at different cell concentrations.

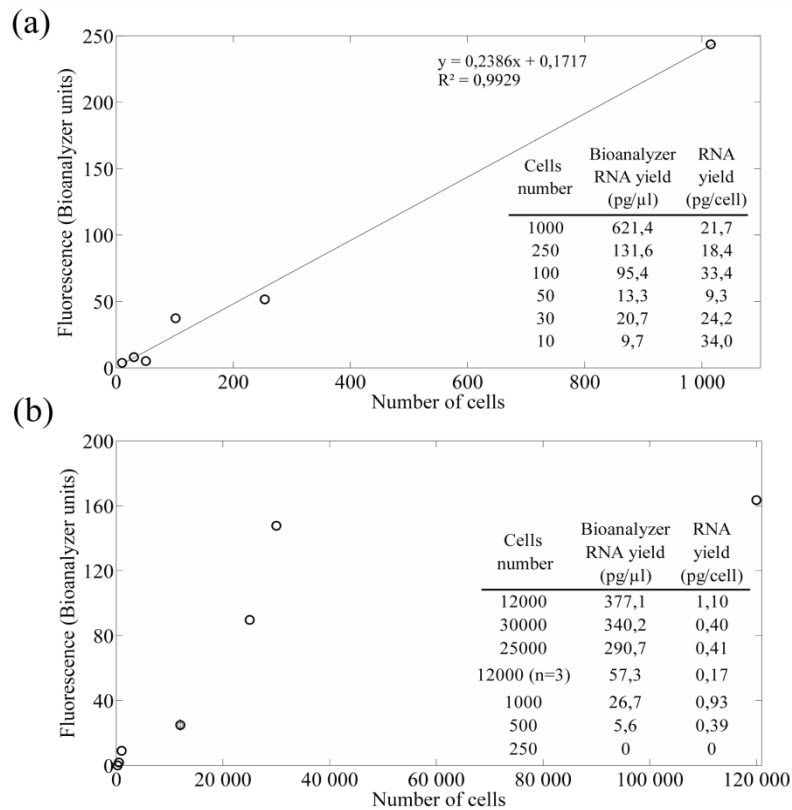


Figure 41 Graphs showing the range of operation for the sample preparation device with the species *Karenia mikimotoi* and *K. brevis*. (a) Bioanalyzer 2100 total RNA fluorescence data from 1,000, 250, 100, 50, 30, and 10 *Karenia mikimotoi* cells extracted on-chip. With table summarising total RNA yields obtained using the on-chip method. (b) Bioanalyzer 2100 total RNA fluorescence data from 120,000, 30,000, 25,000, 12,000, 1,000, 500 and 250 *K. brevis* cells extracted on-chip. With table summarising total RNA yields obtained using the on-chip method.

The data shown in Figure 41b indicates a linear RNA extraction performance in the range 250 – 30,000 *K. Brevis* cells. The device starts to show non-linear performance above 30,000 *K. Brevis* cells. The amount of total RNA extracted from *K. brevis* cultures was on average 0.6 ± 0.30 pg-RNA/cell, whereas for *Karenia mikimotoi* cultures the amount was on average 23 ± 9.3 pg-RNA/cell (Figure 41) well within the expected range (i.e. for *Karenia mikimotoi*) of 10–30 pg-RNA/cell for typical cells (Alberts, Bray et al. 1986). The performance of the sample preparation microdevice varied in terms of the cell species targeted; performance is much lower with *K. brevis* than *Karenia mikimotoi*. This could be due to different biological cycle states and cell wall compositions between species (Bold and Wynne 1978; Graham and Wilcox 2000). It is clear that the performance of the sample preparation microdevice could be improved through customising lysis buffers for specific cells with tough walls such as *K. brevis* (Graham and Wilcox 2000). Nevertheless, the study on complex sample matrixes (mixed population, see section below) was performed using *K. brevis* species because the NASBA assay was available in our laboratory.

3.4.2.d Sample preparation microfluidic performance assessment with mixed population

In this section NASBA and electrophoretic separation analysis was used to quantify the sample preparation microdevice performance in simulated realistic conditions by measuring the amount and purity of the total RNA extracted using Bioanalyzer 2100 and by measuring the amount of target RNA extracted using NASBA. Two different sample preparation methods were compared: the sample preparation microdevice and the bench-top miniMAG® lysis-extraction system. All samples from 125 to 5,000 *K. brevis* cells (in triplicate) were mixed with 10,000 *Tetraselmis suecica* cells and extracted in parallel using both methods. NASBA plots (average of the triplicates sample) comparing both sample preparation methods for *K. brevis* cells mixed with non-targeted cells acquired using the bench-top instrument are shown in Figure 42. The error bars on the data show the standard deviation (n=3, n represents the number of replicated experiments). Figure 43 shows Bioanalyzer 2100 fluorescence data (total RNA amount). Table 9 summarises and compares the two preparation methods in terms of purity and amount of RNA, together with informative qualitative NASBA data analysis.

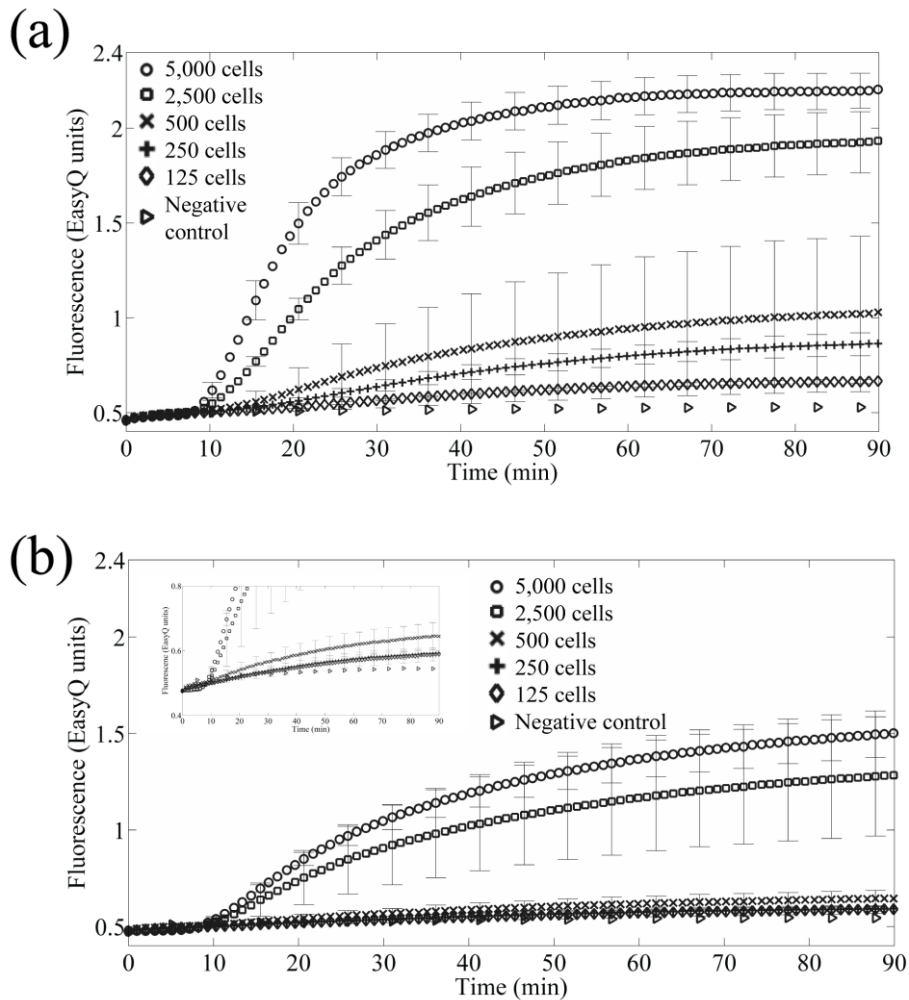


Figure 42 NASBA amplification data. (a) Data for 5,000, 2,500, 500, 250,125 *K. brevis* cells with 10,000 *Tetraselmis suecica* cells extracted using the bench-top miniMAG® lysis-extraction system (each of the five lines show average measurements based on three replicates of the experiment, the error bars represent the standard deviation of the experiments). White triangles represent the negative control. (b) Data for 5,000, 2,500, 500, 250,125 *K. brevis* cells with 10,000 *Tetraselmis suecica* cells extracted using the sample preparation microdevice (each of the five lines show average measurements based on three replicates of the experiment, the error bars represent the standard deviation of the experiments). White triangles represent the negative control.

The performance of both the sample preparation microdevice and the miniMAG® varied in terms of the lowest cell concentration that was detectable by NASBA. An important parameter for assessing the adequacy of the sample preparation system is the amount of material needed to obtain a sufficient amount of mRNA for subsequent NASBA amplification and detection. The lowest cell concentration detectable by NASBA was 125 *K. brevis* cells after using the miniMAG® for RNA extraction. The minimum detectable amount of mRNA after on-chip preparation was 500 *K. brevis* cells (zoom in Figure 42a), indicating 4 times better performance using the miniMAG®. NASBA plots are interpreted with a number of different methods. The time to positivity (TTP) method is very sensitive to experimental variability (i.e. enzymes and instrumentation variability) (Tsaloglou, Bahi et al. 2011), while the linear regression fit method is an alternative to reduce the impact of experimental variability for the data analysis.

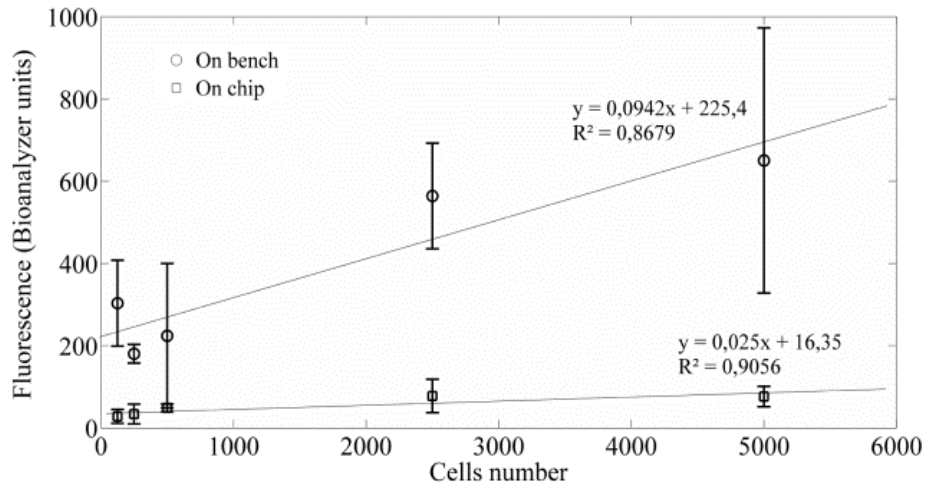


Figure 43 Bioanalyzer total RNA fluorescence data. (a) Open circles are data for 5,000, 2,500, 500, 250,125 *K. brevis* cells with 10,000 *Tetraselmis suecica* cells (n=3, n represents the number of replicated experiments) extracted using the bench-top miniMAG® lysis-extraction system. (b) Open squares are data for 5,000, 2,500, 500, 250,125 *K. brevis* cells with 10,000 *Tetraselmis suecica* cells (n=3, n represents the number of replicated experiments) extracted using the sample preparation microdevice. The error bars represent the standard deviation of the experiments.

Table 9 summarises the linear regression of the relationship between $\ln(k1a1a22)$ and cells for all samples. Table 9 also summarises the Bioanalyzer 2100 data, RNA purity (RIN) and amount, showing that the sample preparation microdevice gave on average a better RNA quality. This may be the result of microfluidic technology allowing complete removal of buffers and contaminant through the nature of laminar flow. However, the miniMAG® preparation method yielded on average approximately seven times more RNA (see Figure 43 and Table 9).

Cells number	Fluorescence (Bioanalyzer units)	RNA Integrity Number (RIN)	ln(cells number)	ln($k_1 a_1 a_2^2$)
Sample preparation on chip (n=3)				
5000	76.2 ± 24.6	Nan	8,51	- 6.02 ± 0.03
2500	77.5 ± 40.4	8.0 ± 0.2	7,82	- 6.13 ± 0.12
500	48.5 ± 9.5	7.3 ± 0.1	6,21	- 6.3 ± 0.12 (n=2)
250	33.6 ± 23.9	9 (n=1)	5,51	- 6.44 ± 0.12
125	27.9 ± 16.8	7.8 ± 0.3 (n=2)	5,26	- 6.49 ± 0.13
Negative control (n=1)	37.2			
Sample preparation on bench (n=3)				
5000	650.2 ± 332.3	5.5 ± 0.8	8,51	- 5.07 ± 0.08
2500	563.9 ± 128.3	4.9 ± 0.51	7,82	- 5.77 ± 0.18
500	224.0 ± 175.5	5.1 ± 0.4 (n=2)	6,21	- 6.23 ± 0.14
250	180.2 ± 22.8	6.1 ± 0.23	5,51	- 6.56 ± 0.09
125	303.3 ± 104.3	6.3 ± 0.3	5,26	- 6.41 ± 0.19 (n=2)
Negative control (n=1)	289.9			

Table 9 Bioanalyzer total RNA fluorescence and NASBA amplification curve kinetic parameters from sample extracted on-chip and bench-top with standard deviation of triplicate samples.

Although we tested the sample preparation microdevice using phytoplankton species that are difficult to lyse, promising results were achieved. Results are comparable between the on-chip and on bench sample preparation. The sample preparation microdevice shows good performance, with detection using the Bioanalyzer 2100 as low as 10 *Karenia mikimotoi* cells prepared on-chip (see Figure 41a).

Concentrations of toxic phytoplankton species that can cause damage to marine life can be as low as 1,000 cells per litre (1 cell/mL) (Blasco, Levasseur et al. 2003; Chang 2011). According to our characterisation of the microdevice; the number of *K. brevis* cells necessary for evident successful amplification was 2,500 cells prepared using the microdevice (Figure 42). This suggests that the device needs to filter 2.5 litres of seawater in order to obtain sufficient mRNA for subsequent successful amplification and detection using NASBA.

For *K. brevis*, a maximum of 30,000 cells allowed successful extraction using the microdevice (operation range, see Figure 41b). In complex sample matrix, if cells are collected from species very similar to *K. brevis*, these will contribute to this upper limit. Therefore, in this condition, to detect a bloom for every 27,500 of non target cells similar to *K. brevis*, at least 2,500 *K. brevis* cells should exist in the sample for subsequent successful NASBA detection.

3.4.3. Discussion and conclusion

3.4.3.a Current challenges

This work has demonstrated a sample preparation microdevice for total RNA extraction from a complex sample matrix. All steps in the sample preparation procedure are performed within a

disposable chip; cell pre-concentration, cell lysis, RNA extraction, and RNA purification. Although the on-bench system demonstrated better performances in terms of RNA extraction efficiency, the microdevice has the advantages of performing cell concentration, extraction providing better RNA quality, and could potentially be used for on-site sample preparation. Eluted samples were of sufficient quality for mRNA amplification and detection using NASBA. Consequently our device could be integrated within a complete microfluidic system for sub-cellular analysis of mRNA using NASBA. However the microdevice performance needs to be improved. The characterisation of the microdevice showed a few limitations including cell lysis and RNA extraction efficiency for the *K. brevis* specie. Phytoplankton cells can be difficult to lyse and there are significant differences in cell wall composition between species (Bold and Wynne 1978; Graham and Wilcox 2000). The performance of the sample preparation microdevice could perhaps be improved through operating process improvement and customising lysis buffers for specific cells with tough walls such as *K. brevis* (Graham and Wilcox 2000). Also the poor lysis efficiency could be the consequence of the volume ratio of cells / lysis buffer being reduced in the microdevice compared to the macroscale technique. This would therefore suggest a better performance can be expected with a stronger lysis buffer for on-chip lysis.

3.4.3.b Possible improvements

A solution to explore could be the use of a lysis/extraction enzymatic-based method to improve lysis efficiency²¹. Alternatively thermal lysis combined with chemical lysis can be tested with this microdevice as a temperature control is already present, Preston et al. have shown a column-based solid phase extraction technique using the thermal-chemical lysis technique (i.e. 85 °C for 8 minutes in a 3M guanidine thiocyanate lysis buffer) (Preston, Harris et al. 2011). It is important to note that a better performance for the microdevice might be obtained using mammalian cells as the Nuclisens miniMAG© commercial lysis buffer which is theoretically versatile for human cell diagnostics. This would make the microdevice attractive for applications other than environmental, but no assessment of performance for alternative applications has been done. Future improvements to the microdevice extraction procedure reported here could include reduction in size (re-design), lysis and extraction optimisation, and sample enrichment by further reduction of elution volume.

The nature of the microfluidic technology (small volume) makes lab-on-a-chip sample preparation very challenging and necessitates the integration of pre-concentration steps. Our sample preparation microdevice based on mechanical filtration does not require integration of complicated concentration steps such as immuno-beads or functionalised beads. These techniques often require active mixing to manipulate these beads in order to decrease the capture time, requiring either additional systems or human intervention. (see section 3.3, page 96) In contrast to beads-based concentration techniques, our

²¹ <http://www.zygem.com/index.html>

sample preparation microdevice can perform fast cell concentrations (within the limits of the microdevice pressure tolerance) and does not rely on bead-cell interaction time.

As discussed in the sections above the characteristics of environmental samples combined with the microfluidic technology offer a few challenges. These are due to low volume handling in microfluidic devices, combined with complex sample matrixes which might contain non-targeted phytoplankton species and a low concentration of the target. Finally the design of the selected devices and techniques should address realistic application scenarios, minimum performances needed and application versatility. A complex sample matrix combined with a low concentration target is often the case for phytoplankton environmental analysis and early stage medical diagnostic (for future work on the sample preparation step, see Chapter 5).

The work above is a unique example of a microchip for environmental sample preparation that enables the rapid concentration of cells from large volumes (in the mL range) onto an on-chip filter where they are chemically lysed, the RNA extracted, purified and eluted. The novelty stems from the use of an on-chip filter which is also used for solid phase extraction and purification of RNA from phytoplankton. We have also shown compatibility with nucleic acid amplification technology. The on-bench system demonstrated better performances in terms of RNA extraction efficiency, however the microdevice has the advantages of performing cell concentration, extraction providing better RNA quality, and could potentially be used for on-site sample preparation.

Analysis of the sample preparation microdevice	
Strengths	Weaknesses
<ul style="list-style-type: none"> • Simple method with no beads manipulation or mixing techniques. • Simple design with a one chamber chip. • Versatile extraction technique using commercial buffers. • Re-usable chips (not filter). • “Fast” and integrated pre-concentration step. • Proof of concept demonstrated with complex sample matrix (i.e. mixed species population). • Integrated device with on-site deployment potential. 	<ul style="list-style-type: none"> • Use of hazardous lysis buffer. • Thermal and flow control require. • Non specific method (i.e. Total RNA capture, non sequence specific). • Chip design limited to the aluminum oxide filter size • Different performance obtained in this work regarding the targeted species. • Input filtration flow rate 200 $\mu\text{L}/\text{min}$ which potentially is the limiting factor in reducing the overall analysis time.
Opportunities	Threats
<ul style="list-style-type: none"> • Unique work on phytoplankton concentration with subsequent RNA extraction using an aluminum oxide filter. • NASBA compatibility - can be part of a “sample-in” “answer-out” system. • Possible medical applications (i.e. commercial buffers). 	<ul style="list-style-type: none"> • Phytoplankton species are especially difficult to lysed. • Method relies on commercial aluminum oxide filter, which can be discontinued at anytime. • The lysis/extraction buffer has to be chaotropic-based therefore a customised buffer needed to meet the requirement. Performance improvement through customization might be restricted.

Table 10 Analysis of the sample preparation microdevice.

Chapter 4 RNA amplification on-chip

4.1. RNA amplification on-chip summary

Objective

As part of a complete bio-analysis microfluidic platform for RNA detection including the key functions, cell concentration, cell lysis, RNA extraction, RNA purification, RNA amplification, and product detection, we demonstrated a microdevice for the detection of the *rbcL* gene of *K. brevis* phytoplankton using NASBA. On-chip RNA amplification was detected with molecular beacons and a custom made fluorescence detection system for real-time detection of the amplification product.

Background

For active estimation of the impact of target organisms, a degree of discrimination between live and dead (or inactive) cells is required. Since DNA can persist for long periods in dead cells, attention has turned to the analysis of shorter lived RNA as a marker for viability as it is only present in active or recently moribund cells (Birch, Dawson et al. 2001). NASBA technology was chosen as the amplification method because it has already been shown that RNA amplification with NASBA is particularly suitable for early detection and quantification of harmful microalga *K. brevis* on a

macro scale system (Casper, Patterson et al. 2007). NASBA is an isothermal process of nucleic acid amplification which occurs at 41 °C, which makes it ideal for lab-on-a-chip applications because of its simplified temperature control requirement. The advantage of being isothermal is that there is no need for thermocycling at high temperatures, which is necessary in the case of a RT-PCR approach.

Methods&Results

Adsorption of nucleic acids and reagents was reduced by including BSA in the assay. Real-time detection of the on-chip RNA amplification product was achieved with a custom made fluorescence detection system. On-chip results were compared against bench top system and previously reported microdevice. The limit of quantification for the on-chip reactions is 10 cells detected as a positive reaction in 2.24 min.

Conclusions

We presented the first on-chip real-time nucleic acid sequence-based amplification of phytoplankton RNA and product detection. This uses a custom made laser induced fluorescence detection system to measure emission of cyanine 5(Cy5)-labelled molecular beacons. The limit of quantification for the on-chip reactions reported was a ten-fold increase in sensitivity compared to the previously reported device (Dimov, Garcia-Cordero et al. 2008). Please see manuscript in the Journal of Physical

Features highlight

- The first PMMA-based microdevice for phytoplankton detection using NASBA is demonstrated.
- The limit of quantification for the on-chip reactions is 10 cells detected as a positive reaction in 2.24 min which is ten-fold increase in sensitivity to the previously reported microdevice.

Chemistry Chemical Physics, entitled “*On-chip real-time quantitative nucleic acid sequence-based amplification for RNA detection and amplification*” by M.-N. Tsaloglou *, M. M. Bahi, E.M Waugh, M. Mowlem and H. Morgan (Tsaloglou, Bahi et al. 2011).

4.2. NASBA-based microdevices

Gulliksen et al. reported a parallel nanolitre microdevice for amplification and detection of artificial human papilloma virus in SiHa human cells. The chip was made of COC polymer and treated with PEG-methanol to avoid enzyme adsorption. Real-time amplification was monitored with a LED induced fluorescence-based detection system combining Fresnel, collimating lenses and a photomultiplier. The system was designed to detect 400 nM of molecular beacons in a 80 nL incubation chamber and reach a limit of detection of 10^{-6} μ M for artificial HPV 16 sequences, and 20,000 cells/mL for the SiHa cell line (Gulliksen, Solli et al. 2004; Gulliksen, Anders Solli et al. 2005). They also demonstrated on-chip storage of dried enzymes (Furuberg, Mielnik et al. 2008). As a result the Institut fur Mikrotechnik Mainz in collaboration with the University of Oslo developed a diagnostic platform for the detection of HPV E6/E7 mRNA (Gulliksen and Hansen-Hagge 2012). A standalone bench-top system using microchips was finalised where nucleic acid analysis is accomplished using different pieces of equipment (see section 1.3.2.b, page 50). The automated platform was made of two on-bench systems using microchips, one for sample preparation and one for amplification and detection (see Figure 44) They developed a stand-alone bench-top system using microchips, where nucleic acid analysis is accomplished using different pieces of equipment. It is clear that these systems are not ready for on-site applications and require further integration (see section 1.3.2.b, page 50).



Figure 44 Automated lab-on-a-chip system for sample preconcentration, nucleic acid extraction, amplification, and real-time fluorescent detection. (a) Sample preparation chip, (b) Sample preparation instrument (c) NASBA chip, (d) NASBA instrument. Taken from (Gulliksen and Hansen-Hagge 2012).

Smith et al. presented a compact hand-held analyser for real-time NASBA monitoring. The device incorporates the amplification and detection steps. Temperature regulation of the capillary reaction chamber (~ 40 μ L) was carried out with a resistive-based heater and a LED-based fluorescence system monitored the real-time amplification. The system had performance detection for fluorescence ranging

from 0.5 to 10 μM with a photodiode. It is worth noting that the NASBA assay for *K. brevis* (Casper, Patterson et al. 2007) used a maximum concentration of 400 μM for the molecular beacon probe, therefore this system would not be able to detect any amplification using the *K. brevis* assay. The device was USB powered and had a weight of as little as 140 g which made it portable for on-site monitoring. However the device could not perform sample preparation steps and the crucial annealing step at 65°C to accomplish NASBA (Smith, Steimle et al. 2007). No performance regarding the assay limit of detection was given. Casper et al. developed a protocol for on-site lysis and extraction from water samples and coupled it with a handheld NASBA device interfaced with a PDA (personal digital assistant) for RNA amplification and detection in a 20 μL chamber. The calculated detection limit was about 400 cells/L (Casper, Patterson et al. 2007). The RNA field extraction protocol was based on manual intervention and could not be performed automatically. The system uses LEDs, photodiodes, and optical filters for detection. Temperature was maintained optically using an infrared heater and no specific treatment against enzymes adsorption is mentioned. It is a macro scale system that could not be deployed for long term deployment, and to our knowledge this system does not use the lab-on-a-chip technology. Dimov et al. were the first to demonstrate a system incorporating RNA purification and NASBA assay on a single chip (see section 1.3) and real-time detection was performed using a fluorescence microscope. The system achieved a detection limit of as little as 100 *Escherichia coli* cells per 10 μL sample (Dimov, Garcia-Cordero et al. 2008). It is worth noting that further developments of the system are necessary in order to finalise a truly portable system (see section 1.3.2.b, page 50).

4.3. On-chip real-time nucleic acid sequence-based amplification for RNA detection and amplification

As part of a complete bio-analysis microfluidic platform for RNA detection including the three key functions, cell lysis, RNA extraction and RNA amplification, we demonstrated the first on-chip real-time nucleic acid sequence-based amplification of phytoplankton RNA and product detection. This uses a custom made laser induced fluorescence detection system to measure emissions of cyanine 5 (Cy5)-labelled molecular beacons. The limit of quantification for the on-chip reactions reported (Tsaloglou, Bahi et al. 2011) was ten cells detected as a positive reaction in 2.24 min which is a ten-fold increase in sensitivity when compared to the previously reported 3 min for 100 *Escherichia coli* cells detected on-chip (Dimov, Garcia-Cordero et al. 2008). The objective was to demonstrate proof of concept for a PMMA-based microdevice using NASBA, a custom fluorescence detection system where optical components were precisely arranged and aligned was assembled to measure emission of Cy5-labelled beacons during RNA amplification. However miniaturization of this optical setup is often difficult and requires further development to integrate and reduce the number of optical components without altering the detection sensitivity (see section 4.5, page 131 and Chapter 5).

4.3.1. Materials and methods

4.3.1.a Algae culture

K. brevis (strain CMPP 2228, Bigelow Laboratory for Ocean Sciences, USA) cells were grown in L1 Aquil* artificial seawater media at 20 °C with 12 h: 12h light: dark at high irradiance. Cell samples were harvested during exponential cell growth. Cell growth was monitored by counting 1 mL culture aliquots fixed in 1% Lugol's solution (Sigma Adrich, UK) in a Sedgwick-Rafter counting chamber (Fisher Scientific, UK).

4.3.1.b Sample preparation

Cells were lysed using a guanidine thiocyanate chaotropic lysis buffer according to the directions of the manufacturer (Nuclisens Lysis Buffer, bioMérieux, Netherlands). RNA from the cell lysate was purified using a commercial kit, which uses magnetic beads according to the directions of the manufacturer (Nuclisens miniMAG©, bioMérieux, Netherlands).

4.3.1.c Bench top NASBA

The pure RNA extract was amplified and measured with a bench-top time resolved fluorescence micro-plate reader instrument (EasyQ™ analyser, bioMérieux, Netherlands). Conditions for NASBA reaction have been previously described (Casper, Paul et al. 2004). Forward primer sequence was ACG TTA TTG GGT CTG TGTA, Reverse primer sequence was incorporating the T7 promoter AATTCTAATACGACTCACTATAGGGAGA AGG TAC ACA CTT TCG TAA ACTA. In order to maximise the fluorescence intensity, the quencher / fluorophore couple was modified and the *K. brevis* beacon was changed to Cy5- GAG TCG CTT AGT CTC GGG TTA TTT TTT CGA CTC- Black Hole Quencher 2 (BHQ2) (see in Appendix A – NASBA design basic succession steps to design a NASBA assay). Oligonucleotides and beacon were purchased from Eurofins MWG Operon (Germany) and were of the highest purity. NASBA Basic EasyQ™ kits were from bioMérieux (UK).

4.3.1.d Microchip fabrication

PMMA microchips (75 x 25 mm) were manufactured from 1.5 mm thick poly-methyl methacrylate (Röhm, Darmstadt, Germany) with features formed using an automated LPKF Protomat S100 micro-mill and bonded using solvent vapour, as previously described (Ogilvie, Sieben et al. 2010). Each chip consisted of a single chamber (8 x 8 mm x 250 µm) with connecting channels (250 x 250 µm) to an inlet and outlet.

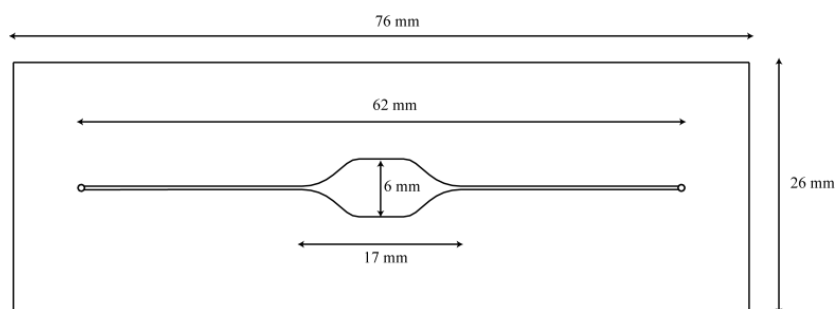


Figure 45 Illustration of the microchip with dimensions of all features shown.

4.3.1.e Material compatibility assessment

As discussed in section 1.4, protein adsorption is a key issue for nucleic acid amplification-based microfluidic systems as this can deteriorate amplification efficiency or even cause complete amplification inhibition. The first objective was to demonstrate the compatibility of the NASBA procedure with PMMA microchips. Fluorescence labelled BSA at a concentration of 2 mg/mL (BSA, Conjugate Alexa 488 nm, Invitrogen, UK) was used to test protein adsorption in PMMA and COC microchips with different surface treatments. COC microchips (5 x 5 mm x 100 μ m) were provided by Ikerlan²² (detailed CAD design was not provided). After fabrication, microchips that were treated were washed sequentially with RNA ZapTM, 70 per cent (v/v) ethanol and 2 per cent (w/v) bovine serum albumin in water. Untreated microchips were washed with RNA ZapTM, 70 per cent (v/v) ethanol and free RNA water only. After treatment, microchips were rinsed with 1 mL free RNA water. Subsequently labelled BSA (2 mg/mL) was loaded into treated (with non labelled BSA for 24 hours) and non-treated microchips and left for 10 minutes incubation. Then the chips were rinsed with 1 mL free RNA water to remove the unabsorbed enzyme. Surface adsorption of the labelled BSA (using the dye Alexa 488 λ_{ex} = 495 nm, λ_{em} = 519 nm) was qualitatively evaluated using fluorescence imaging microscopy (microscope details). Fluorescence images of treated and non-treated microchip were compared.

4.3.1.f On-chip NASBA and fluorescence setup

A custom fluorescence detection system was assembled to measure the emission of Cy5-labelled beacons during RNA amplification (Figure 46a). Excitation light at 635 nm from a 5 mW laser diode (CPS182, Thorlabs, UK) was focused into the reaction chamber by a Nikon 20x Plan Fluor objective. During the NASBA incubation time, custom-made mechanical shutters using a “two positions” DC motors were used to reduce photo-bleaching of the fluorophore by creating a two-second excitation pulse once every minute. The fluorescence light was sampled through the same objective used for focusing. Excitation light was excluded from fluorescence detection using two dichroic mirrors: D1 (XF 2055 400-535-635TBDR, Omega, USA), D2 (XF2018 580DRLP, Omega, USA), and a band pass filter (FF01-660/13-25, IDEX, USA). The fluorescence signal was detected with a compact H5784-20

²² http://www.ikerlan.es/site_preview/index.php

photomultiplier tube (Hamamatsu, Japan). The photomultiplier tube signal was PC-interfaced with a PCI-6289 data acquisition card (National Instruments, Texas, USA). A LabVIEW™-based program was developed for real-time monitoring of the photomultiplier tube electrical signal. Prior to each experiment, adjustment of focus was performed using the resultant image of irradiation separated at D2, focused into a colour camera (Watec WAT-221S, USA). A two-part close-fitting holder (120 x 36 x 40 mm), manufactured from aluminium alloy (grade 6063, Aalco, UK), was used to provide the objective with mechanical alignment and to enable precise temperature regulation with its high thermal mass (Figure 46b).

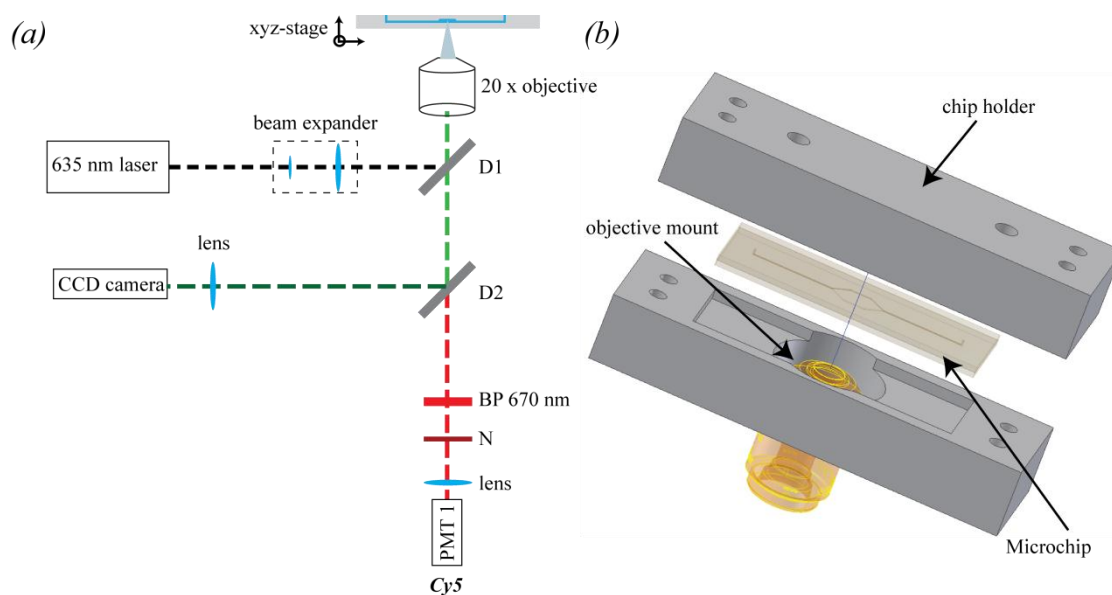


Figure 46 (a) Schematic of optical geometry, where D1 and D2 are dichroic mirrors, N is notch filter, and BP670 is band pass filter at 670 nm. (b) Microchip as housed in thermoregulated chip holder shown with a 20x objective.

The temperature of the chamber was maintained at $41 \pm 0.1^\circ\text{C}$ with an analogue PID control system on each half of the chip holder. Each PID used a 30 W heating resistor (LTO30 Power Resistor T/F 15R, Vishay Intertechnology, USA) and a negative temperature coefficient thermistor (B57540G0303J, Epcos, Germany). Before each microchip-based experiment, temperature control reliability was verified against a reference chip with an embedded thermistor. Optical and thermal controls were PC-interfaced with a PCI-6289 data acquisition card (National Instruments, Texas, USA). A LabVIEW™-based program was developed for real-time monitoring of both optical and thermal control systems.

4.4. Results

4.4.1.a Material compatibility assessment

Figure 47 and Figure 48 show that the non-treated PMMA and COC microchip surface adsorbs large quantities of fluorescent BSA in comparison to the BSA coated surface. While the fluorescently labelled Alexa 488 molecules were uniformly adsorbed over the whole surface of the reaction chamber of the non treated PMMA and COC, the BSA treated microchip showed only smaller areas with high intensity of fluorescence. This measurement revealed clearly that the BSA coated surface had reduced protein adsorption.

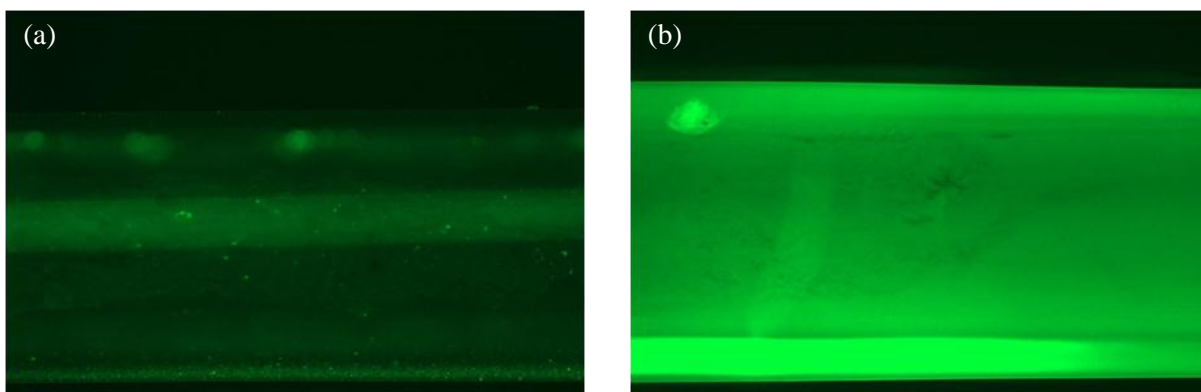


Figure 47 Adsorption of BSA labelled onto PMMA microchips. Microscope fluorescence pictures - Alexa 488 $\lambda_{\text{ex}}=495\text{ nm}$, $\lambda_{\text{em}}=519\text{ nm}$. (a) BSA treated PMMA chip after water rinse, b) native PMMA microchip after water rinse.

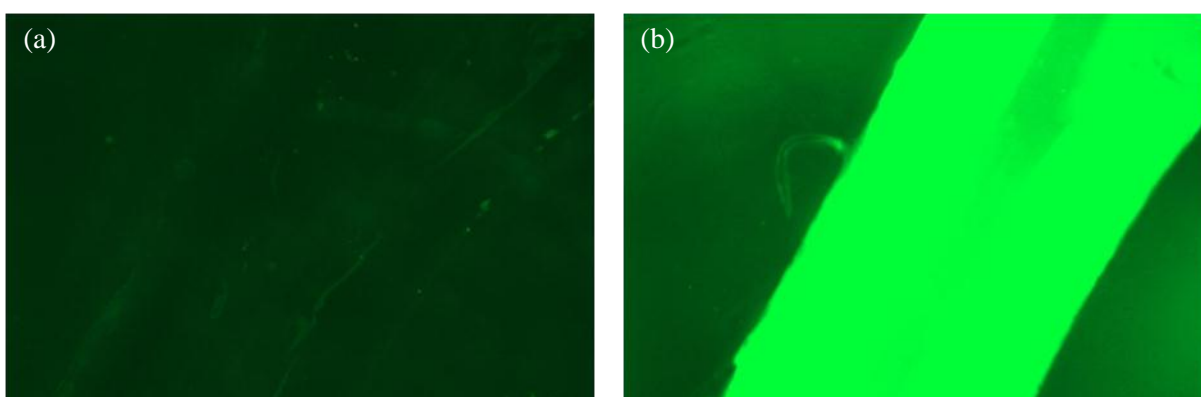


Figure 48 Adsorption of BSA labelled onto COC microchips. Microscope fluorescence pictures - Alexa 488 $\lambda_{\text{ex}}=495\text{ nm}$, $\lambda_{\text{em}}=519\text{ nm}$. (a) BSA treated COC chip after water rinse, b) native COC microchip after water rinse.

4.4.1.b On-chip NASBA and fluorescence setup

Figure 49 shows real-time RNA amplification using PMMA microchips for four different *K. brevis* cell concentrations. The figure shows a clear relationship between the rate of fluorescence increase and the input RNA concentration. The data suggest that the BSA-treated PMMA chambers support NASBA amplification. However the kinetics observed with the microchip do not match the classical bi-exponential amplification curve observed for NASBA. However, this configuration was good enough for end point measurement and a qualitative assessment of the presence of the targeted species: sample with different cell numbers could be distinguished from the negative control. A standard curve of *K. brevis* cell dilution versus NASBA amplification was plotted (Figure 49b). The threshold of detection was set as three time the standard deviation of the negative control (i.e. approximately 10 mV).

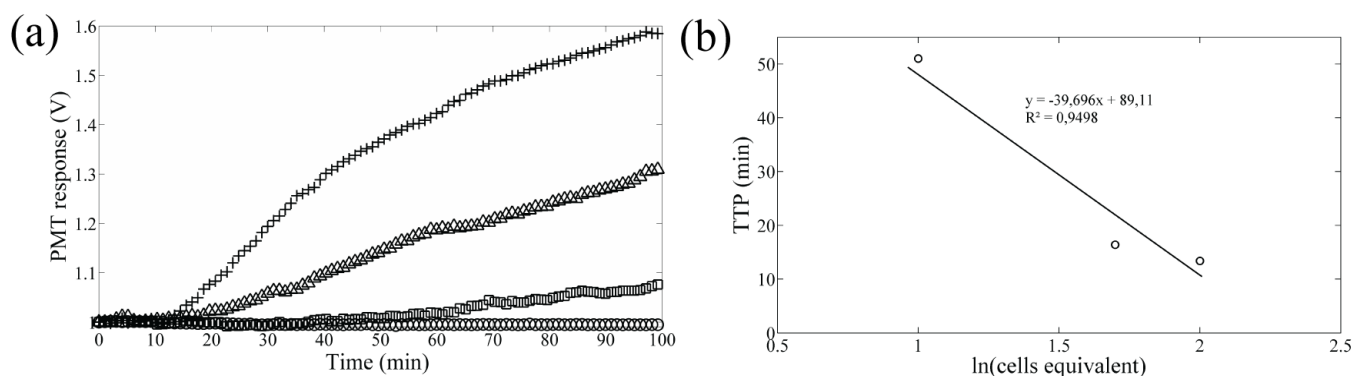


Figure 49 (a) *K. brevis* cells amplified on-chip results for 100 cells (crosses), 50 cells (triangles) and 10 cells (squares) and negative control (circles), the background (DC) fluorescence from the polymer has been subtracted. (b) The standard curve analysis of NASBA.

However after tests and verifications using a dummy chip we observed that the temperature controller was delivering a lower temperature than the NASBA technique requires. After modification of the temperature system microdevice, kinetics were comparable to the conventional bench-top measurement. Typical NASBA plots were obtained for *K. brevis* cells for the microdevice based system and were compared to bench-top measurement (see Figure 50).

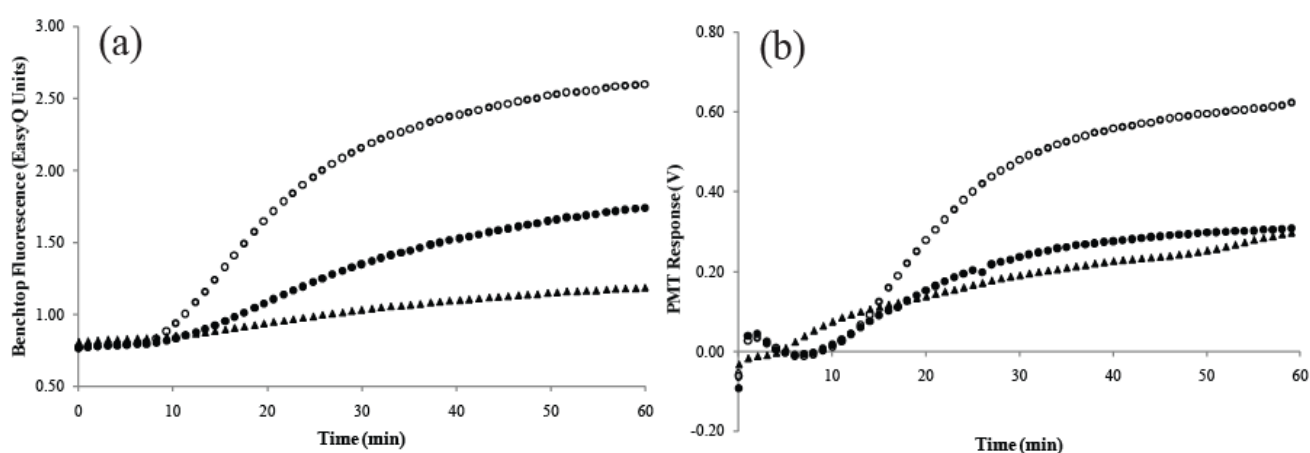


Figure 50 *K. brevis* cells amplified bench-top (a) and on-chip (b). Results for 400 cells (empty circles), 100 cells (full circles) and 10 cells (full triangles). For the on-chip data, the background (DC) fluorescence from the polymer has been subtracted. Taken from (Tsaloglou, Bahi et al. 2011).

Figure 50 shows results for 400, 100 and 10 cell equivalents, corresponding to dilution of RNA extracted from 100,000 *K. brevis* cells in culture. Figure 50a shows the classical bi-exponential amplification curve observed for NASBA. The small offset in the fluorescence level at time zero is due to background from beacons that are not fully quenched. Efficient FRET (see section 1.2.1, page 32) is dependent on key parameters including donor to acceptor molecule distance (between approx. 10 – 100 Å). The short distance (a few nucleotides - equivalent to a distance between 10 to 20 nm) between the fluorophore (donor) and the quencher (acceptor) when the beacon is open can still result in a good quenching efficiency (Lakowicz 1999).

Figure 50b shows the results for the on-chip amplification. A much higher level of background fluorescence was observed (and has been subtracted in the plot), which was the direct result of the PMMA microchip autofluorescence and the wider emission bandpass of the dichroic mirrors D1 (~100 nm), compared to the bench top instrument (~40 nm). Each curve was obtained from a fresh microchip and the background fluorescence varied from chip to chip.

As discussed in the section 1.2.1, NASBA curves can be fitted to Equation 2 using non-linear regression methods. Figure 51a shows a typical NASBA curve and its fitted fluorescence curve using Equation 2. Figure 51b shows the linear relationship obtained between the natural logarithm of $(k_1\alpha_1\alpha_2^2)$ against the natural logarithm of cell equivalents. The results between bench-top and on-chip amplification are comparable and produced equivalent slopes, indicating a similarity in amplification reaction for both methods.

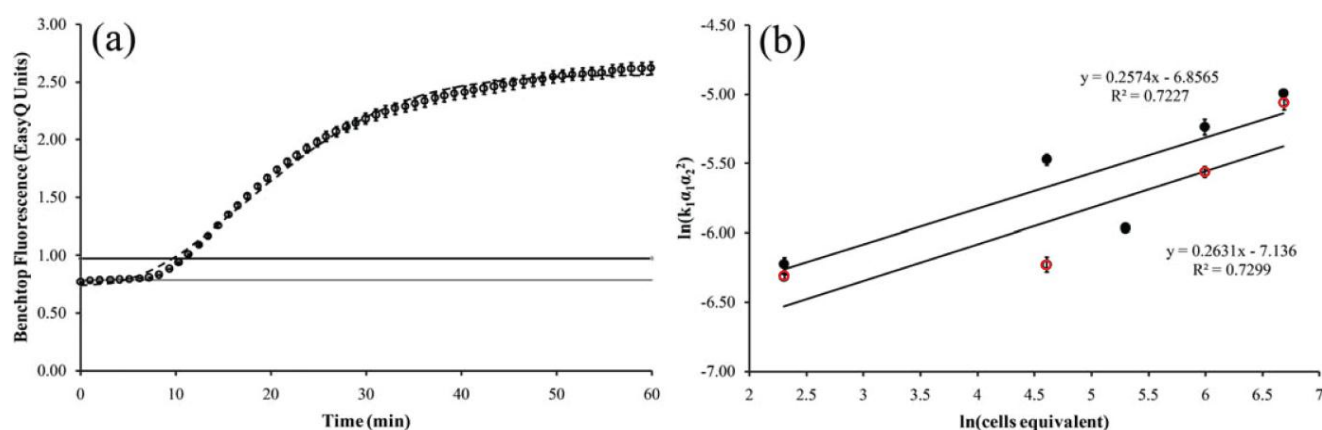


Figure 51 (a) Data for 400 *K. brevis* cells equivalent amplified bench-top (open circles). Dashed line is the fitted fluorescence curve, solid black line is TOD based on negative controls and solid grey line is TOD based on the average of the first five points of measured fluorescence. (b) Relationship between nominal cell number and the observed logarithm of the $k_1\alpha_1\alpha_2^2$ as obtained by on-chip (full circles) and bench-top (red open circles) experiments. Taken from (Tsaloglou, Bahi et al. 2011).

4.5. Discussion and conclusion

We present a microdevice for the detection of RNA using NASBA. The limit of quantification for the on-chip reactions reported (Tsaloglou, Bahi et al. 2011) was 10 cells detected as a positive reaction in 2.24 min which is ten-fold increase in sensitivity compared to the previously reported 3 min for 100 *Escherichia coli* cells detected on-chip (Dimov, Garcia-Cordero et al. 2008). Figure 50b shows the results for the on-chip amplification, for 100 and 10 cells the NASBA fluorescence end points are comparable. Nevertheless as discussed in the Chapter 1 section 1.2.1 the NASBA amplification slope is function to the initial amount of RNA, therefore it should be noted that the NASBA curve for 100 cells has a steeper incline than the NASBA curve for 10 cells. However, the limit of quantification is dependent on several parameters. The limit can vary from assay to assay due to the characteristics of the primers, the molecular beacon, type of sample material, the concentrations of the reagents within

the reaction mixture, surface chemistry, heat transfer, and the quality of the detection system. In our case the better limit of quantification could be the result of the high sensitivity fluorescence detection setup used (i.e. with precisely aligned optics and a high sensitivity photomultiplier). It is worth noting that the molecular beacon design used by Dimov et al. (FAM: Black Hole Quencher 1 (BHQ1)) offers a higher signal to noise ratio compared to our molecular beacon design (Cy5:BHQ2)²³. In contrast to Dimov et al. sample lysis and annealing steps were performed off-chip, therefore further implementations of this key function need to be integrated in our future system by combining our sample preparation device (Chapter 3) with a new version of the NASBA microchip that incorporates an annealing function. Compared to the handheld NASBA analyzer developed by Casper et al. using an IC (Casper, Patterson et al. 2007), only qualitative quantification was performed as no IC was present which can result in significant differences between individual microchip results. Therefore further developments of an IC need to be explored.

The objective was to demonstrate proof of concept for a PMMA-based microdevice using NASBA (a custom fluorescence detection system where optical components were precisely arranged and aligned) which was assembled to measure the emission of Cy5-labelled beacons during RNA amplification. However, miniaturization of this optical setup is often difficult and requires further development to integrate and reduce the number of optical components without altering the detection sensitivity. A first step could be the development of a miniature LED-based fluorescence system using a LED, a PMT, emission and excitation filters and a collimating lens (see Figure 52) similar to the system presented by Xu et al. (Xu, Hsieh et al. 2010).

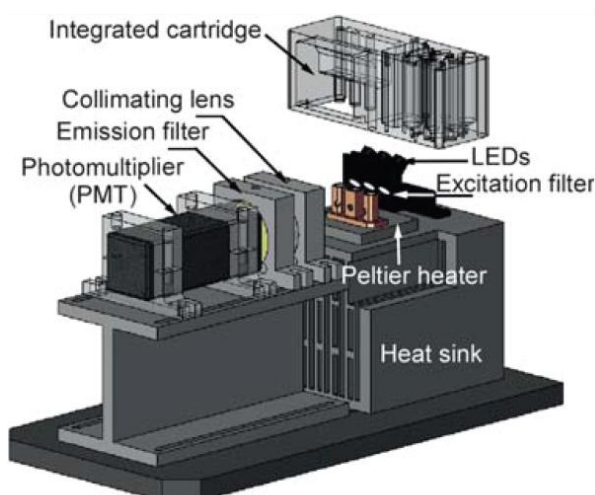


Figure 52 Schematics of the real-time PCR system with integrated sample preparation and fluorescence detection. Taken from (Xu, Hsieh et al. 2010).

The integration of microlenses into microfluidic devices can help to improve fluorescence detection in microsystems by focusing light into the channel to improve the excitation density power, without

²³ <http://www.biosearchtech.com/download/brochures/bhqbrochure.pdf>

using off-chip optical components (e.g. glass lenses). Seo and Luck Lee developed a self-aligned 2D compound microlens for biochip applications. The microsystem has several advantages such as disposability, controllability of optical characteristics, self-alignment and simplified fabrication processes using PDMS (Seo and Lee 2003).

The work above is a unique example of an on-chip real-time nucleic acid sequence-based amplification of phytoplankton RNA and product detection. This technique uses a custom made laser induced fluorescence detection system to measure emission of Cy5-labelled molecular beacons. The limit of quantification for the on-chip reactions reported was a ten-fold increase in sensitivity to the previously reported device. Currently our NASBA microchip strongly relies on extensive manual handling. Still, a number of important issues remain to be studied before satisfactory results can be obtained. Integration and automation of self-contained amplification and detection-chips will be essential in order to constitute a fully automatic, on-site independent monitoring system.

Summary of the NASBA microdevice-based system	
Strengths	Weaknesses
<ul style="list-style-type: none"> • mRNA amplification on a PMMA microdevice. • Low limit and fast detection, 10 cells in 2.24 minutes. • Isothermal method. • Viable species detection. 	<ul style="list-style-type: none"> • Off-chip annealing step at 65 °C. • Bulky fluorescence setup – it is a microdevice in a laboratory. • No quantification – need to incorporate an internal calibrator (i.e. internal control). • It is an early demonstration with no real microfluidic functions.
Opportunities	Threats
<ul style="list-style-type: none"> • Sensitive method that can be use for accurate phytoplankton species monitoring. • Alternative technique to PCR, high temperatures thermocycling method. • Potential for being the first lab-on-a-chip based system for phytoplankton RNA analysis. • The system can be adapted for use as a general RNA amplification device. • Dried reagent storage using protectants is a well known method and can be used for environmental application... 	<ul style="list-style-type: none"> • NASBA is not as well known as PCR. • Greater bio-chemical complexity relative to PCR, NASBA involves 3 enzymes, PCR only one. • Proteins adsorption is a major issue for plastic chips, and treatment methods can be involve complicated protocols. • NASBA is very susceptible to inhibition. • Annealing temperature (65 °C) could modify chip surface in long term and inhibit the reaction.

Table 11 Summary of the NASBA microdevice-based system.

Chapter 5 Discussion and further work

5.1. Conclusion

Traditional methods for HAB monitoring require sample collection and preservation for later study in the laboratory (Galluzzi, Penna et al. 2004; Anderson 2009). Alternatively, laboratory equipment has been adapted for ship-board use. For example, instruments which utilise optical characters that are unique to the target organism have been developed and these have been mounted on board research vessels (Kirkpatrick, Orrico et al. 2003). However in some cases these methods are slow and do not provide the temporal and spatial resolution (i.e. particular location and depth - (Gentien, Lunven et al. 1995)) essential for the true understanding of HAB evolution (Rantajaervi, Olsonen et al. 1998; Vila, Camp et al. 2001; Anderson, Cembella et al. 2011; Erickson, Hashemi et al. 2011). This can only be addressed using submersible sensors small enough to be integrated into autonomous underwater vehicles (AUVs) and argo float station networks (Anderson, Cembella et al. 2011; Erickson, Hashemi et al. 2011).

The purpose of this work has been to develop key functions in independent microdevices that perform elements of a complete biological assay for RNA phytoplankton metrology, from the sample preparation to the detection step. Whilst a complete sample-to-result chip or device has not been realised, the developments described in this thesis are important innovations leading to this final goal. Specifically this thesis reports the development of three lab-on-a-chip devices which perform microalga concentration, cell lysis, nucleic acid purification and real-time RNA detection. The aim was to demonstrate proof-of concept for each device separately in order to decouple the complications of system integration, whilst understanding performance needed and characterising the system to most likely scenarios for real-world applications. To achieve this, most of the available literature was reviewed with the focus given to sample preparation methods including concentration steps and molecular biology assays for RNA amplification. These methods were selected based on their advantages including simple sample concentration techniques, molecular biology assay availability in our laboratory and simple fluidic and thermal designs etc. To our knowledge, this work presents the first work employing SPE and NASBA in microchip format for preparation, detection and amplification of phytoplankton RNA. Still, a number of important issues remain to be studied before satisfactory results can be obtained. Integration of self-contained sample preparation chips along with amplification and detection chips will be essential in order to constitute a fully automatic, on-site independent monitoring system. Further, the integrated system has to be validated with regard to sensitivity, risk of cross-contamination, robustness and the reliability of the system for trial deployments.

Firstly, we presented the first demonstration of electrical lysis for RNA extraction from phytoplankton cells. Lysis efficiency results were comparable to the commercial bench top lysis method - the amount of total RNA extracted from cells using electric field-mediated cell lysis was around 15 pg.

Dielectrophoresis at 1 V_{pp}, 200 kHz for 10 s duration was used to concentrate the cells from suspension onto electrodes. Total membrane destruction was observed at a voltage of 45 V, 600 kHz for 60 seconds duration, and optimal lysis conditions were found to be, 1 V, 120 s, and 30 V, 1 s. However for on-site preparation (i.e. seawater medium), cells are in seawater which is a highly conductive medium. This means that only negative DEP occurs, and this is with a force weaker than positive DEP (real Clausius-Mossotti factor has a maximum value of 0.5 for negative DEP, see Figure 21). Moreover, subsequent high electric field mediated lysis cannot be performed after negative DEP, as cells are attracted to low electric field zones. Therefore for on-site application cells need to be re-suspended or transferred into a non conductive medium in order to enable positive DEP and high electric field mediated lysis. This could result in the implementation of complex design and sample preparation techniques.

Secondly, for the sample preparation step we explored an alternative technique based on filtering technology for sample concentration and nucleic acid extraction (Kim and Gale 2008; Baier, Hansen-Hagge et al. 2009). We developed a RNA sample preparation microdevice (see Chapter 3) with cell concentration using a mechanical filter (nanoporous aluminium oxide), chemical lysis, and nucleic acid extraction and purification using the same filter as used for mechanical filtering. This was also the first demonstration and characterisation of a sample preparation microdevice for phytoplankton cells in simulated environmental conditions (i.e. complex sample matrix). A series of biological experiments were conducted to validate the efficiency of the designed microdevice by lysing cells and extracting released RNA molecules. At least 200,000 cells can concentrate onto the filter in the microdevice. The RNA binding efficiency of the microdevice method was 47.1%. As few as 10 *Karenia mikimotoi* cells prepared on-chip provided sufficient RNA for Bioarray detection. The number of *K. brevis* cells necessary for subsequent NASBA detection was 2,500 cells prepared using the microdevice. The on-bench system demonstrated better performance in terms of RNA extraction efficiency, however the microdevice has the advantage of performing cell concentration, extraction providing better RNA quality, and could potentially be used for on-site sample preparation. Further improvements are discussed below.

Finally, in this thesis was presented the first on-chip real-time nucleic acid sequence-based amplification of phytoplankton RNA and product detection. This uses a custom made laser induced fluorescence detection system to measure emissions of Cy5-labelled molecular beacons. The first PMMA-based microdevice for phytoplankton detection using NASBA was demonstrated. The limit of quantification for the on-chip reactions was 10 cells detected as a positive reaction in 2.24 min, which is a ten-fold increase in sensitivity when compared to the previously reported microdevice (Dimov, Garcia-Cordero et al. 2008). However our system needs further development and integration in order to achieve a truly portable system.

The sample preparation microdevice characterised in Chapter 3 showed that the number of *K. brevis* cells necessary for successful on-bench subsequent amplification was approximately 2,500 cells prepared using the microdevice with a sample matrix ratio of 1:4 (targeted species : non targeted species). For the RNA amplification on-chip, we demonstrated a limit of detection of 10 *K. brevis* cells using a custom-made macro-scale fluorescence system. Currently the combined system from sample preparation to detection using our microdevices is strongly limited by the sample preparation step performance. Below we discuss further improvements for both sample preparation and amplification steps.

5.1.1. Sample preparation

In the Chapter 3 demonstrated a microdevice for sample preparation, which is both a fundamental component for molecular biology analysis and a challenging function to integrate into a microchip. As discussed in Chapter 3, real-world samples are often large and sometimes incompatible with micro scale technology. For a complex sample matrix, a specific preparation technique is required. For example using cell-specific capture techniques, or using nucleic acid sequence-specific capture with functionalized beads. Therefore an ideal sample preparation system would require, for example, a concentration step using a mechanical filter where targeted and non targeted species concentration will increase making feasible the use of high volume samples in a microfluidic device. The system would then use a chemical lysis technique compatible with a high discriminatory extraction technique to capture the targeted analyte, for example combining mixing and the use of functionalized beads for nucleic acid sequence specific capture (Mangiapan, Vokurka et al. 1996; Chernesky and Jang 2006). The sample preparation technique can be based on specific RNA sequence capture, which uses hybridization and magnetic particles to isolate the target sequences and separate them from non target analytes in the complex sample matrix, which may contain amplification inhibitors (Wang, Lien et al. 2011). However it is important to note that sequence specific techniques rely on nucleic acid hybridization, which can be time consuming and sometimes non specific bindings can occur. It might be worth exploring a less discriminatory method (i.e. mRNA can be specifically extracted by introducing coated beads with an oligo (dT), see section 3.3.1.c, page 97). An alternative design could create a large volume loop (3 mL) in a microfluidic device where lysis buffer (see Figure 53), sample and functionalized beads can be mixed at a high flow rate. Then beads can be separated from the lysate, transferred and captured (i.e. using a magnet) into a low volume chamber for the washing and elution steps.

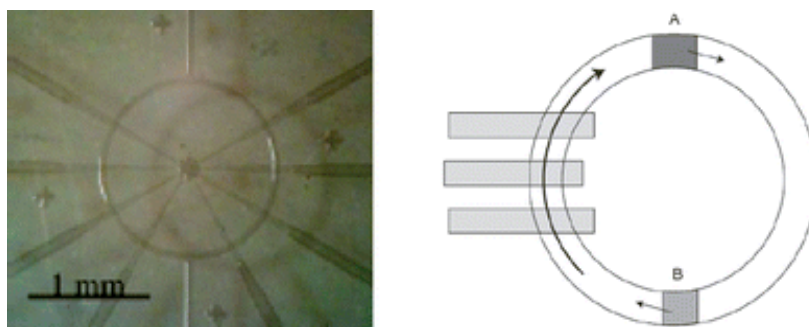


Figure 53 Illustration of a micromixer. “The three rectangles on the left represent a peristaltic micropump and A and B represent two spots which will eventually mix in the rotary micromixer”. Taken from (Tabeling 2009).

Another important requirement for seawater sampling is the separation of particles with a range of different sizes as encountered in natural samples. This often leads to the clogging of filters. A strategy to address this issue could be the use of different filters in series of descending pore size from the front end (i.e. seawater) to the back end (i.e. microchip inlet) of the collection system. Combining this architecture with a washing protocol using bleach could reduce filter clogging. (Preston, Harris et al. 2011).

5.1.2. Integration

The long term goal of this work is that separate microdevices may be integrated into a fully automated single chip for field operation which can receive and treat fresh samples to obtain a pure solution of nucleic acids which, in turn, can be transferred to the amplification chip. All analytical functions should be integrated without forgetting instrumentations integration (fluorescence detection system, microfluidic actuation) and fully automated. In my view this is where the gap is: efforts should focus on integration to avoid the development of a macro scale system using a microchip. Many laboratories aiming to develop portable systems eventually generate stand-alone bench-top systems using microchips, where nucleic acid analysis is accomplished using separate pieces of equipment. Potential portable instrument systems that incorporate sample preparation and detection have also been developed for environmental applications. However, very few are suitable for real environmental deployment and often require laboratory infrastructure or personnel to facilitate sample collection and processing (Bruckner-Lea, Tsukuda et al. 2002; Belgrader, Elkin et al. 2003; Regan, Makarewicz et al. 2008; Lefevre, Chalifour et al. 2012). To achieve full integration, key functions on microchips have to be improved in order to deliver better performance through re-design, fluidic actuation implementation (see section 1.4.7, page 60), reagent storage strategy (see section 1.4.3, page 58), quantification strategy and fluorescence detection system integration (see section 1.4.4, page 58). For ease of use, if the system requires on-chip reagent, stored reagent must be stably stored on-chip. The protocol for dried NASBA reagents has been previously described²⁴ (Carpenter, Prestrelski et al. 1993; Prestrelski,

²⁴ de Rosier. A, de la Cruz. B, and Wilkosz. K, (2001) Method and formulation for stabilization of enzymes, US patent <http://www.patentstorm.us/patents/6294365/description.html> (for NASBA)

Arakawa et al. 1993; Roy and Gupta 2004; Seetharam, Wada et al. 2006; Gulliksen, Marek. et al. 2007). Finally reagent dispensing could be fully automated with the integration of fluid actuation components (i.e. valves, pumps and mixers). It is worth highlighting that it is essential to understand the performances needed and most likely scenarios that the system will be exposed to for real world applications.

Molecular biology analyses are inherently slow compared to most chemical measurements. In our case the challenge is in the sample preparation technique used - how to collect a large volume sample, separate unwanted species and concentrate analyte in a micro scale device as fast as possible. Alternatively an equivalent method of electronic buffers could be reproduced where a sample queue processing technique could be performed combined with sample conservation techniques and prior sensor analysis. However AUVs might not have the capacity to store hundreds of millilitres of seawater and sample conservation techniques might still degrade nucleic acid, particularly mRNA. In my view molecular biology-based microchips have key features suitable for on-coast seawater analysis (i.e. portable, low volume consumption), but the current level of maturity of this technology is restricting potential incorporation into AUVs (i.e. fluidic actuation components, optical components integration, amplification time).

High throughput-based methods (i.e. droplets) that offer fast nucleic acid analysis could be an alternative solution. Microdroplet technology has recently been utilized to perform PCR in droplets, which offers shorter thermal-cycling times, lower surface adsorption and offers great potential for single DNA molecule and single-cell amplification (Mohr, Zhang et al. 2007; Zhang and Ozdemir 2009; Hatch, Fisher et al. 2011). Combining PCR or NASBA to droplet technology in which a single cell could be statistically isolated, and where lysis and RT-PCR / NASBA reactions could be performed has the potential to offer automation and parallelization processes. High throughput droplet methods rely on the sufficiently direct analysis of the cell lysate and often sample preparation is not required ahead of the analysis (Mary, Dauphinot et al. 2011). This could avoid the use of a complicated extraction process with separation and isolation. However droplet technology is still in development and requires more complex system design than traditional lab-on-a-chip techniques (Guzowski, Korczyk et al. 2011; Hatch, Fisher et al. 2011). Moreover, sample preparation functions (cell concentration, nucleic acid extraction and purification) need to be demonstrated for these microdroplet-based systems

Finally the different microchip developments are promising proof of concept for on-site or on-coast environmental analysis of phytoplankton species. The final aim will be to demonstrate a self-contained microdevice, in which all reagents are stored on-chip and which benefits from minimal handling by the user enabling the analysis to be performed automatically. The future microdevice might not only be limited to environmental applications, it could be adapted for use as a general RNA analysis

platform for medical and clinical applications. It is very important to appreciate the level of interdisciplinary input needed and the magnitude of the task to develop these complex systems for gene analysis. This has led to the emergence of a highly interdisciplinary field bringing biologists, chemists and engineers closer.

5.2. Further work

This section focuses on making some suggestions to further extend and improve this research. These suggestions are listed as follows:

5.2.1. Sample preparation

- As discussed in Chapter 3, further improvement of lysis efficiency. Thermal lysis combined with chemical lysis can be tested with our microdevice as a temperature control is already present.
- More optimisations are necessary to obtain a rapid and simple extraction protocol with efficient buffer conditions (lower reagents to sample ratio) suitable for chip-based extraction process.
- As a temperature control is already present in the sample preparation device, this can be used to investigate the efficiency of the on-chip NASBA on the aluminium oxide filter. Since this process could be performed in the same extraction chamber, it reduces the fluidic problems as well as fabrication complexity. In addition, the elution step can be eliminated.
- Alternative extraction techniques based on functionalized beads should be tested, characterised (including maximum binding capacity), optimised and compared on bench. As discussed above, the use of functionalized beads for nucleic acid sequence specific capture should be explored. Sample preparation techniques can be based on specific RNA sequence capture which uses hybridization and magnetic particles to isolate the target sequences (Wang, Lien et al. 2011) and separate them from non target analytes in the complex sample matrix. This should be tested on bench top instruments. A less discriminatory method using coated beads with an oligo (dT) should also be tested on bench top instruments and compared to other methods.
- A solution to explore could be the use of a lysis/extraction enzymatic-based method to improve lysis efficiency²⁵.
- The microdevice for sample preparation should be redesigned according to the technique chosen. Mixing functions should be studied and explored.

²⁵ <http://www.zygem.com/index.html>

- Another important requirement for seawater sampling is the separation of particles with a range of different size as encountered in natural samples. This often leads to clogging of filters. Filter architecture, and washing protocols using bleach should be investigated.

5.2.2. Integration and automation

- To achieve full integration, key functions on microchips have to be improved in order to deliver better performance through re-design, on-chip fluidic actuation implementation, on-chip reagent storage strategy, quantification strategy and fluorescence detection system integration. Also an automated electronic control system is also necessary to omit manual controlling.
- And finally, further development should integrate these separate chips into an integrated single chip design to achieve fully automated chips with “sample-in” to “answer-out” capability.

Summary of the general discussion for future work.	
Strengths	Weaknesses
<ul style="list-style-type: none"> • Proof of concept of key functions with “real word” constraints applied (i.e. sample preparation chip) • Fast detection NASBA (i.e. 10 cells detected in 3 minutes). • Isothermal method with easier engineering design compare to PCR. • Improved version could be use for on-site or on coast analysis. 	<ul style="list-style-type: none"> • Still in development with important challenges still to be addressed (i.e. on-chip storage, sample preparation, detection integration). • Poor sample preparation performances for <i>K. brevis</i> species. • High analysis rate might not be achievable
Opportunities	Threats
<ul style="list-style-type: none"> • Unique system with on-chip storage for phytoplankton species analysis. • Unique system using lab-on-a-chip technology for phytoplankton species analysis. • Potential to be the first lab-on-a-chip incorporated to an AUV. • The system could be adapted for use as a general RNA analysis device. • Improvement of the sample preparation microdevice could make the system set to be use for on coast trial. 	<ul style="list-style-type: none"> • NASBA is very susceptible to inhibitions which make the technique very restrictive. • The system could be limited technologically for potential AUV incorporation. • Laboratory competitors are a step ahead using macro-system-based. • Focus could be on technology innovation instead of application requirements. • Risk to develop a macro system for microchips. • Interdisciplinary field, talents are difficult to attract for environmental-based lab-on-a-chip.

Table 12 Summary of the general discussion.

This work was funded by EU FP7 LABONFOIL grant project 224306, the Natural Environment Research Council, and my studentship through EPSRC/NERC grant EP/E016774/1.

References

- Adams, M. L., M. Enzelberger, et al. (2003). "Microfluidic integration on detector arrays for absorption and fluorescence micro-spectrometers." Sensors and Actuators A: Physical **104**(1): 25-31.
- Agrawal, N., Y. A. Hassan, et al. (2007). "A pocket-sized convective PCR thermocycler." Angewandte Chemie-International Edition **46**(23): 4316-4319.
- Alberts, B., D. Bray, et al. (1986). "MOLECULAR BIOLOGY OF THE CELL." Alberts, B., D. Bray, J. Lewis, M. Raff, K. Roberts and J. D. Watson. Molekularbiologie Der Zelle (Molecular Biology of the Cell). Xlviii+1310p. Vch Verlagsgesellschaft/Physik-Verlag: Weinheim, West Germany; Vch Publishers: New York, New York, USA. Illus: XLVIII+1310P.
- Alcantar, N. A., E. S. Aydil, et al. (2000). "Polyethylene glycol-coated biocompatible surfaces." Journal of Biomedical Materials Research **51**(3): 343-351.
- Am, J., Z. Zhiwei, et al. (2011). "State-of-the-art lab chip sensors for environmental water monitoring." Measurement Science and Technology **22**(3): 032001.
- Anderson, D. M. (2009). "Approaches to monitoring, control and management of harmful algal blooms (HABs)." Ocean & Coastal Management **52**(7): 342-347.
- Anderson, D. M., A. D. Cembella, et al. (2011). "Progress in Understanding Harmful Algal Blooms: Paradigm Shifts and New Technologies for Research, Monitoring, and Management." Annual Review of Marine Science **4**(1): 143-176.
- Andrade, J. D., V. Hlady, et al. (1996). Poly(ethylene oxide) and Protein Resistance. Hydrophilic Polymers, American Chemical Society. **248**: 51-59.
- Bahi, M. M., M.-N. Tsaloglou, et al. (2010). "Electroporation and lysis of marine microalga *Karenia brevis* for RNA extraction and amplification." Journal of The Royal Society Interface.
- Baier, T., T. E. Hansen-Hagge, et al. (2009). "Hands-free sample preparation platform for nucleic acid analysis." Lab on a Chip **9**(23): 3399-3405.
- Beaton, A. D., V. J. Sieben, et al. (2011). "An automated microfluidic colourimetric sensor applied in situ to determine nitrite concentration." Sensors and Actuators B: Chemical **156**(2): 1009-1014.
- Becker, H. (2010). "Mind the gap!" Lab on a Chip **10**(3): 271-273.
- Belgrader, P., C. J. Elkin, et al. (2003). "A reusable flow-through polymerase chain reaction instrument for the continuous monitoring of infectious biological agents." Analytical Chemistry **75**(14): 3446-3450.
- Belgrader, P., S. Young, et al. (2000). "A Battery-Powered Notebook Thermal Cycler for Rapid Multiplex Real-Time PCR Analysis." Analytical Chemistry **73**(2): 286-289.
- Bell, D. J., J. P. Brody, et al. (1998). "Using poly(ethylene glycol) silane to prevent protein adsorption in microfabricated silicon channels." Micro- and Nanofabricated Structures and Devices for Biomedical Environmental Applications **3258**: 134-140.
- Bentsink, L., G. O. M. Leone, et al. (2002). "Amplification of RNA by NASBA allows direct detection of viable cells of *Ralstonia solanacearum* in potato." Journal of Applied Microbiology **93**(4): 647-655.
- Bi, H. Y., S. Meng, et al. (2006). "Deposition of PEG onto PMMA microchannel surface to minimize nonspecific adsorption." Lab on a Chip **6**(6): 769-775.
- Birch, L., C. E. Dawson, et al. (2001). "A comparison of nucleic acid amplification techniques for the assessment of bacterial viability." Letters in Applied Microbiology **33**(4): 296-301.
- Birnboim, H. C. (1983). "A RAPID ALKALINE EXTRACTION METHOD FOR THE ISOLATION OF PLASMID DNA." Methods in Enzymology **100**: 243-255.
- Blasco, D., M. Levasseur, et al. (2003). "Patterns of paralytic shellfish toxicity in the St. Lawrence region in relationship with the abundance and distribution of *Alexandrium tamarense*." Scientia marina. **67**: 261-278.
- Boesch, D. (1997). Harmful algal blooms in coastal waters options for prevention, control and mitigation. D. F. Boesch. U.S. Dept. of Commerce National Oceanic and Atmospheric Administration Coastal Ocean Office, Silver Spring, MD.

- Böhmer, A., V. Schildgen, et al. (2009). "Novel application for isothermal nucleic acid sequence-based amplification (NASBA)." Journal of Virological Methods **158**(1-2): 199-201.
- Bold, H. C. and M. J. Wynne (1978). Introduction to the algae : structure and reproduction. Englewood Cliffs, N.J., Prentice-Hall.
- Bonnet, G., S. Tyagi, et al. (1999). "Thermodynamic basis of the enhanced specificity of structured DNA probes." Proceedings of the National Academy of Sciences of the United States of America **96**(11): 6171-6176.
- Boom, R., C. J. A. Sol, et al. (1990). "RAPID AND SIMPLE METHOD FOR PURIFICATION OF NUCLEIC-ACIDS." Journal of Clinical Microbiology **28**(3): 495-503.
- Brask, A., J. P. Kutter, et al. (2005). "Long-term stable electroosmotic pump with ion exchange membranes." Lab on a Chip **5**(7): 730-738.
- Brown, R. B. and J. Audet (2008). "Current techniques for single-cell lysis." Journal of The Royal Society Interface **5**(Suppl 2): S131-S138.
- Brown, T. A. (2001). Gene cloning and DNA analysis : an introduction. Oxford; Malden, Mass., Blackwell Science.
- Bruckner-Lea, C. J., T. Tsukuda, et al. (2002). "Renewable microcolumns for automated DNA purification and flow-through amplification: from sediment samples through polymerase chain reaction." Analytica Chimica Acta **469**(1): 129-140.
- Buckingham, L. (2012). Molecular diagnostics : fundamentals, methods, and clinical applications. Philadelphia, F.A. Davis Co.
- Buijs, J., P. A. W. van den Berg, et al. (1996). "Adsorption Dynamics of IgG and Its F(ab')₂ and Fc Fragments Studied by Reflectometry." Journal of Colloid and Interface Science **178**(2): 594-605.
- Burchill, S. A., L. Perebolte, et al. (2002). "Comparison of the RNA-amplification based methods RT-PCR and NASBA for the detection of circulating tumour cells." British journal of cancer **86**(1): 102-109.
- Burkholder, J. M., E. J. Noga, et al. (1992). "NEW PHANTOM DINOFLAGELLATE IS THE CAUSATIVE AGENT OF MAJOR ESTUARINE FISH KILLS (NATURE, VOL 358, PG 407, 1992)." Nature **360**(6406): 768-768.
- Burton, R. S. (1996). "Molecular tools in marine ecology." Journal of Experimental Marine Biology and Ecology **200**(1-2): 85-101.
- Bustin, S. A. (2000). "Absolute quantification of mRNA using real-time reverse transcription polymerase chain reaction assays." Journal of Molecular Endocrinology **25**(2): 169-193.
- Bustin, S. A., V. Benes, et al. (2009). "The MIQE Guidelines: Minimum Information for Publication of Quantitative Real-Time PCR Experiments." Clinical Chemistry **55**(4): 611-622.
- Cady, N. C., S. Stelick, et al. (2003). "Nucleic acid purification using microfabricated silicon structures." Biosensors & Bioelectronics **19**(1): 59-66.
- Cady, N. C., S. Stelick, et al. (2005). "Real-time PCR detection of *Listeria monocytogenes* using an integrated microfluidics platform." Sensors and Actuators B-Chemical **107**(1): 332-341.
- Carlo, D. D., K.-H. Jeong, et al. (2003). "Reagentless mechanical cell lysis by nanoscale barbs in microchannels for sample preparation." Lab on a Chip **3**(4): 287-291.
- Carpenter, J. F., S. J. Prestrelski, et al. (1993). "SEPARATION OF FREEZING-INDUCED AND DRYING-INDUCED DENATURATION OF LYOPHILIZED PROTEINS USING STRESS-SPECIFIC STABILIZATION .1. ENZYME-ACTIVITY AND CALORIMETRIC STUDIES." Archives of Biochemistry and Biophysics **303**(2): 456-464.
- Casper, E. T., S. S. Patterson, et al. (2007). "A handheld NASBA analyzer for the field detection and quantification of *Karenia brevis*." Harmful Algae **6**(1): 112-118.
- Casper, E. T., J. H. Paul, et al. (2004). "Detection and quantification of the red tide dinoflagellate *Karenia brevis* by real-time nucleic acid sequence-based amplification." Applied and Environmental Microbiology **70**(8): 4727-4732.
- Chang, F. H. (2011). "Toxic effects of three closely-related dinoflagellates, *Karenia concordia*, *K. brevisulcata* and *K. mikimotoi* (Gymnodiniales, Dinophyceae) on other microalgal species." Harmful Algae **10**(2): 181-187.
- Chantratita, W., W. Pongtanapisit, et al. (2004). "Development and comparison of the real-time amplification based methods - NASBA-Beacon, RT-PCR Taqman and RT-PCR hybridization

- probe assays - for the qualitative detection of SARS coronavirus." *Southeast Asian Journal of Tropical Medicine and Public Health* **35**(3): 623-629.
- Chen, C., S. W. Smye, et al. (2006). "Membrane electroporation theories: a review." *Medical and Biological Engineering and Computing* **44**(1): 5-14.
- Chernesky, M. A. and D. E. Jang (2006). "APTIMA® transcription-mediated amplification assays for *Chlamydia trachomatis* and *Neisseria gonorrhoeae*." *Expert Review of Molecular Diagnostics* **6**(4): 519-525.
- Chin, C. D., V. Linder, et al. (2007). "Lab-on-a-chip devices for global health: Past studies and future opportunities." *Lab on a Chip* **7**(1): 41-57.
- Chin, C. D., V. Linder, et al. (2012). "Commercialization of microfluidic point-of-care diagnostic devices." *Lab on a Chip* **12**(12): 2118-2134.
- Cho, Y.-K., J.-G. Lee, et al. (2007). "One-step pathogen specific DNA extraction from whole blood on a centrifugal microfluidic device." *Lab on a Chip* **7**(5): 565-573.
- Choi, Z. Z., P. Boccazzi, P.E. Laibinis, A.J. Sinskey and K.F. Jensen (2003). "Poly(ethylene glycol) (PEG)- modified poly(dimethylsiloxane) (PDMS) for protein- and cell-resistant surfaces in microbio-reactor." *7th International Conference on Miniaturized Chemical and Biochemical Analysis Systems*: pp. 1105–1108.
- Christensen, T. B., C. M. Pedersen, et al. (2007). "PCR biocompatibility of lab-on-a-chip and MEMS materials." *Journal of Micromechanics and Microengineering* **17**(8): 1527.
- Christensen, T. B., C. M. Pedersen, et al. (2007). "PCR biocompatibility of lab-on-a-chip and MEMS materials." *Journal of Micromechanics and Microengineering* **17**(8): 1527-1532.
- Cleary, J., C. Slater, et al. (2009). Analysis of phosphate in wastewater using an autonomous microfluidics-based analyser, World Academy of Science, Engineering and Technology.
- Collins, K. D. (1997). "Charge density-dependent strength of hydration and biological structure." *Biophysical Journal* **72**(1): 65-76.
- Compton, J. (1991). "nucleic-acid sequence-based amplification." *Nature* **350**(6313): 91-92.
- Cook, N. (2003). "The use of NASBA for the detection of microbial pathogens in food and environmental samples." *Journal of Microbiological Methods* **53**(2): 165-174.
- Coombs, L. M., D. Pigott, et al. (1990). "Simultaneous isolation of DNA, RNA, and antigenic protein exhibiting kinase activity from small tumor samples using guanidine isothiocyanate." *Analytical Biochemistry* **188**(2): 338-343.
- Coster, H. G. L. (1965). "A quantitative analysis of the voltage-current relationships of fixed charge membranes and the associated property of "punch-through"." *Biophys J* **5**(5): 669-686.
- Crevillén, A. G., M. Hervás, et al. (2007). "Real sample analysis on microfluidic devices." *Talanta* **74**(3): 342-357.
- Dames, S., L. K. Bromley, et al. (2006). "A Single-Tube Nucleic Acid Extraction, Amplification, and Detection Method Using Aluminum Oxide." *The Journal of molecular diagnostics : JMD* **8**(1): 16-21.
- Dandin, M., P. Abshire, et al. (2007). "Optical filtering technologies for integrated fluorescence sensors." *Lab on a Chip* **7**(8): 955-977.
- de Baar, M. P., M. W. van Dooren, et al. (2001). "Single rapid real-time monitored isothermal RNA amplification assay for quantification of human immunodeficiency virus type 1 isolates from groups M, N, and O." *Journal of Clinical Microbiology* **39**(4): 1378-1384.
- de la Rosa, C., P. A. Tilley, et al. (2008). "Microfluidic Device for Dielectrophoresis Manipulation and Electrodisruption of Respiratory Pathogen *Bordetella pertussis*." *Biomedical Engineering, IEEE Transactions on* **55**(10): 2426-2432.
- Delaney, J. A., R. M. Ulrich, et al. (2011). "Detection of the toxic marine diatom *Pseudo-nitzschia multiseries* using the RuBisCO small subunit (rbcS) gene in two real-time RNA amplification formats." *Harmful Algae* **11**(0): 54-64.
- DeLong, E. F. (2009). "The microbial ocean from genomes to biomes." *Nature* **459**(7244): 200-206.
- Derjaguin, B. V. and L. Landau (1941). "Theory of the Stability of Strongly Charged Lyophobic Sols and of the Adhesion of Strongly Charged Particles in Solutions of Electrolytes." *Acta Phys. Chim. URSS* **14**: 633-662.
- Dimov, I. K., J. L. Garcia-Cordero, et al. (2008). "Integrated microfluidic tmRNA purification and real-time NASBA device for molecular diagnostics." *Lab on a Chip* **8**(12): 2071-2078.

- Doucette, G. J., M. M. Logan, et al. (1997). "Development and preliminary validation of a microtiter plate-based receptor binding assay for paralytic shellfish poisoning toxins." Toxicon **35**(5): 625-636.
- Elgort, M. G., M. G. Herrmann, et al. (2004). "Extraction and amplification of genomic DNA from human blood on nanoporous aluminum oxide membranes." Clinical Chemistry **50**(10): 1817-1819.
- Erali, M., J. D. Durtschi, et al. (2004). "Localization and imaging of nucleic acids on nanoporous aluminum oxide membranes." Clinical Chemistry **50**(10): 1819-1821.
- Erickson, J. S., N. Hashemi, et al. (2011). "In Situ Phytoplankton Analysis: There's Plenty of Room at the Bottom." Analytical Chemistry.
- Ferrari, M., L. Cremonesi, et al. (1996). "Molecular diagnosis of genetic diseases." Clinical biochemistry **29**(3): 201-208.
- Fleige, S. and M. W. Pfaffl (2006). "RNA integrity and the effect on the real-time qRT-PCR performance." Molecular Aspects of Medicine **27**(2-3): 126-139.
- Focke, M., D. Kosse, et al. (2010). "Lab-on-a-Foil: microfluidics on thin and flexible films." Lab on a Chip **10**(11): 1365-1386.
- Fries, D., J. Paul, et al. (2007). "The Autonomous Microbial Genosensor, an in situ Sensor for Marine Microbe Detection." Microscopy and Microanalysis **13**(SupplementS02): 514-515.
- Fu, J. L., Q. Fang, et al. (2006). "Laser-induced fluorescence detection system for microfluidic chips based on an orthogonal optical arrangement." Analytical Chemistry **78**(11): 3827-3834.
- Fukuba, T., A. Miyaji, et al. (2011). "Integrated in situ genetic analyzer for microbiology in extreme environments." RSC Advances **1**(8): 1567-1573.
- Furuberg, L., M. Mielnik, et al. (2008). "RNA amplification chip with parallel microchannels and droplet positioning using capillary valves." Microsystem Technologies-Micro-and Nanosystems-Information Storage and Processing Systems **14**(4-5): 673-681.
- Galluzzi, L., A. Penna, et al. (2004). "Development of a real-time PCR assay for rapid detection and quantification of *Alexandrium minutum* (a dinoflagellate)." Applied and Environmental Microbiology **70**(2): 1199-1206.
- Gentien, P., M. Lunven, et al. (1995). "In-situ depth profiling of particle sizes." Deep Sea Research Part I: Oceanographic Research Papers **42**(8): 1297-1312.
- Giacobbe, M., A. Penna, et al. (2007). "Recurrent high-biomass blooms of *Alexandrium taylorii* (Dinophyceae), a HAB species expanding in the Mediterranean." Hydrobiologia **580**(1): 125-133.
- Gilbride, K. A., D. Y. Lee, et al. (2006). "Molecular techniques in wastewater: Understanding microbial communities, detecting pathogens, and real-time process control." Journal of Microbiological Methods **66**(1): 1-20.
- Gimsa, J., P. Marszalek, et al. (1991). "DIELECTROPHORESIS AND ELECTROROTATION OF NEUROSPORA SLIME AND MURINE MYELOMA CELLS." Biophysical Journal **60**(4): 749-760.
- Giovannoni, S. and M. Rappé (2000). Evolution, diversity, and molecular ecology of marine prokaryotes. D. L. Kirchman. New York, Wiley-Liss Inc: 47-84.
- Gjerde, D. T., L. Hoang, et al. (2009). Biological and Chemical RNA, Wiley-VCH Verlag GmbH & Co. KGaA.
- Gjerde, D. T., L. Hoang, et al. (2009). RNA Extraction and Analysis, Wiley-VCH Verlag GmbH & Co. KGaA.
- Gjerde, D. T., L. Hoang, et al. (2009). RNA Extraction, Separation, and Analysis, Wiley-VCH Verlag GmbH & Co. KGaA.
- Graham, L. E. and L. W. Wilcox. (2000). "Algae." from <http://catalog.hathitrust.org/api/volumes/oclc/40964928.html>.
- Granéli, E. and J. T. Turner. (2006). "Ecology of harmful algae." from <http://site.ebrary.com/id/10145287>.
- Green, N. G. and H. Morgan (1997). "Dielectrophoretic separation of nano-particles." Journal of Physics D: Applied Physics **30**(11): L41.
- Greenfield, D. I., R. Marin, et al. (2006). "Application of environmental sample processor (ESP) methodology for quantifying *Pseudo-nitzschia australis* using ribosomal RNA-targeted probes

- in sandwich and fluorescent in situ hybridization formats." Limnology and Oceanography-Methods **4**: 426-435.
- Grimes, D. J. (2009). "Oceans and Human Health: Risks and Remedies from the Sea." from <http://www.pubmedcentral.nih.gov/articlerender.fcgi?artid=2661934>.
- Gross, D., L. M. Loew, et al. (1986). "Optical imaging of cell membrane potential changes induced by applied electric fields." Biophysical Journal **50**(2): 339-348.
- Grosse, C. and H. P. Schwan (1992). "Cellular membrane potentials induced by alternating fields." Biophysical Journal **63**(6): 1632-1642.
- Gulliksen, A., L. Anders Solli, et al. (2005). "Parallel nanoliter detection of cancer markers using polymer microchips." Lab on a Chip **5**(4): 416-420.
- Gulliksen, A. and T. Hansen-Hagge (2012). "Towards a Sample-In, Answer-Out& Point-of-Care Platform for Nucleic Acid Extraction and Amplification: Using an HPV E6/E7 mRNA Model System." Journal of Oncology **2012**.
- Gulliksen, A., M. M. Marek., et al. (2007). Storage and reactivation of enzymes in a disposable, self-contained lab-on-a-chip system
- Micro total analysis systems : proceedings of [Mu]TAS 2007 : Eleventh International Conference on Miniaturized Systems for Chemistry and Life Sciences, Paris, France, 7-11 October 2007, Paris, Chemical and Biological Microsystems Society.
- Gulliksen, A., L. Solli, et al. (2004). "Real-time nucleic acid sequence-based amplification in nanoliter volumes." Analytical Chemistry **76**(1): 9-14.
- Gulliksen, A., L. A. Solli, et al. (2005). "Parallel nanoliter detection of cancer markers using polymer microchips." Lab on a Chip **5**(4): 416-420.
- Guzowski, J., P. M. Korczyk, et al. (2011). "Automated high-throughput generation of droplets." Lab on a Chip **11**(21): 3593-3595.
- Hagan, K. A., C. R. Reedy, et al. (2011). "An integrated, valveless system for microfluidic purification and reverse transcription-PCR amplification of RNA for detection of infectious agents." Lab on a Chip.
- Hallegraef, G. M. (1993). "A REVIEW OF HARMFUL ALGAL BLOOMS AND THEIR APPARENT GLOBAL INCREASE." Phycologia **32**(2): 79-99.
- Hatch, A. C., J. S. Fisher, et al. (2011). "1-Million droplet array with wide-field fluorescence imaging for digital PCR." Lab on a Chip **11**(22): 3838-3845.
- Hoettges, K. F., M. P. Hughes, et al. (2003). "Optimizing particle collection for enhanced surface-based biosensors." Engineering in Medicine and Biology Magazine, IEEE **22**(6): 68-74.
- Hong, J. W., V. Studer, et al. (2004). "A nanoliter-scale nucleic acid processor with parallel architecture." Nat Biotech **22**(4): 435-439.
- Hoorfar, J., B. Malorny, et al. (2004). "Practical Considerations in Design of Internal Amplification Controls for Diagnostic PCR Assays." Journal of Clinical Microbiology **42**(5): 1863-1868.
- Houde, A., D. Leblanc, et al. (2006). "Comparative evaluation of RT-PCR, nucleic acid sequence-based amplification (NASBA) and real-time RT-PCR for detection of noroviruses in faecal material." Journal of Virological Methods **135**(2): 163-172.
- Huang, Y., R. Holzel, et al. (1992). "Differences in the AC electrodynamic of viable and non-viable yeast cells determined through combined dielectrophoresis and electrorotation studies." Physics in Medicine and Biology **37**(7): 1499.
- Huang, Y., E. Mather, et al. (2002). "MEMS-based sample preparation for molecular diagnostics." Analytical and Bioanalytical Chemistry **372**(1): 49-65.
- Huang, Y. and B. Rubinsky (2003). "Flow-through micro-electroporation chip for high efficiency single-cell genetic manipulation." Sensors and Actuators A: Physical **104**(3): 205-212.
- Iglesias-Rodriguez, M. D., P. R. Halloran, et al. (2008). "Phytoplankton Calcification in a High-CO2 World." Science **320**(5874): 336-340.
- Ikeda, N., N. Tanaka, et al. (2007). "On-chip single-cell lysis for extracting intracellular material." Japanese Journal of Applied Physics Part 1-Regular Papers Brief Communications & Review Papers **46**(9B): 6410-6414.
- Invitrogen "Molecular Probes: The Handbook."

- Irimajiri, A., T. Hanai, et al. (1979). "A dielectric theory of "multi-stratified shell" model with its application to a lymphoma cell." Journal of Theoretical Biology **78**(2): 251-269.
- Isaac, P. G. (2009). "Essentials of nucleic acid analysis: a robust approach." Annals of Botany **104**(2): vi.
- Iverson, B. D. and S. V. Garimella (2008). "Recent advances in microscale pumping technologies: a review and evaluation." Microfluidics and Nanofluidics **5**(2): 145-174.
- Jesús-Pérez, N. M. and B. H. Lapizco-Encinas (2011). "Dielectrophoretic monitoring of microorganisms in environmental applications." Electrophoresis **32**(17): 2331-2357.
- Jones, T. B. and J. P. Kraybill (1986). "ACTIVE FEEDBACK-CONTROLLED DIELECTROPHORETIC LEVITATION." Journal of Applied Physics **60**(4): 1247-1252.
- Keightley, M. C., P. Sillekens, et al. (2005). "Real-time NASBA detection of SARS-associated coronavirus and comparison with real-time reverse transcription-PCR." Journal of Medical Virology **77**(4): 602-608.
- Khan, U., N. Benabderrazik, et al. (2010). "UV and solar TiO₂ photocatalysis of brevetoxins (PbTx_s)." Toxicon **55**(5): 1008-1016.
- Kim, J. and B. K. Gale (2008). "Quantitative and qualitative analysis of a microfluidic DNA extraction system using a nanoporous AIO membrane." Lab on a Chip **8**(9): 1516-1523.
- Kim, J., M. Johnson, et al. (2009). "Microfluidic sample preparation: cell lysis and nucleic acid purification." Integrative Biology **1**(10): 574-586.
- Kim, J., M. Mauk, et al. (2010). "A PCR reactor with an integrated alumina membrane for nucleic acid isolation." Analyst **135**(9): 2408-2414.
- Kirkpatrick, G. J., C. Orrico, et al. (2003). "Continuous hyperspectral absorption measurements of colored dissolved organic material in aquatic systems." Applied Optics **42**(33): 6564-6568.
- Krishnan, R. S., M. E. Mackay, et al. (2007). "Improved polymer thin-film wetting behavior through nanoparticle segregation to interfaces." Journal of Physics: Condensed Matter **19**(35): 356003.
- Lagally, E. T. and H. T. Soh (2005). "Integrated Genetic Analysis Microsystems." Critical Reviews in Solid State and Materials Sciences **30**(4): 207-233.
- Lakowicz, J. (1999). Principles of Fluorescence Spectroscopy. New York, Boston, Dordrecht, London, Moscow, Kluwer Academic/Plenum Publishers.
- Lanciotti, R. S. and A. J. Kerst (2001). "Nucleic acid sequence-based amplification assays for rapid detection of West Nile and St. Louis encephalitis viruses." Journal of Clinical Microbiology **39**(12): 4506-4513.
- Lapizco-Encinas, B. H., R. V. Davalos, et al. (2005). "An insulator-based (electrodeless) dielectrophoretic concentrator for microbes in water." Journal of Microbiological Methods **62**(3): 317-326.
- Lapizco-Encinas, B. H. and M. Rito-Palomares (2007). "Dielectrophoresis for the manipulation of nanobioparticles." Electrophoresis **28**(24): 4521-4538.
- Lee, B. S., J.-N. Lee, et al. (2009). "A fully automated immunoassay from whole blood on a disc." Lab on a Chip **9**(11): 1548-1555.
- Lee, H., J. Jung, et al. (2010). "High-speed RNA microextraction technology using magnetic oligo-dT beads and lateral magnetophoresis." Lab on a Chip **10**(20): 2764-2770.
- Lee, H. J., J.-H. Kim, et al. (2010). "Electrochemical cell lysis device for DNA extraction." Lab on a Chip **10**(5): 626-633.
- Lee, K. H. (2001). "Proteomics: a technology-driven and technology-limited discovery science." Trends in Biotechnology **19**(6): 217-222.
- Lee, S.-W. and Y.-C. Tai (1999). "A micro cell lysis device." Sensors and Actuators A: Physical **73**(1-2): 74-79.
- Lefevre, F., A. Chalifour, et al. (2012). "Algal fluorescence sensor integrated into a microfluidic chip for water pollutant detection." Lab on a Chip.
- Leone, G., B. van Gemen, et al. (1998). "Molecular beacon probes combined with amplification by NASBA enable homogeneous, real-time detection of RNA." Nucleic Acids Research **26**(9): 2150-2155.
- Li, D. (2008). "Encyclopedia of microfluidics and nanofluidics." from <http://dx.doi.org/10.1007/978-0-387-48998-8>.
- Li, D. (2008). Encyclopedia of Microfluidics and Nanofluidics, Springer.

- Lien, K.-Y., Y.-H. Chuang, et al. (2010). "Rapid isolation and detection of cancer cells by utilizing integrated microfluidic systems." Lab on a Chip **10**(21): 2875-2886.
- Lien, K. Y., J. L. Lin, et al. (2007). "Purification and enrichment of virus samples utilizing magnetic beads on a microfluidic system." Lab on a Chip **7**(7): 868-875.
- Lim, D. V., J. M. Simpson, et al. (2005). "Current and Developing Technologies for Monitoring Agents of Bioterrorism and Biowarfare." Clinical Microbiology Reviews **18**(4): 583-607.
- Lin, Y.-C., C.-M. Jen, et al. (2001). "Electroporation microchips for continuous gene transfection." Sensors and Actuators B: Chemical **79**(2-3): 137-143.
- Lin, Y.-Y., M. Risk, et al. (1981). "Isolation and structure of brevetoxin B from the "red tide" dinoflagellate *Ptychodiscus brevis* (Gymnodinium breve)." Journal of the American Chemical Society **103**(22): 6773-6775.
- Lionello, A., J. Jossierand, et al. (2005). "Protein adsorption in static microsystems: effect of the surface to volume ratio." Lab on a Chip **5**(3): 254-260.
- Liu, C.-J., K.-Y. Lien, et al. (2009). "Magnetic-bead-based microfluidic system for ribonucleic acid extraction and reverse transcription processes." Biomedical Microdevices **11**(2): 339-350.
- Liu, R. H., J. Yang, et al. (2004). "Self-Contained, Fully Integrated Biochip for Sample Preparation, Polymerase Chain Reaction Amplification, and DNA Microarray Detection." Analytical Chemistry **76**(7): 1824-1831.
- Loens, K., D. Ursi, et al. (2005). Nucleic Acid Sequence-Based Amplification: 273-291.
- Logemann, J., J. Schell, et al. (1987). "IMPROVED METHOD FOR THE ISOLATION OF RNA FROM PLANT-TISSUES." Analytical Biochemistry **163**(1): 16-20.
- Lou, X. J., N. J. Panaro, et al. (2004). "Increased amplification efficiency of microchip-based PCR by dynamic surface passivation." Biotechniques **36**(2): 248-+.
- Lu, H., M. A. Schmidt, et al. (2005). "A microfluidic electroporation device for cell lysis." Lab on a Chip **5**(1): 23-29.
- Lui, C., N. C. Cady, et al. (2009). "Nucleic Acid-based Detection of Bacterial Pathogens Using Integrated Microfluidic Platform Systems." Sensors **9**(5): 3713-3744.
- Mangiapan, G., M. Vokurka, et al. (1996). "Sequence capture-PCR improves detection of mycobacterial DNA in clinical specimens." Journal of Clinical Microbiology **34**(5): 1209-1215.
- Manz, A., N. Graber, et al. (1990). "Miniaturized total chemical analysis systems: A novel concept for chemical sensing." Sensors and Actuators B: Chemical **1**(1-6): 244-248.
- Marcus, J. S., W. F. Anderson, et al. (2006). "Microfluidic single-cell mRNA isolation and analysis." Analytical Chemistry **78**(9): 3084-3089.
- Margraf, R. L., S. Page, et al. (2004). "Single-tube method for nucleic acid extraction, amplification, purification, and sequencing." Clinical Chemistry **50**(10): 1755-1761.
- Marie, D., C. P. D. Brussaard, et al. (1999). "Enumeration of marine viruses in culture and natural samples by flow cytometry." Applied and Environmental Microbiology **65**(1): 45-52.
- Mary, P., L. Dauphinot, et al. (2011). "Analysis of gene expression at the single-cell level using microdroplet-based microfluidic technology." Biomicrofluidics **5**(2).
- Mas, A., V. Soriano, et al. (1998). "The ultrasensitive NASBA assay for quantifying HIV-1 viral load." Antiviral Therapy **3**(1): 43-44.
- Masserini, R. T. and K. A. Fanning (2000). "A sensor package for the simultaneous determination of nanomolar concentrations of nitrite, nitrate, and ammonia in seawater by fluorescence detection." Marine Chemistry **68**(4): 323-333.
- Meese, E. and N. Blin (1987). "Simultaneous isolation of high molecular weight RNA and DNA from limited amounts of tissues and cells." Gene Analysis Techniques **4**(3): 45-49.
- Melzak, K. A., C. S. Sherwood, et al. (1996). "Driving forces for DNA adsorption to silica in perchlorate solutions." Journal of Colloid and Interface Science **181**(2): 635-644.
- Mohr, S., Y. H. Zhang, et al. (2007). "Numerical and experimental study of a droplet-based PCR chip." Microfluidics and Nanofluidics **3**(5): 611-621.
- Moore, C., E. M. Clark, et al. (2004). "Evaluation of a broadly reactive nucleic acid sequence based amplification assay for the detection of noroviruses in faecal material." Journal of clinical virology : the official publication of the Pan American Society for Clinical Virology **29**(4): 290-296.

- Muller, T., T. Schnelle, et al. (1998). "Dielectric single cell spectra in snow algae." *Polar Biology* **20**(5): 303-310.
- Murray, M. G. and W. F. Thompson (1980). "RAPID ISOLATION OF HIGH MOLECULAR-WEIGHT PLANT DNA." *Nucleic Acids Research* **8**(19): 4321-4325.
- Myers, F. B. and L. P. Lee (2008). "Innovations in optical microfluidic technologies for point-of-care diagnostics." *Lab on a Chip* **8**(12): 2015-2031.
- Nakanishi, K., T. Sakiyama, et al. (2001). "On the adsorption of proteins on solid surfaces, a common but very complicated phenomenon." *Journal of Bioscience and Bioengineering* **91**(3): 233-244.
- Napper, D. H. (1983). *Polymeric stabilization of colloidal dispersions*, Academic Press.
- Neumann, E., S. Kakorin, et al. (1999). "Fundamentals of electroporative delivery of drugs and genes." *Bioelectrochemistry and Bioenergetics* **48**(1): 3-16.
- Nguyen, T. H. and M. Elimelech (2007). "Plasmid DNA adsorption on silica: Kinetics and conformational changes in monovalent and divalent salts." *Biomacromolecules* **8**(1): 24-32.
- Niesters, H. G. M. (2001). "Quantitation of viral load using real-time amplification techniques." *Methods* **25**(4): 419-429.
- Nolan, T., R. E. Hands, et al. (2006). "Quantification of mRNA using real-time RT-PCR." *Nature Protocols* **1**(3): 1559-1582.
- Norde, W. (1994). "PROTEIN ADSORPTION AT SOLID-SURFACES - A THERMODYNAMIC APPROACH." *Pure and Applied Chemistry* **66**(3): 491-496.
- Northrup, M. A., B. Benett, et al. (1998). "A miniature analytical instrument for nucleic acids based on micromachined silicon reaction chambers." *Analytical Chemistry* **70**(5): 918-922.
- Ogilvie, I. R. G., V. J. Sieben, et al. (2010). "Reduction of surface roughness for optical quality microfluidic devices in PMMA and COC." *Journal of Micromechanics and Microengineering* **20**(6): 065016.
- Okamura, K., H. Kimoto, et al. (2001). "Development of a deep-sea in situ Mn analyzer and its application for hydrothermal plume observation." *Marine Chemistry* **76**(1-2): 17-26.
- Palchetti, I. and M. Mascini (2008). "Nucleic acid biosensors for environmental pollution monitoring." *Analyst* **133**(7): 846-854.
- Panaro, N. J., X. J. Lou, et al. (2004). "Surface effects on PCR reactions in multichip microfluidic platforms." *Biomedical Microdevices* **6**(1): 75-80.
- Pasloske, B. L., C. R. Walkerpeach, et al. (1998). "Armored RNA technology for production of ribonuclease-resistant viral RNA controls and standards." *Journal of Clinical Microbiology* **36**(12): 3590-3594.
- Patterson, S. S., E. T. Casper, et al. (2005). "Increased precision of microbial RNA quantification using NASBA with an internal control." *Journal of Microbiological Methods* **60**(3): 343-352.
- Patterson, S. S., E. T. Casper, et al. (2005). "Increased precision of microbial RNA quantification using NASBA with an internal control." *Journal of Microbiological Methods* **60**(3): 343-352.
- Pavlin, M., T. Kotnik, et al. (2008). Chapter Seven Electroporation of Planar Lipid Bilayers and Membranes. *Advances in Planar Lipid Bilayers and Liposomes*. A. L. Liu, Academic Press. **Volume 6**: 165-226.
- Pennathur (2008). "Improving fluorescence detection in lab on chip devices." *Lab on a Chip* **8**(5): 649-652.
- Peperzak, L. (2005). "Future increase in harmful algal blooms in the North Sea due to climate change." *Water Science and Technology* **51**(5): 31-36.
- Pethig, R. and G. H. Markx (1997). "Applications of dielectrophoresis in biotechnology." *Trends in Biotechnology* **15**(10): 426-432.
- Plakas, S. M. and R. W. Dickey (2010). "Advances in monitoring and toxicity assessment of brevetoxins in molluscan shellfish." *Toxicon* **56**(2): 137-149.
- Polstra, A. M., J. Goudsmit, et al. (2002). "Development of real-time NASBA assays with molecular beacon detection to quantify mRNA coding for HHV-8 lytic and latent genes." *Bmc Infectious Diseases* **2**.
- Prausnitz, M. R., V. G. Bose, et al. (1993). "Electroporation of mammalian skin: a mechanism to enhance transdermal drug delivery." *Proceedings of the National Academy of Sciences* **90**(22): 10504-10508.

- Preston, C. M., A. Harris, et al. (2011). "Underwater Application of Quantitative PCR on an Ocean Mooring." *PLoS ONE* **6**(8): e22522.
- Prestrelski, S. J., T. Arakawa, et al. (1993). "Separation of Freezing- and Drying-Induced Denaturation of Lyophilized Proteins Using Stress-Specific Stabilization: II. Structural Studies Using Infrared Spectroscopy." *Archives of Biochemistry and Biophysics* **303**(2): 465-473.
- Price, C. W., D. C. Leslie, et al. (2009). "Nucleic acid extraction techniques and application to the microchip." *Lab on a Chip* **9**(17): 2484-2494.
- Prien, R. D. (2007). "The future of chemical in situ sensors." *Marine Chemistry* **107**(3): 422-432.
- Puren, A., J. L. Gerlach, et al. (2010). "Laboratory operations, specimen processing, and handling for viral load Testing and surveillance." *Journal of Infectious Diseases* **201**(Supplement 1): S27-S36.
- Rantajaervi, E., R. Olsonen, et al. (1998). "Effect of sampling frequency on detection of natural variability in phytoplankton: unattended high-frequency measurements on board ferries in the Baltic Sea." *ICES MARINE SCIENCE SYMPOSIA*(206): 697-704.
- Ratner, B. D. (1995). "SURFACE MODIFICATION OF POLYMERS - CHEMICAL, BIOLOGICAL AND SURFACE ANALYTICAL CHALLENGES." *Biosensors & Bioelectronics* **10**(9-10): 797-804.
- Regan, J. F., A. J. Makarewicz, et al. (2008). "Environmental Monitoring for Biological Threat Agents Using the Autonomous Pathogen Detection System with Multiplexed Polymerase Chain Reaction." *Analytical Chemistry* **80**(19): 7422-7429.
- Roach, P., D. Farrar, et al. (2005). "Interpretation of Protein Adsorption: Surface-Induced Conformational Changes." *Journal of the American Chemical Society* **127**(22): 8168-8173.
- Robidart, J. C., C. M. Preston, et al. (2011). "Seasonal Synechococcus and Thaumarchaeal population dynamics examined with high resolution with remote in situ instrumentation." *ISME J.*
- Rodríguez-Lazaro, D., M. D'Agostino, et al. (2004). "Construction Strategy for an Internal Amplification Control for Real-Time Diagnostic Assays Using Nucleic Acid Sequence-Based Amplification: Development and Clinical Application." *Journal of Clinical Microbiology* **42**(12): 5832-5836.
- Rodríguez-Lazaro, D., M. Hernandez, et al. (2006). APPLICATION OF NUCLEIC ACID SEQUENCE-BASED AMPLIFICATION FOR THE DETECTION OF VIABLE FOODBORNE PATHOGENS: PROGRESS AND CHALLENGES, Blackwell Publishing Inc. **14**: 218-236.
- Rodríguez-Lazaro, D., M. Hernandez, et al. (2006). "APPLICATION OF NUCLEIC ACID SEQUENCE-BASED AMPLIFICATION FOR THE DETECTION OF VIABLE FOODBORNE PATHOGENS: PROGRESS AND CHALLENGES." *Journal of Rapid Methods & Automation in Microbiology* **14**(3): 218-236.
- Romano, J. W., R. N. Shurtliff, et al. (1995). "Detection of HIV-1 infection in vitro using NASBA: an isothermal RNA amplification technique." *Journal of Virological Methods* **54**(2-3): 109-119.
- Roy, I. and Munishwar N. Gupta (2004). "Freeze-drying of proteins: some emerging concerns." *Biotechnol. Appl. Biochem. Biotechnology and Applied Biochemistry* **39**(2).
- Ryu, G., J. Huang, et al. (2011). "Highly sensitive fluorescence detection system for microfluidic lab-on-a-chip." *Lab on a Chip* **11**(9): 1664-1670.
- Saiki, R. K., S. Scharf, et al. (1985). "ENZYMATIC AMPLIFICATION OF BETA-GLOBIN GENOMIC SEQUENCES AND RESTRICTION SITE ANALYSIS FOR DIAGNOSIS OF SICKLE-CELL ANEMIA." *Science* **230**(4732): 1350-1354.
- Sambrook, J. and D. W. Russell (2001). *Molecular cloning : a laboratory manual*. Cold Spring Harbor, N.Y., Cold Spring Harbor Laboratory Press.
- Sarmiento, J. L. and N. Gruber (2006). *Ocean Biogeochemical Dynamics*. Princeton, Woodstock, Princeton University Press.
- Sasaki, S., Y. Ando, et al. (1998). "A fluorescence-based sensor for ammonium and nitrate." *Analytical Letters* **31**(4): 555-567.
- Sauer-Budge, A. F., P. Mirer, et al. (2009). "Low cost and manufacturable complete microTAS for detecting bacteria." *Lab on a Chip* **9**(19): 2803-2810.

- Schneider, P., L. Wolters, et al. (2005). "Real-time nucleic acid sequence-based amplification is more convenient than real-time PCR for quantification of *Plasmodium falciparum*." Journal of Clinical Microbiology **43**(1): 402-405.
- Scholin, C. A. (2010). "What are "ecogenomic sensors?" A review and thoughts for the future." Ocean Science **6**(1): 51-60.
- Schroeder, A., O. Mueller, et al. (2006). "The RIN: an RNA integrity number for assigning integrity values to RNA measurements." BMC Molecular Biology **7**.
- Sedgwick, H., F. Caron, et al. (2008). "Lab-on-a-chip technologies for proteomic analysis from isolated cells." Journal of The Royal Society Interface **5**(Suppl 2): S123-S130.
- Seetharam, R., Y. Wada, et al. (2006). "Long-term storage of bionanodevices by freezing and lyophilization." Lab on a Chip **6**(9): 1239-1242.
- Seo, J. and L. P. Lee (2003). "Fluorescence amplification by self-aligned integrated microfluidic optical systems." Boston Transducers'03: Digest of Technical Papers, Vols 1 and 2: 1136-1139.
- Shaw, K. J., D. A. Joyce, et al. (2011). "Development of a real-world direct interface for integrated DNA extraction and amplification in a microfluidic device." Lab on a Chip **11**(3): 443-448.
- Shoffner, M. A., J. Cheng, et al. (1996). "Chip PCR. I. Surface Passivation of Microfabricated Silicon-Glass Chips for PCR." Nucleic Acids Research **24**(2): 375-379.
- Sieben, V. J., C. F. A. Floquet, et al. (2010). "Microfluidic colourimetric chemical analysis system: Application to nitrite detection." Analytical Methods **2**(5): 484-491.
- Sims, C. E. and N. L. Allbritton (2007). "Analysis of single mammalian cells on-chip." Lab on a Chip **7**(4): 423-440.
- Smith, M. C., G. Steimle, et al. (2007). "An integrated portable hand-held analyser for real-time isothermal nucleic acid amplification." Analytica Chimica Acta **598**(2): 286-294.
- Sposito, G. (1989). The Environmental chemistry of aluminum / editor, Garrison Sposito. Boca Raton, Fla. :, CRC Press.
- Squires, T. M. and S. R. Quake (2005). "Microfluidics: Fluid physics at the nanoliter scale." Reviews of Modern Physics **77**(3): 977-1026.
- Starikov, D., F. Benkabou, et al. (2002). "Integrated multi-wavelength fluorescence sensors." Proceedings of the Isa/Ieee Sensors for Industry Conference: 15-18.
- Stevens, D. Y., C. R. Petri, et al. (2008). "Enabling a microfluidic immunoassay for the developing world by integration of on-card dry reagent storage." Lab on a Chip **8**(12): 2038-2045.
- Suzuki, M. T., L. T. Taylor, et al. (2000). "Quantitative analysis of small-subunit rRNA genes in mixed microbial populations via 5'-nuclease assays." Applied and Environmental Microbiology **66**(11): 4605-4614.
- Tabeling, P. (2009). "A brief introduction to slippage, droplets and mixing in microfluidic systems." Lab on a Chip **9**(17): 2428-2436.
- Tabor, S. and C. C. Richardson (1992). "A bacteriophage T7 RNA polymerase/promoter system for controlled exclusive expression of specific genes. 1985." Biotechnology (Reading, Mass.) **24**: 280-284.
- Tan, S. C. and B. C. Yiap (2009). "DNA, RNA, and protein extraction: the past and the present." J Biomed Biotechnol **2009**: 574398.
- Teissie, J. and T. Y. Tsong (1981). "Electric field induced transient pores in phospholipid bilayer vesicles." Biochemistry **20**(6): 1548-1554.
- Tian, H., A. F. R. Hühmer, et al. (2000). "Evaluation of Silica Resins for Direct and Efficient Extraction of DNA from Complex Biological Matrices in a Miniaturized Format." Analytical Biochemistry **283**(2): 175-191.
- Torres-Chavolla, E. and E. C. Alocilja (2009). "Aptasensors for detection of microbial and viral pathogens." Biosensors & Bioelectronics **24**(11): 3175-3182.
- Tsaloglou, M.-N., M. M. Bahi, et al. (2011). "On-chip real-time nucleic acid sequence-based amplification for RNA detection and amplification." Analytical Methods **3**(9): 2127-2133.
- Tsong, T. Y. (1991). "ELECTROPORATION OF CELL-MEMBRANES." Biophysical Journal **60**(2): 297-306.
- Tyagi, S. and F. R. Kramer (1996). "Molecular beacons: Probes that fluoresce upon hybridization." Nature Biotechnology **14**(3): 303-308.

- Van Dolah, F. M., K. B. Lidie, et al. (2009). "The Florida red tide dinoflagellate *Karenia brevis*: New insights into cellular and molecular processes underlying bloom dynamics." Harmful Algae **8**(4): 562-572.
- Vet, J. A. M. and S. A. E. Marras (2005). "Design and optimization of molecular beacon real-time polymerase chain reaction assays." Methods in Molecular Biology: 273-290.
- Vila, M., J. Camp, et al. (2001). "High Resolution Spatio-temporal Detection of Potentially Harmful Dinoflagellates in Confined Waters of the NW Mediterranean." Journal of Plankton Research **23**(5): 497-514.
- Wang, C.-H., K.-Y. Lien, et al. (2011). "An integrated microfluidic loop-mediated-isothermal-amplification system for rapid sample pre-treatment and detection of viruses." Biosensors and Bioelectronics **26**(5): 2045-2052.
- Wang, J. (2002). On-chip enzymatic assays, WILEY-VCH Verlag GmbH. **23**: 713-718.
- Wang, J., V. L. Sukhorukov, et al. (1997). "Electrorotational spectra of protoplasts generated from the giant marine alga <i>Valonia utricularis</i>." Protoplasma **196**(3): 123-134.
- Watkins, S., A. Reich, et al. (2008). "Neurotoxic Shellfish Poisoning." Marine Drugs **6**(3): 431-455.
- Weaver, J. C. (1993). "Electroporation: A general phenomenon for manipulating cells and tissues." Journal of Cellular Biochemistry **51**(4): 426-435.
- Weaver, J. C. (2000). "Electroporation of cells and tissues." Plasma Science, IEEE Transactions on **28**(1): 24-33.
- Weaver, J. C. and Y. A. Chizmadzhev (1996). "Theory of electroporation: A review." Bioelectrochemistry and Bioenergetics **41**(2): 135-160.
- Weusten, J., W. M. Carpay, et al. (2002). "Principles of quantitation of viral loads using nucleic acid sequence-based amplification in combination with homogeneous detection using molecular beacons." Nucleic Acids Research **30**(6).
- Weusten, J. J. A. M., W. M. Carpay, et al. (2002). "Principles of quantitation of viral loads using nucleic acid sequence-based amplification in combination with homogeneous detection using molecular beacons." Nucleic Acids Research **30**(6): e26.
- Whitesides, G. M. (2011). "What Comes Next?" Lab on a Chip **11**(2): 191-193.
- Wu, H.-W., R.-C. Hsu, et al. (2010). "An integrated microfluidic system for isolation, counting, and sorting of hematopoietic stem cells." Biomicrofluidics **4**(2): Article No.: 024112.
- Xu, G., T.-M. Hsieh, et al. (2010). "A self-contained all-in-one cartridge for sample preparation and real-time PCR in rapid influenza diagnosis." Lab on a Chip **10**(22): 3103-3111.
- Yager, P., G. J. Domingo, et al. (2008). "Point-of-Care Diagnostics for Global Health." Annual Review of Biomedical Engineering **10**(1): 107-144.
- Yun, S.-S., S. Y. Yoon, et al. (2010). "Handheld mechanical cell lysis chip with ultra-sharp silicon nano-blade arrays for rapid intracellular protein extraction." Lab on a Chip **10**(11): 1442-1446.
- Zehr, J. P., I. Hewson, et al. (2008). "Molecular biology techniques and applications for ocean sensing." Ocean Sci. Discuss. Ocean Science Discussions **5**(4): 625-657.
- Zhang, C. and D. Xing (2007). "Miniaturized PCR chips for nucleic acid amplification and analysis: latest advances and future trends." Nucleic Acids Research **35**(13): 4223-4237.
- Zhang, C., J. Xu, et al. (2006). "PCR microfluidic devices for DNA amplification." Biotechnology Advances **24**(3): 243-284.
- Zhang, Y. and P. Ozdemir (2009). "Microfluidic DNA amplification-A review." Analytica Chimica Acta **638**(2): 115-125.
- Zhang, Z., X. Feng, et al. (2009). Environmentally friendly surface modification of PDMS using PEG polymer brush.
- Zhang, Z. W., X. J. Feng, et al. (2010). "'Click' chemistry-based surface modification of poly(dimethylsiloxane) for protein separation in a microfluidic chip." Electrophoresis **31**(18): 3129-3136.
- Zheng, S., H. Lin, et al. (2007). "Membrane microfilter device for selective capture, electrolysis and genomic analysis of human circulating tumor cells." Journal of Chromatography A **1162**(2): 154-161.
- Zimmermann, U. (1982). "Electric field-mediated fusion and related electrical phenomena." Biochimica et Biophysica Acta (BBA) - Reviews on Biomembranes **694**(3): 227-277.

Appendix A – NASBA design

Below are the different steps for designing a NASBA assay. In this example the targeted species is *Dunaliella primolecta* a phytoplankton studied for biofuel development. NASBA design recommendations have been previously published (Rodriguez-Lazaro, Hernandez et al. 2006).

A real-time NASBA assay has been developed for the detection of rbcL mRNA from *Dunaliella primolecta*. Molecular beacon and primer design were evaluated using online data base searches. Once the species' sequence was found, primers were designed and chosen using

<http://frodo.wi.mit.edu/primer3/>.

Different primer site are suggested:

Primer sets 1

599' AAAACGTAAACTCACAACCA TTCATGCGTTGGAGAGACCGTTTCTTATTCGTAGCTGAAGCTAT
TTACAAATCACAAGCAGAACTGGTGAAATTAAGGTCACTACTTAAACGCTACAGCAGGTACTGC
TGAAGGAATGCTTCAACGTGCACAAT'754 (NASBA will produce antisense amplicon from this sequence)

Forward primer (primer B, see NASBA 1.2.1, page 32): AAA ACG TAA ACT CAC AAC CA

Reverse primer (primer A): AATTCTAATACGACTCACTATAGGGAGAAG ATT GTG CAC GTT GAA
GCA TT (reverse primer is designed to be complementary to the sense)

After choosing primers, the beacon site needs to be selected.

Beacon

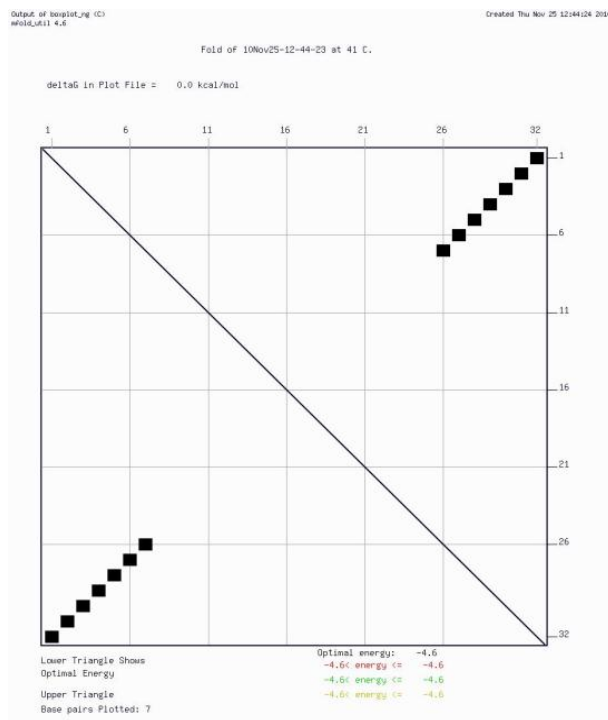
599' AAAACGTAAACTCACAACCA TTCATGCGTTGGAGAGACCGTTTCTTATTCGTAGCTGAAGCTAT
TTACAAATCACAAGCAGAACTGGTGAAATTAAGGTCACTACTTAAACGCTACAGCAGGTACTGC
TGAAGGAATGCTTCAACGTGCACAAT'754

Beacon: 5'-cy5- GAGTCG GGTCACTACTTAAACGCTAC CGACTC -ECLIPS-3' (the beacon is designed to be complementary to the antisense amplicon)

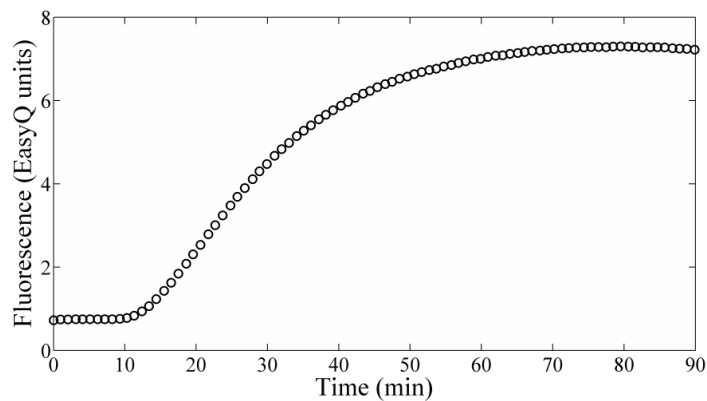
Then the primers and beacon will be analysed on <http://primerdigital.com/tools/> regarding the melting temperature calculation for standard and degenerate oligonucleotides, GC content, primer PCR efficiency, sequence linguistic complexity and molecular weight. Self dimer and cross dimer between the different oligonucleotides and the specie sequence can also be assessed. A primer self-dimer is formed by intermolecular interactions between the two primers and primer cross dimers are formed by intermolecular interaction between sense and antisense primers. When designing primers, it is important to have a minimum of intramolecular or intermolecular homology. Dimers could result in assay interferences.

Name	Sequence	Tm°C	CG%	nt	A	T	C	G	Extinction	Molecular	nmol	µg/OD260	Linguistic	Primer's	F
Forward	aaaacgtaactcacaacca	50.48	35	20	11	2	6	1	208300	6056.04	4.8	29.07	88	85	
Revers	aattctaatacgcactactataggagaagattgtgcacgttgaagcatt	64.76	38	50	17	14	8	11	503000	15456.16	1.99	30.73	94	66	
Beacon	gagtcgggtcactactaaacgcctaccgactc	63.9	53.13	32	8	7	10	7	303500	9769.39	3.29	32.19	95	71	

Beacon folding and design can be checked on the following website <http://mfold.bioinfo.rpi.edu/cgi-bin/dna-form1.cgi>.



Beacon folding energy diagram.



NASBA amplification data for approximately 100,000 *Dunaliella primolecta* cells equivalent.